

Electronic Thesis and Dissertation Repository

6-22-2022 1:30 PM

Luminescent Group 11 Metal Chalcogen Clusters with Bidentate Phosphine Ligands

Mansha Nayyar, *The University of Western Ontario*

Supervisor: Corrigan, John F., *The University of Western Ontario*

A thesis submitted in partial fulfillment of the requirements for the Master of Science degree in Chemistry

© Mansha Nayyar 2022

Follow this and additional works at: <https://ir.lib.uwo.ca/etd>

Recommended Citation

Nayyar, Mansha, "Luminescent Group 11 Metal Chalcogen Clusters with Bidentate Phosphine Ligands" (2022). *Electronic Thesis and Dissertation Repository*. 8599.
<https://ir.lib.uwo.ca/etd/8599>

This Dissertation/Thesis is brought to you for free and open access by Scholarship@Western. It has been accepted for inclusion in Electronic Thesis and Dissertation Repository by an authorized administrator of Scholarship@Western. For more information, please contact wlsadmin@uwo.ca.

Abstract

Luminescent group 11 metal chalcogen clusters have been of interest in the past few decades due to their potential applications in light emitting materials. These complexes can be synthesized by a controlled reaction between a phosphine solubilized metal complex ($M = \text{Cu}, \text{Ag}$) and trimethylsilylchalcogen reagents ($\text{R}(\text{SiMe}_3)$ and $\text{E}(\text{SiMe}_3)_2$, $\text{R} = \text{organic moiety}$, $\text{E} = \text{S}, \text{Se}$) which results in polynuclear metal chalcogen complexes ((M-ER) or (M_2E)) with protective phosphine ligands. These phosphine stabilized clusters can exhibit emission at room temperature (RT) which can be changed depending on the phosphine ligand. This thesis focuses on incorporating 4,6 - *bis*(diphenylphosphino)dibenzofuran (DBFDP) and related diphosphine ligands in group 11 metal chalcogen clusters to determine how the incorporation of these bidentate phosphines affect the structural and the luminescence properties of these compounds. It was observed that the incorporation of DBFDP in metal chalcogenolate clusters resulted in $[(\text{M}(\text{EPh}))_x(\text{dbfdp})_2]$ ($\text{Ph} = \text{phenyl}$, $x = 4, 5, 6$) with efficient PLQY's of up to 73 % at RT while the incorporation of the related DBFDP resulted in $[\text{Cu}_{12}\text{E}_6(\text{etdfbdp})_4]$ with protective phosphine ligands with red - orange emission at RT. An analysis of the structure and the photophysical properties of group 11 metal chalcogen clusters is discussed.

Keywords: metal chalcogenolates, metal chalcogenides, phosphine ligands, luminescence, emission, photoluminescence quantum yields

Summary for Lay Audience

Group 11 metals refer to copper, silver and gold while chalcogens refer to the group 16 elements oxygen, sulfur, selenium and tellurium. The chalcogens in combination with group 11 metals can form group 11 metal chalcogenolate or chalcogenide clusters. Chalcogenolates (RE^- , R = organic moiety, E = S, Se) have a 1^- charge on the chalcogen atom which has the ability to bond to group 11 metals with a 1^+ charge resulting in a core made of M-ER (M = Cu, Ag) with a ratio of 1:1 between M:E. The R groups in the chalcogenolates provide kinetic control in the assembly of the desired compound. Moreover, phosphorus containing organic compounds (phosphine ligands) can also be incorporated in these compounds which can provide a way to change the properties (such as luminescence - emission of light in the visible region) of group 11 metal chalcogenolate clusters. On the other hand, chalcogenides have a 2^- charge on the chalcogen and when reacted with $M^{(I)}$, they result in a M_2E core with a 2:1 ratio between the M and E. The metal is protected by the incorporation of phosphine ligands and provides kinetic control in synthesizing the desired species and preventing the formation of bulk M_2E . The protective phosphine ligands can result in properties such as luminescence for group 11 metal chalcogen clusters which have potential applications in light emitting materials, optical sensors and bioimaging. This thesis describes the incorporation of a custom / tailored phosphine ligand that has the ability to bond two metal atoms in group 11 metal chalcogen clusters and an examination of their luminescence.

Co-Authorship Statement

The work in this thesis contains contributions from the author as well as Kenneth Chu, Daniela Capello, Jonathan Adsetts, Dr. Florian Weigend and Dr. John F. Corrigan. The contributions are described.

Chapter 1 was written by the author and edited by Dr. Corrigan.

Chapter 2 reports compounds synthesized by the author. The crystallography experiments as well as structure resolution and refinement were performed by Dr. Corrigan. Kenneth Chu and Jonathan Adsetts performed the emission and excitation measurements of the complexes. Daniela Capello measured the photoluminescent quantum yields of the reported compounds. Dr. Florian Weigend performed the theoretical calculations for the complexes reported in Chapter 2. The chapter was written by the author and edited by Dr. Corrigan.

Chapter 3 reports compounds synthesized by the author. The crystallography experiments as well as structure resolution and refinement were performed by Dr. Corrigan. The chapter was written by the author and edited by Dr. Corrigan.

Chapter 4 provides conclusion and future outlooks for Chapter 2 and 3. The chapter was written by the author and edited by Dr. Corrigan.

Acknowledgements

I would like to thank the Department of Chemistry for making the past three years very memorable. It was all possible because of the contribution of the staff and the faculty. I am thankful to all the professors in the department because each one of them has shaped me into the person I am today.

I am the most thankful to my supervisor, Dr. John F. Corrigan who not only taught me how to be a better scientist, a better team member and a better individual but also inspired me to pursue a Masters in inorganic synthetic chemistry. I owe it all to his support and faith in me. All my accomplishments and the chemist I am today, is because of him. I am also grateful for my colleagues. Thank you, Nils, for always helping me out when I get stuck and the stopcock gets stuck. Thank you, Andy, for the craziest ideas and conversations (play mobile + baby monitor). Thank you, Alex, for always being the most normal one and being there for the laughs. I would also like to thank my undergraduate students. Thank you, Jeffrey (who is now my colleague), for making me a mentor, the Timmies runs and all the silly ideas / discussions. Thank you, Aaron, for making me an even better mentor and accompanying the group on the Timmies runs.

I want to thank Dr. Chris Levy and Benjamin Bridge for allowing me to use the undergraduate instruments for ATR - IR and UV - Vis Spectroscopy. Thank you to Dr. F. Weigend for acquiring the DFT data for my compound. I am indebted to Dr. John F. Corrigan who collected and analyzed the data for single crystal X - ray diffraction which was a crucial piece of data for my thesis. Thank you to Jonathan Adsetts and Kenneth Chu from the *Ding* group for running and analyzing my emission and excitation data. I also want to acknowledge Daniela Cappello from the *Gilroy* group for running and analyzing the quantum yields.

I want to thank my friends for their motivation and support throughout these past years. I have met some of the most amazing people throughout these years who have now turned into family. I want to thank my best friend (more like sister) Zahra Mohamad Sharif or better known as my “partner in crime” (- as stated by John) for always helping me and believing in me. This past year has been a hell of a roller coaster for me and there was not one moment where I felt alone and that was all because of her. I also want to thank Jeffrey Li (who is basically my brother at this point) for always helping me and spending money with me on food / coffee. It has been a blast sharing an office with you and working beside you in the lab. Most of all, it has been very fun to discuss the messy NMR spectra, “nerding” out on crystals and arguing like siblings with you. I am going to miss seeing you & Zahra every day, but I know nothing will ever change between us. I also want to thank Clement Lee for being one of my best friends since my first year of

university. You have always been there to help me in any way possible. We've both come a long way in our friendship and careers, and I couldn't be happier for you and everything you have accomplished. Special thanks to Zahra, Jeffrey, Haley Marier and Clement who stayed up nights with me to make sure I was not alone in finishing my thesis.

Lastly, I want to thank my family for always encouraging me to strive for the best. My parents have been two of the most important people who have supported me, always believed in me and given me the strength through the best and the worst times. They have been my biggest backbone through everything in my life. Moreover, I would like to thank my grandparents, my aunt, uncle and my little cousin. They would call me every time I accomplished something just to congratulate me and tell me how proud they are of me. Everything my family and friends have done means the world to me. This would not have been possible without any of you. Thank you.

Table of Contents

<i>Abstract</i>	<i>i</i>
<i>Summary for Lay Audience</i>	<i>ii</i>
<i>Co-Authorship Statement</i>	<i>iii</i>
<i>Acknowledgements</i>	<i>iv</i>
<i>List of Figures</i>	<i>ix</i>
<i>List of Schemes</i>	<i>xiii</i>
<i>List of Tables</i>	<i>xiv</i>
<i>List of Compounds</i>	<i>xv</i>
<i>List of Abbreviations</i>	<i>xvi</i>
Chapter 1	1
1.0 Introduction	1
1.1 Group 11 Metal Chalcogen Clusters	1
1.1.1 Group 11 Metal Chalcogenolate Clusters (M-ER)	1
1.1.2 Group 11 Metal Chalcogenide Clusters (M₂E)	4
1.2 Synthesis Methods for Group 11 Metal Chalcogen Clusters	7
1.2.1 Silylated Chalcogen Reagents for the Synthesis of Group 11 Metal Chalcogen Clusters	9
1.3 Phosphine Stabilized Group 11 Metal Chalcogen Clusters	10
1.4 Luminescence, Photoluminescence: Fluorescence, Phosphorescence, Thermally Activated Delayed Fluorescence and Photoluminescence Quantum Yields	11
1.5 Luminescent Group 11 Metal Chalcogen Complexes incorporating Phosphine Ligands	13
1.6 A Better Phosphine Ligand: 4,6 - bis(diphenylphosphino)dibenzofuran (DBFDP)	16
1.7 Scope of Thesis	19
1.8 References	20
Chapter 2	23
2.0 Luminescent Group 11 Metal Chalcogenolate Clusters with Conjugated Diphosphine Ligands ..	23
2.1 Introduction	23
2.2 Results and Discussion	25
2.2.1 Synthesis and Characterization of [Cu₄(μ_{2/3}-SePh)₄(μ-dbfdp)₂] (2.3), [Ag₆(μ_{2/3}-SePh)₆(μ-dbfdp)₂] (2.4), [Cu₅(μ_{2/3}-SPh)₅(μ-dbfdp)₂] (2.5), [Cu₅(μ_{2/3}-SPh)₄Cl(μ-dbfdp)₂] (2.6), and [Ag₄(μ_{2/3}-SPh)₄(μ-dbfdp)₂] (2.7)	25
2.2.2 Photophysical properties of Metal Chalcogenolate Complexes (2.3) - (2.7)	34
2.2.3 Theoretical Calculations for [Cu₄(μ_{2/3}-SePh)₄(μ-dbfdp)₂] (2.3)	39
2.3 Experimental	41
2.3.1 General Considerations	41

2.3.2 Synthesis of $[Cu_4(SePh)_4(dbfdp)_2]$ (2.3)	42
2.3.3 Synthesis of $[Ag_6(SePh)_6(dbfdp)_2]$ (2.4)	43
2.3.4 Synthesis of $[Cu_5(SPh)_5(dbfdp)_2]$ (2.5)	43
2.3.5 Synthesis of $[Cu_5(SPh)_4Cl(dbfdp)_2]$ (2.6)	44
2.3.6 Synthesis of $[Ag_4(SPh)_4(dbfdp)_2]$ (2.7)	44
2.4 Conclusions	45
2.5 References	46
Chapter 3	49
3.0 Luminescent Copper Chalcogenide Clusters with Conjugated Diphosphine Ligands	49
3.1 Introduction	49
3.2 Results and Discussion	53
3.2.1 Synthesis and Characterization of EtDBF (3.1) and EtDBFDP (3.2)	53
3.2.2 Synthesis and Characterization of $[Cu_{12}Se_6(etdbfdp)_4]$ (3.3)	56
3.2.3 Synthesis and Characterization of $[Cu_{12}S_6(etdbfdp)_4]$ (3.4)	59
3.2.4 Photophysical Properties of $[Cu_{12}Se_6(etdbfdp)_4]$ (3.3) and $[Cu_{12}S_6(etdbfdp)_4]$ (3.4)	60
3.3 Experimental	64
3.3.1 General Considerations	64
3.3.2 Synthesis of EtDBF (3.1)	64
3.3.3 Synthesis of EtDBFDP (3.2)	65
3.3.4 Synthesis of $[Cu_{12}Se_6(etdbfdp)_4]$ (3.3)	65
3.3.5 Synthesis of $[Cu_{12}S_6(etdbfdp)_4]$ (3.4)	66
3.4 Conclusions	67
3.5 References	68
4.0 Conclusions and Outlook	70
4.1 Summary and Conclusions	70
4.2 Outlook - Luminescent Group 11 Metal Chalcogenolate Clusters with Conjugated Diphosphine Ligands	74
4.3 Outlook - Luminescent Copper Chalcogenolate Clusters with Conjugated Diphosphine Ligands	75
4.4 References	76
Appendices	77
Appendix 1.0 Permission to Reuse Copyright Material	77
Appendix 2.0 Supporting Information for Chapter 2	84
Appendix 2.1: 1H and $^{31}P\{^1H\}$ NMR data for compounds (2.3) - (2.7)	84
Appendix 2.2: X - ray structure analysis and data for compounds (2.3) - (2.7)	94

<i>Appendix 3.0 Supporting Information for Chapter 3</i>	105
<i>Appendix 3.1: ^1H, $^{13}\text{C}\{^1\text{H}\}$ and $^{31}\text{P}\{^1\text{H}\}$ NMR data for compounds (3.1) and (3.2)</i>	105
<i>Appendix 3.2: X - ray structure analysis and data for (3.3)</i>	109
<i>Curriculum Vitae</i>	113

List of Figures

Figure 1.1: Molecular structure of $[\text{Cu}_2(\mu_2\text{-S-C}_6\text{H}_4\text{-OMe})_2(\text{dpppt})_2]$ (I.I) (H atoms are omitted for clarity). ^[9]	2
Figure 1.2: Molecular structure of $[\text{Cu}_7(\text{p-S-C}_6\text{H}_4\text{-NMe}_2)_7(\text{PPh}_3)_4]$ (I.II) (H atoms are omitted for clarity). ^[11]	3
Figure 1.3: Molecular structure of $[\text{Ag}_{12}(\text{SCH}_2\text{C}_6\text{H}_5)_6(\text{CF}_3\text{COO})_6(\text{pyridine})_6]$ (I.III) (H atoms are omitted for clarity). ^[16]	4
Figure 1.4: (a) Molecular structure of $[\text{Cu}_{12}\text{S}_6(\text{dppo})_4]$ (I.IV) (H atoms are omitted for clarity) ^[18] (b) Molecular structure of $[\text{Cu}_{12}\text{Se}_6(\text{dppo})_4]$ (I.V) (H atoms are omitted for clarity). ^[21]	6
Figure 1.5: (a) Molecular structure of $[\text{Ag}_{58}\text{S}_{13}(\text{SAd})_{32}]$ (I.VII) (H atoms are omitted for clarity) (b) $(\text{Ag}_2\text{S})_{13}$ core (only sulfide atoms that form the core are shown for clarity) (c) S_{13} centered icosahedral core made of S^{2-} shown in orange and S_{32} shell of RS^- shown in yellow (Lines between S centres are only shown for geometric arrangement) (figure adapted from S. Bestgen, X. Yang, I. Issac, O. Fuhr, P. W. Roesky, D. Fenske, Chem. - A Eur. J. 2016, 22, 9933–9937. Copyright 2022 John Wiley and Sons). ^[19]	7
Figure 1.6: Molecular structure of $[\text{Cu}_2(\text{SePh})_2(\text{dpppt})_2]$ (I.XIII) (H atoms are omitted for clarity). ^[9]	10
Figure 1.7: Simplified version of emission from the singlet state showing fluorescence and triplet state showing phosphorescence (figure adapted from literature). ^[41]	12
Figure 1.8: Simplified version of emission shown as thermally activated delayed fluorescence (TADF) and phosphorescence (figure adapted from literature). ^{[41][47]}	13
Figure 1.9: General core structures of copper (I) sulfide clusters with phosphine ligands (a) $[\text{Cu}_{12}\text{S}_6(\text{dpppt})_4]$ (I.XIX) (b) $[\text{Cu}_{20}\text{S}_{10}(\text{PPh}_3)_8]$ (I.XX) (c) $[\text{Cu}_{24}\text{S}_{12}(\text{PEt}_3\text{Ph})_{12}]$ (I.XXI) (d) $[\text{Cu}_{20}\text{S}_{10}(\text{P}^t\text{Bu}_3)_8]$ (I.XXII) (C and H atoms are omitted for clarity) (adapted with permission from A. Eichhöfer, G. Buth, S. Lebedkin, M. Kühn, F. Weigend, Inorg. Chem. 2015, 54, 9413–9422. Copyright 2022 American Chemical Society). ^[21]	14
Figure 1.10: (a) Molecular structure of $[\text{Cu}_2(\text{S-C}_6\text{H}_4\text{-OMe})_2(\text{dpppt})_2]$ (I.I) (H atoms are omitted for clarity) (b) Emission of $[\text{Cu}_2(\text{S-C}_6\text{H}_4\text{-OMe})_2(\text{dpppt})_2]$ (I.I) (adapted from B. Hu, C. Y. Su, D. Fenske, O. Fuhr, Inorg. Chim. Acta 2014, 419, 118–123. Copyright 2022 Elsevier). ^[9]	15
Figure 1.11: (a) Molecular structure of $[\text{Ag}_{14}(\text{SC}_6\text{H}_3\text{F}_2)_{12}(\text{PPh}_3)_8]$ (I.XXIV) (H atoms are omitted for clarity) (b) Emission of $[\text{Ag}_{14}(\text{SC}_6\text{H}_3\text{F}_2)_{12}(\text{PPh}_3)_8]$ (I.XXIV) in DCM (c) Emission of $[\text{Ag}_{14}(\text{SC}_6\text{H}_3\text{F}_2)_{12}(\text{PPh}_3)_8]$ (I.XXIV) in the solid state (adapted with permission from H. Yang, J. Lei, B. Wu, Y. Wang, M. Zhou, A. Xia, L. Zheng, N. Zheng, Chem. Commun. 2013, 49, 300–302. Copyright 2022 Royal Society of Chemistry). ^[52]	16
Figure 1.12: Molecular structure of $[\text{CuITTPP}]$ (I.XXV) (H atoms are omitted for clarity). ^[54]	17
Figure 1.13: Temperature dependent TADF and PH emission of $[(\text{Cu}_4\text{I}_4)(\text{dbfdp})_2]$ (I.XXVI) with lifetime decays (figure adapted from M. Xie, C. Han, J. Zhang, G. Xie, H. Xu, Chem. Mater. 2017, 29, 6606–6610. Copyright 2022 American Chemical Society). ^[53]	17
Figure 1.14: (a) 4,6 - bis(diphenylphosphino)dibenzofuran (DBFDP) (b) Molecular structure of $[(\text{Cu}_4\text{I}_4)(\text{dbfdp})_2]$ (I.XXVI) in the crystal (H atoms are omitted for clarity). ^[53]	18

Figure 1.15: DFT Calculations for $[(Cu_4I_4)(dbfdp)_2]$ (LXXVI) (figure adapted from M. Xie, C. Han, J. Zhang, G. Xie, H. Xu, <i>Chem. Mater.</i> 2017, 29, 6606–6610. Copyright 2022 American Chemical Society).^[53]	18
Figure 2.1: $[Cu_4(P^{\wedge}S)_4(CH_3CN)_2]$ ($P^{\wedge}S = 2-(diphenylphosphino)benzenethiolate$) (II.III) (H atoms are omitted for clarity).^[14]	24
Figure 2.2: 4,6 - bis(diphenylphosphino)dibenzofuran (DBFDP).^[15]	25
Figure 2.3: Molecular structure of $[Cu_4(SePh)_4(dbfdp)_2]$ (2.3) in the crystal (Cu - Se: 2.3651(3) - 2.5797(3) Å, Cu - P: 2.2022(6) - 2.2412(5) Å, Cu(1) ... Cu(2): 2.6246(4) Å) (H atoms are omitted for clarity). The molecule resides about a crystallographic inversion centre.	27
Figure 2.4: Molecular structure of $[Ag_6(SePh)_6(dfbdp)_2]$ (2.4) in the crystal (Ag - Se: 2.5145(9) - 3.0222(9) Å, Ag - P: 2.4371(18) - 2.4769(19) Å, Ag ... Ag: 2.9910(8) - 3.1320(8) Å) (H atoms are omitted for clarity).	29
Figure 2.5: Molecular structure of $[Cu_5(SPh)_5(dbfdp)_2]$ (2.5) in the crystal (Cu - S: 2.2111(10) - 2.4494(10) Å, Cu - P: 2.1816(10) - 2.2617(10) Å, Cu ... Cu: 2.6942(6) - 2.8223(6) Å) (H atoms are omitted for clarity).	31
Figure 2.6: Molecular structure of $[Cu_5(SPh)_4Cl(dbfdp)_2]$ (2.6) in the crystal (Cu - S: 2.2371(10) - 2.3050(7) Å, Cu - P: 2.2253(9) - 2.2369(9) Å, Cu - Cl: 2.2429(15) Å) (H atoms are omitted for clarity). The molecule resides about a mirror plane bisecting Cu(3)/S(2)/S(3)/Cl.	32
Figure 2.7: Molecular structure of $[Ag_4(SPh)_4(dbfdp)_2]$ (2.7) in the crystal (Ag - S: 2.442(8) - 2.897(16) Å, Ag - P: 2.414(8) - 2.442(8) Å) (H atoms are omitted for clarity). (The molecule resides about a crystallographic inversion centre).	34
Figure 2.8: (a) Emission of $[Cu_4(SePh)_4(dbfdp)_2]$ ((2.3)·THF) (b) Emission of $[Cu_4(SePh)_4(dbfdp)_2]$ (2.3) (c) Emission of $[Ag_6(SePh)_6(dfbdp)_2]$ (2.4) (d) Emission of $[Cu_5(SPh)_5(dbfdp)_2]$ (2.5) (e) Emission of $[Cu_5(SPh)_4Cl(dbfdp)_2]$ (2.6) (f) Emission of $[Ag_4(SPh)_4(dbfdp)_2]$ (2.7). (Qualitative observation of the emission of solid - state samples at room temperature when irradiated at 365 nm).	35
Figure 2.9: (a) Emission of $[Cu_4(SePh)_4(dbfdp)_2]$ (2.3) (in DCM and heptane) (b) Emission of $[Cu_4(SePh)_4(dbfdp)_2]$ ((2.3)·DCM) after isolation and removal of DCM under vacuum. (Qualitative observation of the emission of solid - state samples at room temperature when irradiated at 365 nm).	36
Figure 2.10: Excitation spectra of (2.3) - (2.7) in the solid state at room temperature. The selected $\lambda_{exc(max)}$ for these complexes range between 360 nm - 470 nm.	37
Figure 2.11: Emission spectra of (2.3) - (2.7) in the solid state at room temperature. ($\lambda_{exc} = 470$ nm ((2.3)·THF)), $\lambda_{exc} = 475$ nm (2.3), $\lambda_{exc} = 400$ nm (2.4), $\lambda_{exc} = 465$ nm (2.5), $\lambda_{exc} = 390$ nm (2.6), $\lambda_{exc} = 360$ nm (2.7)) The λ_{em} for these complexes range between 510 nm - 570 nm. (The noise seen in (2.4) and (2.7) is due to the low emission intensity of the compounds).	38
Figure 2.12: DFT Calculations for $[Cu_4(SePh)_4(dbfdp)_2]$ (2.3) displaying the HOMOs and LUMOs 40	
Figure 2.13: (a) Emission of the reaction mixture of $[Cu_4(SePh)_4(dbfdp)_2]$ (2.3) (b) $[Cu_5(SPh)_5(dbfdp)_2]$ (2.5) and (c) $[Cu_5(SPh)_4Cl(dbfdp)_2]$ (2.6) at room temperature when irradiated at 365 nm. (Qualitative observation of the emission of solution - state samples at room temperature when irradiated at 365 nm).	45
Figure 3.1: 4,6 - bis(diphenylphosphino)dibenzofuran (DBFDP).^[18]	50

Figure 3.2: Molecular structure of [(Cu₄I₄)(dbfdp)₂] (III.II) (H atoms are omitted for clarity).^[18]	51
Figure 3.3: Substituted 4,6 - bis(diphenylphosphino)dibenzofuran.^[20]	52
Figure 3.4: (a) ¹H NMR spectrum (CDCl₃): EtDBF (3.1) (b) Zoomed in aliphatic region of EtDBF (3.1) displaying the triplet and the quartet multiplicities of the ethyl group.	55
Figure 3.5: ³¹P {¹H} NMR spectrum (CDCl₃): EtDBFDP (3.2) δ: -16 ppm.	56
Figure 3.6: Molecular structure of [(CuOAc)₂(dfbdp)₂] (III.IX) (H atoms are omitted for clarity).^[19]	56
Figure 3.7: Molecular structure of [Cu₁₂Se₆(dbfdp)₄] (3.3) in the crystal (Cu - Se: 2.2705(14) - 2.4632(16) Å, Cu - P: 2.298(3) - 2.318(3) Å, Cu ... Cu: 2.5966(16) - 2.9868(15) Å) (H atoms are omitted for clarity). (The molecule resides about a crystallographic inversion centre).	58
Figure 3.8: Molecular structure of [Cu₁₂Se₆(dppo)₄] (III.X).^[17]	59
Figure 3.9: (a) Emission of the reaction mixture of EtDBFDP (3.2) with CuOAc and Se(SiMe₃)₂ in THF at -40 °C (b) Emission of crystals of [Cu₁₂Se₆(etdbfdp)₄] (3.4) (Qualitative observation of the emission of the reaction solution and solid - state samples at room temperature when irradiated at 365 nm).	61
Figure 3.10: Excitation spectrum of [Cu₁₂Se₆(etdbfdp)₄] (3.3) in the solid state at room temperature. The selected λ_{exc(max)} for this complex is at 475 nm.	62
Figure 3.11: Emission spectra of [Cu₁₂Se₆(etdbfdp)₄] (3.3) in the solid state at room temperature. The highest intensity for λ_{em} (653 nm) is when the sample is irradiated at 475 nm.	62
Figure 3.12: Emission of the reaction mixture solution of EtDBFDP (3.2) and CuOAc with S(SiMe₃)₂ in THF at -40 °C with a handheld UV lamp. (Qualitative observation of the emission of the reaction solution when irradiated at 365 nm).	63
Figure 4.1: (a) Molecular structure [Cu₄(SePh)₄(dbfdp)₂] (2.3), (b) [Ag₆(SePh)₆(dbfdp)₂] (2.4), (c) [Cu₅(SPh)₅(dbfdp)₂] (2.5), (d) [Cu₅(SPh)₄Cl(dbfdp)₂] (2.6), (e) [Ag₄(SPh)₄(dbfdp)₂] (2.7).	71
Figure 4.2: Molecular structure of [Cu₁₂Se₆(etdbfdp)₄] (3.3) in the crystal (H atoms are omitted for clarity). (The molecule resides about a crystallographic inversion centre).	73
Figure 4.3: Substituted 4,6 - bis(diphenylphosphino)dibenzofuran.^[6]	75
Figure S2.1: ¹H NMR spectrum in CDCl₃ (298 K) of [Cu₄(SePh)₄(dbfdp)₂] (2.3)	84
Figure S2.2: ³¹P{¹H} NMR spectrum in CDCl₃ (298 K) of [Cu₄(SePh)₄(dbfdp)₂] (2.3)	85
Figure S2.3: ¹H NMR spectrum in CDCl₃ (298 K) of [Ag₆(SePh)₆(dbfdp)₂] (2.4)	86
Figure S2.4: ³¹P{¹H} NMR spectrum in CDCl₃ (298 K) of [Ag₆(SePh)₆(dbfdp)₂] (2.4)	87
Figure S2.5: ¹H NMR spectrum in CDCl₃ (298 K) of [Cu₅(SPh)₅(dbfdp)₂] (2.5)	88
Figure S2.6: ³¹P{¹H} NMR spectrum in CDCl₃ (298 K) of [Cu₅(SPh)₅(dbfdp)₂] (2.5)	89
Figure S2.7: ¹H NMR spectrum in CDCl₃ (298 K) of [Cu₅(SPh)₄Cl(dbfdp)₂] (2.6)	90
Figure S2.8: ³¹P{¹H} NMR spectrum in CDCl₃ (298 K) of [Cu₅(SPh)₄Cl(dbfdp)₂] (2.6)	91
Figure S2.9: ¹H NMR spectrum in CDCl₃ (298 K) of [Ag₄(SPh)₄(dbfdp)₂] (2.7)	92
Figure S2.10: ³¹P{¹H} NMR spectrum in CDCl₃ (298 K) of [Ag₄(SPh)₄(dbfdp)₂] (2.7)	93
Figure S3.1: ¹³C{¹H} NMR spectrum in CDCl₃ (298 K) of (EtDBF) (3.1)	105

<i>Figure S3.2: ^1H NMR spectrum in CDCl_3 (298 K) of (EtDBFDP) (3.2)</i>	106
<i>Figure S3.3: $^{13}\text{C}\{^1\text{H}\}$ NMR spectrum in CDCl_3 (298 K) of (EtDBFDP) (3.2)</i>	107
<i>Figure S3.4: $^{31}\text{P}\{^1\text{H}\}$ NMR spectrum in CDCl_3 (298 K) of (EtDBFDP) (3.2) (* unknown impurities)</i>	108

List of Schemes

<i>Scheme 1.1: Reaction scheme (a) Deprotonation of H₂S (b) Synthesis of a copper sulfide complex using deprotonated sulfide.</i> ^[25]	8
<i>Scheme 1.2: Reaction scheme for the synthesis of [CuSAr^{iPr4}]₂ (I.X) (Dipp = -C₆H₃-2,6-(C₆H₃-2,6-iPr₂).</i> ^[31]	8
<i>Scheme 1.3: General reaction scheme for the synthesis of metal chalcogen clusters (n = 1,2,3... y = 1,2,3...) (Metal in the metal salts is also bonded to a ligand).</i> ^{[1][2][34][36][37]}	9
<i>Scheme 1.4: General reaction scheme for the synthesis of phosphine stabilized metal complexes (x = 1,2,3... y = 1,2,3...).</i> ^{[1][3][39]}	11
<i>Scheme 2.1: Synthesis schemes of group 11 metal chalcogenolate complexes (2.3) - (2.7).</i>	26
<i>Scheme 3.1: Synthesis of 2,8 - dibromo - dibenzofuran.</i> ^[20]	53
<i>Scheme 3.2: Synthesis of carbzole substituted dibenzofuran.</i> ^[20]	53
<i>Scheme 3.3: Synthesis of 2,8-diethyl-dibenzofuran (EtDBF) (3.1).</i>	54
<i>Scheme 3.4: Synthesis of 2,8-diethyl(4,6 - bis-(diphenylphosphino))dibenzofuran (EtDBFDP) (3.2).</i> ^[18]	55
<i>Scheme 3.5: Synthesis of [Cu₁₂Se₆(etdbfdp)₄] (3.3).</i>	57
<i>Scheme 3.6: Synthesis of [Cu₁₂S₆(etdbfdp)₄] (3.4).</i>	59
<i>Scheme 4.1: Proposed scheme to synthesise metal chalcogenide / chalcogenolate clusters.</i>	74

List of Tables

<i>Table S2.1: Summary of Crystal Data of [Cu₄(SePh)₄(dbfdp)₂] (2.3)</i>	94
<i>Table S2.2: Selected bond lengths of [Cu₄(SePh)₄(dbfdp)₂] (2.3)</i>	95
<i>Table S2.3: Selected bond angles of [Cu₄(SePh)₄(dbfdp)₂] (2.3)</i>	95
<i>Table S2.4: Summary of Crystal Data of [Ag₆(SePh)₆(dbfdp)₂] (2.4)</i>	96
<i>Table S2.5: Selected bond lengths of [Ag₆(SePh)₆(dbfdp)₂] (2.4)</i>	97
<i>Table S2.6: Selected bond angles of [Ag₆(SePh)₆(dbfdp)₂] (2.4)</i>	97
<i>Table S2.7: Summary of Crystal Data of [Cu₅(SPh)₅(dbfdp)₂] (2.5)</i>	99
<i>Table S2.8: Selected bond lengths of [Cu₅(SPh)₅(dbfdp)₂] (2.5)</i>	100
<i>Table S2.9: Selected bond angles of [Cu₅(SPh)₅(dbfdp)₂] (2.5)</i>	100
<i>Table S2.10: Summary of Crystal Data of [Cu₅(SPh)₄Cl(dbfdp)₂] (2.6)</i>	101
<i>Table S2.11: Selected bond lengths of [Cu₅(SPh)₄Cl(dbfdp)₂] (2.6)</i>	102
<i>Table S2.12: Selected bond angles of [Cu₅(SPh)₄Cl(dbfdp)₂] (2.6)</i>	102
<i>Table S2.13: Summary of Crystal Data of [Ag₄(SPh)₄(dbfdp)₂] (2.7)</i>	103
<i>Table S2.14: Selected bond lengths of [Ag₄(SPh)₄(dbfdp)₂] (2.7) (Molecule shows disorder, ₁ – fraction 1, ₂ – fraction 2)</i>	104
<i>Table S2.15: Selected bond angles of [Ag₄(SPh)₄(dbfdp)₂] (2.7) (Molecule shows disorder, ₁ – fraction 1, ₂ – fraction 2)</i>	104
<i>Table S3.1: Summary of Crystal Data of [Cu₁₂Se₆(etdbfdp)₂] (3.3)</i>	109
<i>Table S3.2: Selected bond lengths of [Cu₁₂Se₆(etdbfdp)₂] (3.3)</i>	110
<i>Table S3.3: Selected bond angles of [Cu₁₂Se₆(etdbfdp)₂] (3.3)</i>	110

List of Compounds

2.1 [(CuOAc)₂(dbfdp)₂]

2.2 [(AgOAc)₂(dbfdp)₂]

2.3 [Cu₄(SePh)₄(dbfdp)₂]

2.4 [Ag₆(SePh)₆(dbfdp)₂]

2.5 [Cu₅(SPh)₅(dbfdp)₂]

2.6 [Cu₅(SPh)₄Cl(dbfdp)₂]

2.7 [Ag₄(SPh)₄(dbfdp)₂]

3.1 EtDBF

3.2 EtDBFDP

3.3 [Cu₁₂Se₆(dbfdp)₄]

3.4 [Cu₁₂S₆(dbfdp)₄]

List of Abbreviations

Å	Angstrom
μ	Bridging
δ	Chemical shift
κ	Kappa (coordination)
ε	Molar absorptivity coefficient
λ _{em(max)}	Wavelength of emission
λ _{exc(max)}	Wavelength of excitation
λ _{max}	Wavelength maximum
°	Degrees
°C	Degrees Celsius
°C _{decomp}	Decomposition temperature
ΔE	Difference in energy
μm	Micrometres
a.u.	Arbitrary units
Ar ^{iPr4}	-C ₆ H ₃ -2,6-(C ₆ H ₃ -2,6-iPr ₂) ₂
ATR-IR	Attenuated Total Reflectance Infrared
EtBr	Bromoethane
CC	Cluster centered
DBF	Dibenzofuran
DBFDP	4,6 - <i>bis</i> (diphenylphosphino)dibenzofuran
DCM	Dichloromethane
DCz	Carbazole
DCzDBFDP	2,8 - dicarbazole - (4,6 - <i>bis</i> (diphenylphosphino))dibenzofuran
DtBCz	<i>Tert</i> butyl carbazole
DtBCzDBFDP	2,8 - di - <i>tert</i> - butylcarbazole - (4,6 - <i>bis</i> (diphenylphosphino))dibenzofuran
def2-TZVP	Polarized triple zeta valence set
DFT	Density functional theory
Dipp	2,6 - diisopropylphenyl
dpP	Diphenylphosphine
dppm	<i>bis</i> (diphenylphosphino)methane
dppo	1, 8 <i>bis</i> (diphenylphosphino)octane
dpppt	1, 2 <i>bis</i> (diphenylphosphino)pentane
E	Chalcogen: S, Se, Te
ER	Chalcogenolate
Et	Ethyl
EtDBP	2,8 - diethyl - dibenzofuran
EtDBFDP	2,8 - diethyl - (4,6 - <i>bis</i> (diphenylphosphino))dibenzofuran
equiv.	Equivalents
EUE	Exciton Utilization Efficiency
eV	Electron Volt (-1.6022 x 10 ⁻¹⁹ J)
<i>f</i>	Oscillator strength
g	Grams
HOMO	Highest occupied molecular orbital
HSAB	Hard soft acid base
K	Kelvin
LMCT	Ligand to metal charge transfer

LUMO	Lowest unoccupied molecular orbital
Me	Methyl
meV	Millielectron volt
MHz	Megahertz
mL	Milliliter
M	Group 11 metal
MLCT	Metal to ligand charge transfer
(M+X)LCT	Metal + halide to ligand charge transfer
mmol	Millimole
MOAc	Metal acetate
m.p.	Melting point
N _{abs}	Number of photons absorbed
N _{em}	Number of photons emitted
nm	Nanometers
NMR	Nuclear Magnetic Resonance
⁻ OAc	Acetate
OLED	Organic Light Emitting Diodes
P [^] S	2 - (diphenylphosphino)benzenethiolate
PBE	Perdew - Burke - Ernzerhof
Ph	Phenyl
PH	Phosphorescence
PLQY	Photoluminescence Quantum Yield
ppm	Parts per million
PR ₃	Tertiary phosphine
QY	Quantum Yield
R	Organic group
RT	Room temperature
S ₀	Singlet ground state
S ₁	Singlet excited state
SAd	1 - adamantanethiolate
SOC	Spin orbit coupling
T ₁	Triplet excited state
TADF	Thermally activated delayed fluorescence
THF	Tetrahydrofuran
TMEDA	Tetramethylethylenediamine
TTPP	2,2' - (phenylphosphinediyl) <i>bis</i> (2,1 - phenylene) <i>bis</i> (diphenylphosphine)
UV – Vis	Ultraviolet - Visible
W _{1/2}	Full width half maximum

Chapter 1

1.0 Introduction

1.1 Group 11 Metal Chalcogen Clusters

Polynuclear metal chalcogen complexes have been researched extensively due to their rich structural, chemical and physical properties. These properties depend on the elements of the cluster, the ligands and the spatial arrangement of the atoms.^{[1]-[6]} Specifically, coinage metal (group 11) clusters have been of interest due to their structural and photophysical properties with potential application in catalysis, sensors, polymers, photovoltaic cells, luminescence signalling devices and organic light emitting diodes (OLEDs).^{[4][5][7][8]}

1.1.1 Group 11 Metal Chalcogenolate Clusters (M-ER)

Group 11 metal chalcogenolate complexes show that clusters with different nuclearities and dimensionalities can be synthesized with Cu or Ag with protective chalcogenolates and organic ligands bonded to the metal. A common feature observed throughout these compounds is the trigonal planar / tetrahedral geometries of the metal atoms with μ_2 , μ_3 and μ_4 bridging chalcogenolates and protective ligands present at the periphery. An interesting characteristic of the high nuclearity complexes indicates the presence of metallophilic interactions which are attractive forces between metal centres that reduce the vibrations within the cluster reducing the loss of energy through vibrational energy. Discussed below are examples that highlight these factors.

Coinage metal elements (copper, silver and gold) in combination with chalcogenolates have gained interest in the past few decades due to their high potential as modifiable complexes in regard to the dimensionality of the structure and the functionality of the organic substituents to change the molecular, electronic and conductive properties.^{[9][10]} The M-ER (M = Cu, Ag, E = S, Se, R = organic moiety) bond is favoured due to the soft base - soft acid interaction between the metal and the chalcogen. The favourability of the M-ER bond with the incorporation of different sized organic ligands can result in molecular complexes of different sizes.^{[9][10]} These complexes have a core composed of $M^{(I)}$ and RE^{1-} resulting in a $(ME)_x$ core with organic ligands (bonded to the metal) and the R groups (bonded to the chalcogen) present at the periphery. Chalcogenolates (RE^- , E = S, Se) are known to have multiple coordination modes with group 11 metals resulting in different structural and photophysical properties (emission).^[11] An example of a smaller sized complex is $[Cu_2(\mu_2-S-C_6H_4-OMe)_2(dpppt)_2]$ (dpppt =

diphenylphosphinopentane) (**I.I**) shown in *Figure 1.1*.^[9] This represents a binuclear compound with a copper - thiolate core with organic ligands present at the periphery. As seen in *Figure 1.1*, the chalcogenolate adopts μ_2 coordination.^[9] Another example to compare to (**I.I**) is $[\text{Cu}_7(p\text{-S-C}_6\text{H}_4\text{-NMe}_2)_7(\text{PPh}_3)_4]$ (**I.II**) (*Figure 1.2*) reported by *Fuhr and co-workers*.^[11] This represents a heptanuclear cluster with a copper thiolate core with organic ligands bonded to the copper.^[11] The size and the structural geometry of (**I.I**) and (**I.II**) are very different from each other.^[11]

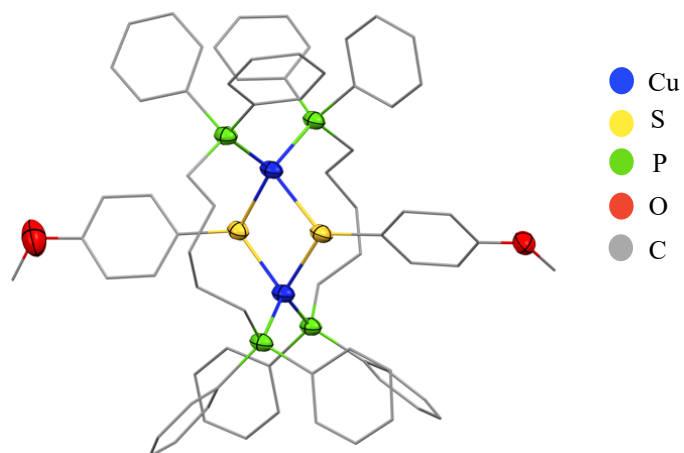


*Figure 1.1: Molecular structure of $[\text{Cu}_2(\mu_2\text{-S-C}_6\text{H}_4\text{-OMe})_2(\text{dpppt})_2]$ (**I.I**) (*H atoms are omitted for clarity*).^[9]*

In (**I.I**), each copper atom has a tetrahedral geometry due to bonding to two thiolates and two phosphines. In (**I.II**), four of the seven Cu centres represent tetrahedral geometry (three bonds to thiolate and one to phosphine) while the other three Cu centres have a trigonal planar geometry due to solely bonding to thiolates. A significant difference between (**I.I**) and (**I.II**) is that (**I.II**) has some Cu centres stabilized by thiolate ligands only due to thiolates having more coordination modes (μ_2 , μ_3 and μ_4). Moreover, the short distances between the copper atoms in (**I.II**) indicate the presence of metallophilic (cuprophilic) interactions.^[11]

Metallophilic interactions refer to the weak attractive forces between metal atoms. These attractive forces are known as weak bonds or secondary bonds and can be observed in univalent group 11 metal atoms ($\text{Au}^{(I)}$, $\text{Ag}^{(I)}$ and $\text{Cu}^{(I)}$).^[12] Auophilic interactions have been largely investigated and the short intermetallic distances between Au centres (2.5 - 3.5 Å) are used to indicate the presence of metallophilic interactions. These $\text{Au}^{(I)} \cdots \text{Au}^{(I)}$ interactions (7 - 11 kcal / mol) are slightly stronger than van der Waals forces and are considered unique due to the univalent atoms having closed shell configurations.^[12] The linear coordinated geometry of the Au atoms results in d orbital overlap resulting in auophilicity. The most

accepted theory for these $\text{Au}^{(I)} \cdots \text{Au}^{(I)}$ interactions is the relativistic contraction of the valence electrons which is the most pronounced in heavier elements.^[12] Argentophilic interactions are less studied than aurophilic interactions since linear coordinated geometry is predominantly observed in Au containing compounds than Ag. Similar to aurophilic interactions, argentophilicity is indicated by the short $\text{Ag}^{(I)} \cdots \text{Ag}^{(I)}$ distances (shorter than 2.5 - 3.4 Å).^[12]

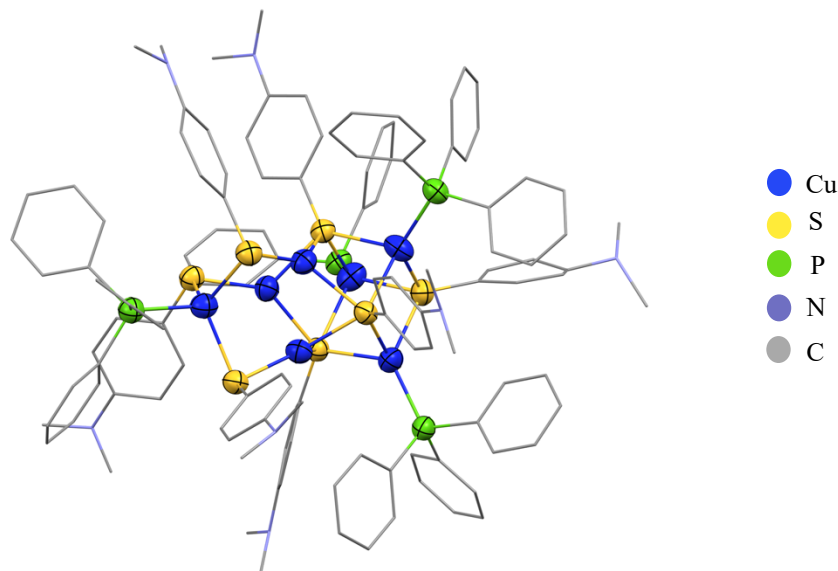


Figure 1.2: Molecular structure of $[\text{Cu}_7(\text{p-S-C}_6\text{H}_4\text{-NMe}_2)_7(\text{PPh}_3)_4]$ (**I.II**) (*H atoms are omitted for clarity*).^[11]

Cuprophilicity refers to $d^{10} - d^{10}$ $\text{Cu}^{(I)} \cdots \text{Cu}^{(I)}$ interactions which are weaker than aurophilic and argentophilic forces. Cuprophilic interactions are equivalent to van der Waals forces.^[12] These interactions are studied even less than their Ag counterparts. Since relativistic effects are more pronounced in heavier elements, the presence of cuprophilic interactions has been controversial.^[12] The major supporting evidence for an interaction to be classified as a cuprophilic interaction is the short distance between the Cu centres. The distance of the “bond” must be shorter than the sum of the van der Waals radii of two $\text{Cu}^{(I)}$ atoms, with the former having a distance of 2.4 - 2.8 Å.^[12]

Cuprophilic interactions have similar structural and dynamic characteristics when compared to the well-studied aurophilicity and argentophilicity. However, $\text{Cu}^{(I)}$ and $\text{Ag}^{(I)}$ are more likely to adopt trigonal planar / tetrahedral geometries resulting in higher coordination numbers.^[12] Copper is also a lighter element and therefore has weak relativistic effects which also result in $\text{Cu}^{(I)}$ having a higher coordination number. Cuprophilic interactions are relatively weak interactions and can be difficult to discern when present along with other stronger forces such as crystal packing, hydrogen bonding and $\pi - \pi$ interactions

but one of the key ways to determine the indication of cuprophilicity is through single crystal X - ray diffraction.^[12]

Silver chalcogenolate complexes are also considered interesting due to their structural diversity and their emission properties.^[13] They are not explored as extensively due to their instability under light and moisture which often leads to decomposition.^{[14][15]} An example of a stable silver chalcogenolate cluster is $[\text{Ag}_{12}(\text{SCH}_2\text{C}_6\text{H}_5)_6(\text{CF}_3\text{COO})_6(\text{pyridine})_6]$ (**I.III**) shown in *Figure 1.3*.^[16]

The silver atoms are bridged by the thiolates via μ_4 coordination forming a Ag_{12} cuboctahedron. The silver atoms have a distorted tetrahedral and trigonal planar geometries. The trigonal planar geometry arises from bonding to two thiolates and either one pyridine or one CF_3COO^- .^[16] The coordination ability of the CF_3COO^- ligand results in two of the silvers having distorted tetrahedral geometry. Another interesting feature of these clusters is the short distances (2.935 - 3.218 Å) between silver centres which indicates the presence of argentophilic interactions.^[16] Argentophilic interactions follow the same rule as cuprophilic interactions where the distance of the “bond” must be shorter than the sum of the van der Waals radii of two Ag atoms, with the former having a distance shorter than 3.4 Å.^{[12][17]}

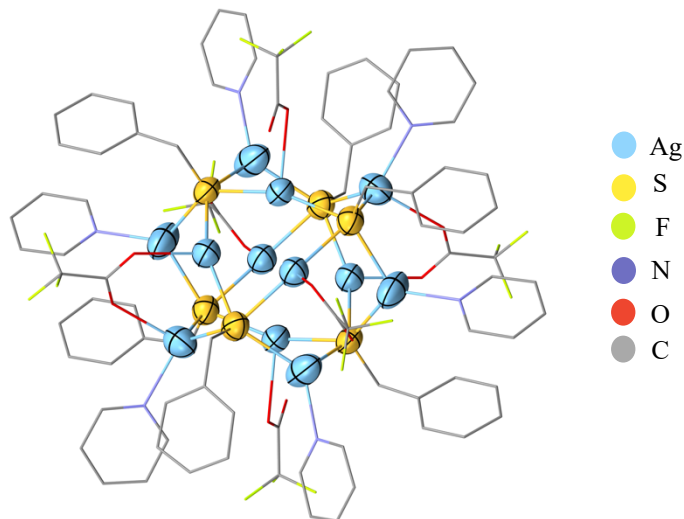


*Figure 1.3: Molecular structure of $[\text{Ag}_{12}(\text{SCH}_2\text{C}_6\text{H}_5)_6(\text{CF}_3\text{COO})_6(\text{pyridine})_6]$ (**I.III**) (H atoms are omitted for clarity).^[16]*

1.1.2 Group 11 Metal Chalcogenide Clusters (M_2E)

Group 11 metal chalcogenides exhibit a 2:1 ratio of M:E in the core with protective ligands bonded to the metal. Metal atoms in these clusters can have a linear, trigonal planar or tetrahedral geometry with μ_2 , μ_3

and μ_4 bridging chalcogenides. Metal atoms in the corners of the core are bonded to organic ligands and chalcogenides while the metal atoms in the center of the core can be solely bridged and stabilized by chalcogenides. These complexes can have different nuclearities and dimensionalities with a consistent core ratio of 2:1 between M:E.

These clusters are researched extensively due to their ability to exhibit high ionic and high electric conductivity in the solid state^{[2][3]} with luminescent properties which allow them to be potentially used in medicine, catalysis and OLEDs.^{[4][5][7][8]} The difference between the metal chalcogenide and the metal chalcogenolate clusters is that the core is composed of $M^{(I)}$ ($M = \text{Cu}, \text{Ag}$) and E^{2-} ($E = \text{S}, \text{Se}$) resulting in a $(M_2E)_x$ core with protective ligands at the periphery.^{[1]-[3][19]} These complexes are usually insoluble, and this results in a challenge to characterize them. One of the best and most used methods to characterize such clusters is through single crystal X - ray crystallography.^[20] An example of a stable copper chalcogenide cluster is $[\text{Cu}_{12}\text{S}_6(\text{dppo})_4]$ (**I.IV**) ($\text{dppo} = \text{dipheynlphosphinoctane}$) shown in *Figure 1.4 (a)*.^[18] This core is composed solely of $\text{Cu}^{(I)}$ and S^{2-} with a ratio of 2:1 with the phosphine ligands bonded to the copper atoms while the sulfide ligands adopt μ_4 coordination modes.^[18] The copper atoms in the corners have a trigonal planar geometry due to bonding to two S^{2-} and a single PR_3 ligand.^[18] The Cu atoms in the middle of the core are each stabilized by two S^{2-} resulting in a linear coordinated geometry. The short distances between the copper atoms indicate the presence of cuprophilic interactions.^[18]

$[\text{Cu}_{12}\text{Se}_6(\text{dppo})_4]$ (**I.V**) presents as a nice comparison to determine how a different chalcogen could affect the molecular structure of these complexes (*Figure 1.4 (b)*).^[21] Both of these clusters have a copper chalcogenide core with a ratio of 2:1 between Cu and E ($E = \text{S}, \text{Se}$). $[\text{Cu}_{12}\text{Se}_6(\text{dppo})_4]$ (**I.V**) is isostructural to $[\text{Cu}_{12}\text{S}_6(\text{dppo})_4]$ (**I.IV**) with slight geometric differences. Bond lengths for Cu-Se in (**I.V**) are 2.295 - 2.458 Å while the bond lengths for Cu-S in (**I.IV**) are 2.155 - 2.378 Å. The longer bond lengths in (**I.V**) are due to the larger covalent radii of Se (1.16 Å) compared to the covalent radii of S (1.03 Å).^[21] Comparing these two complexes, it can be seen that when using the same metal and organic ligand with a different chalcogenide, the resulting cluster can be similar in structure and size.^[21]

In terms of silver chalcogenide clusters, they are much more difficult to synthesize even with the presence of surface organic ligands as it can result in the formation of insoluble Ag_2E ($E = \text{S}, \text{Se}$).^[22] There are not many reports on silver chalcogenide clusters where the core is solely composed of $\text{Ag}^{(I)}$ and E^{2-} as most result in bulk Ag_2E but there have been many Ag clusters with both chalcogenide (E^{2-}) and chalcogenolate (RE^-) stabilizing ligands.^[23]

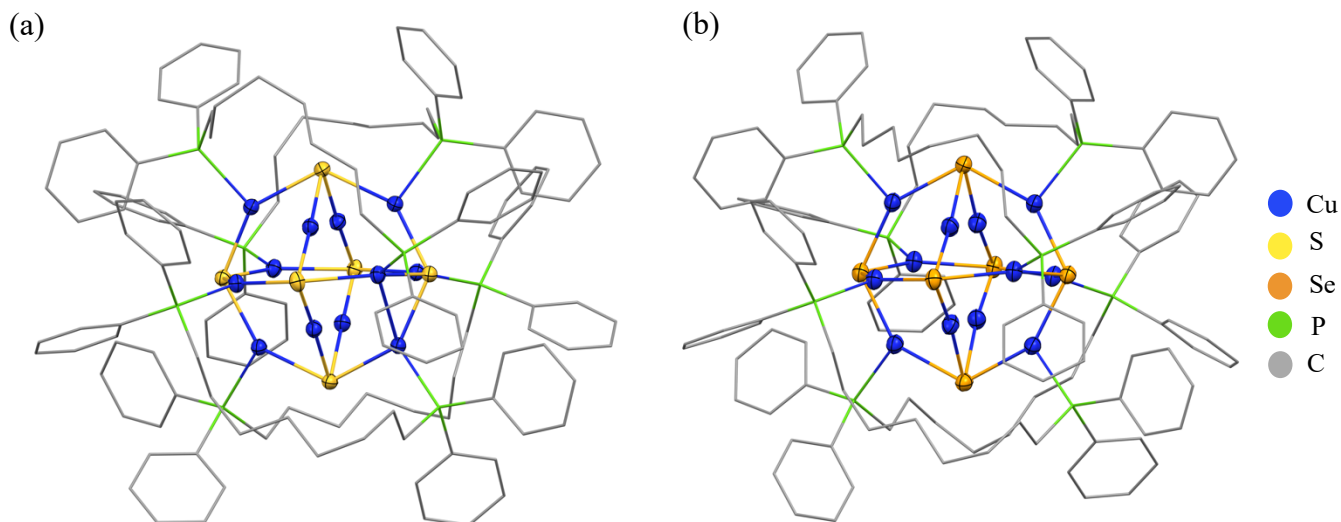


Figure 1.4: (a) Molecular structure of $[Cu_{12}S_6(dppo)_4]$ (**I.IV**) (*H atoms are omitted for clarity*)^[18] (b) Molecular structure of $[Cu_{12}Se_6(dppo)_4]$ (**I.V**) (*H atoms are omitted for clarity*).^[21]

One example of a stable silver chalcogenide complex that has a 2:1 ratio of Ag:S for the core is $[Ag_{188}S_{94}(PnPr_3)_{30}]$ (**I.VI**)^[24] reported by *Fenske and co-workers*. This cluster is unique as all the $Ag^{(I)}$ are stabilized by S^{2-} with the phosphine ligands present at the periphery.^[24] Most of the silver chalcogenide clusters are core-shell clusters where the inorganic core $(Ag_2S)_x$ is protected by a shell of silver thiolates and / or organic ligands.^[20] An example for such a core-shell cluster is the $[Ag_{58}S_{13}(SAd)_{32}]$ ($SAd = 1$ -adamantanethiolate) (**I.VII**) shown in *Figure 1.5*.^[19]

The centered icosahedral core is neutral and made of $(Ag_2S)_{13}$ while the shell is encapsulated by 32 $AgSAd$ moieties. The $Ag^{(I)}$ atoms in the core are stabilized by S^{2-} while the $Ag^{(I)}$ atoms in the shell are stabilized by the AdS^- ligands. The silver atoms exhibit various geometries (linear, trigonal planar and tetrahedral) and the sulfide has various coordination modes ($\mu_2 - \mu_7$).^[19] The cluster also has short distances between the silver atoms indicating the presence of argentophilic interactions.^{[17][19]}

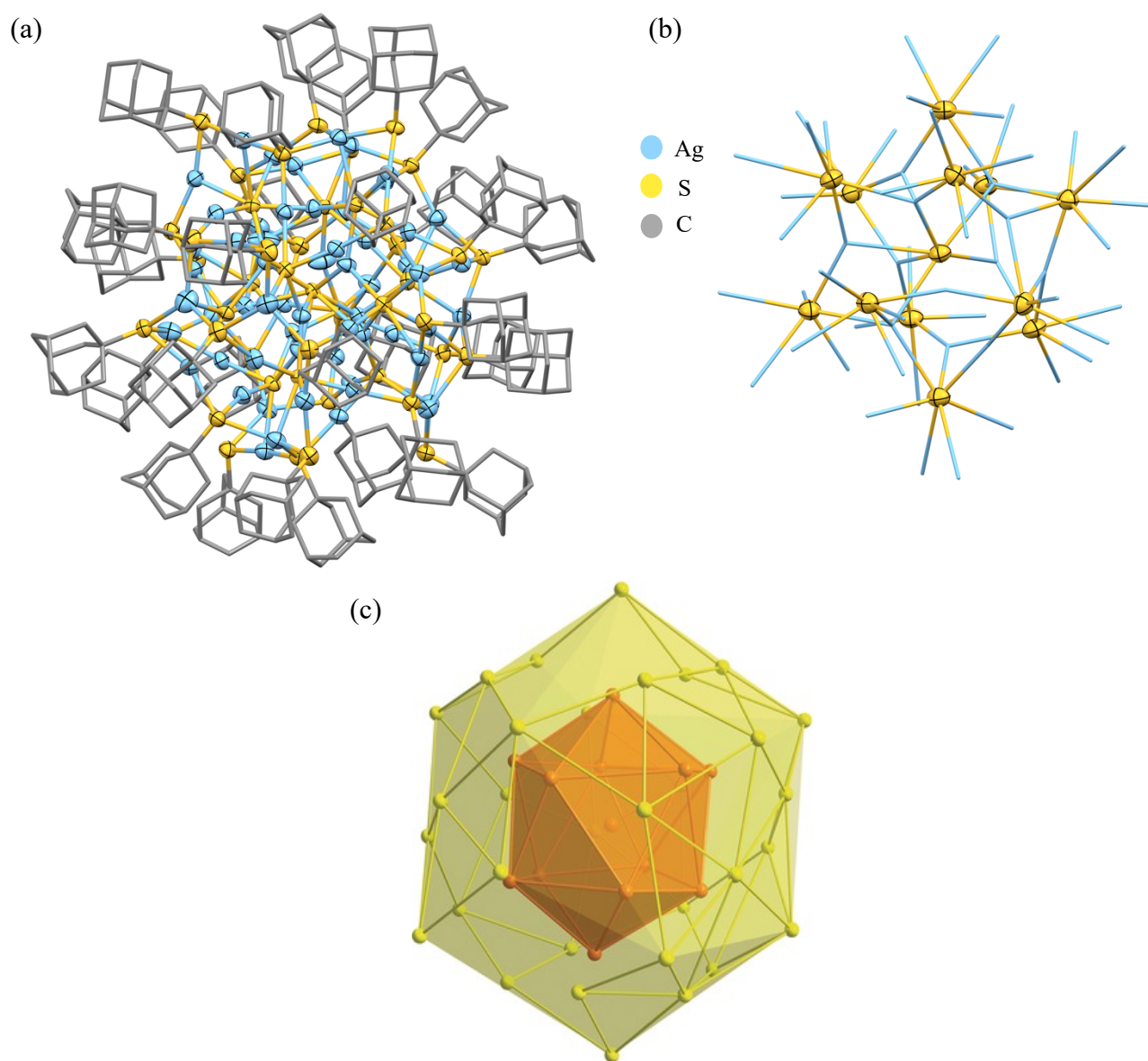
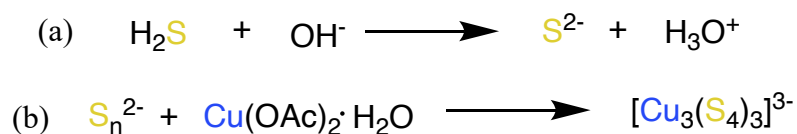


Figure 1.5: (a) Molecular structure of $[Ag_{58}S_{13}(SAd)_{32}]$ (I.VII) (H atoms are omitted for clarity) (b) $(Ag_2S)_{13}$ core (only sulfide atoms that form the core are shown for clarity) (c) S_{13} centered icosahedral core made of S^{2-} shown in orange and S_{32} shell of RS^I- shown in yellow (Lines between S centres are only shown for geometric arrangement) (figure adapted from S. Bestgen, X. Yang, I. Issac, O. Fuhr, P. W. Roesky, D. Fenske, *Chem. - A Eur. J.* **2016**, 22, 9933–9937. Copyright 2022 John Wiley and Sons).^[19]

1.2 Synthesis Methods for Group 11 Metal Chalcogen Clusters

There have been various ways to synthesize metal chalcogen clusters. One of the earliest and still heavily used ways is the use of H_2S .^[25] Hydrogen sulfide can be either used in a condensation reaction to displace metal oxides or it can be deprotonated by bubbling it through an aqueous base solution, resulting in sulfide

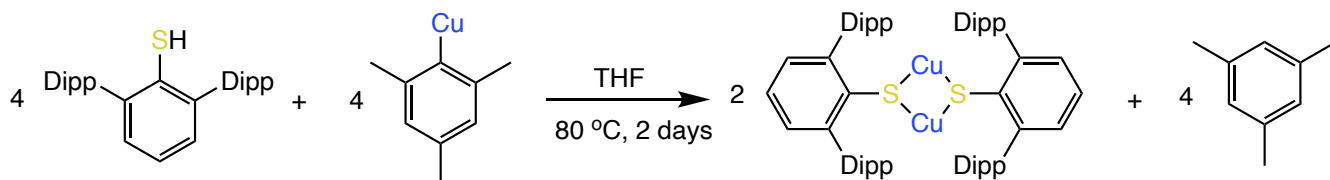
or polysulfide which can be then reacted with metal salts to result in metal sulfide complexes as shown in *Scheme 1.1*.^[25]



Scheme 1.1: Reaction scheme (a) Deprotonation of H₂S (b) Synthesis of a copper sulfide complex using deprotonated sulfide.^[25]

This method of synthesis is not as efficient when using H₂Se because it can lead to impure products.^[25] Both H₂S and H₂Se can be highly toxic and lethal thus, scientists have transitioned into finding safer ways to synthesize metal chalcogen clusters.^{[25][26]} Yam and co-workers reported the synthesis of [Cu₄(μ-dppm)₄(μ₄-S)](PF₆)₂ (dppm = diphenylphosphinomethane) (**I.VIII**) produced by reacting [Cu₂(μ-dppm)₂(CH₃CN)₂]²⁺ (**I.IX**) with Na₂S (3).^[27] They also reported several other copper chalcogenide and silver chalcogenide clusters by using Na₂S and Li₂Se as reagents.^[27]

Similar to the early synthesis method of using H₂S to synthesize metal chalcogenide complexes, free chalcogenol reagents (REH, E = S, Se, R = organic moiety) can be used to synthesize metal chalcogenolate clusters.^{[28]-[30]} These reactions proceed under mild conditions and result in products with high yield. An example of this cluster is the [CuSAr^{iPr4}]₂ (**I.X**) synthesized by reacting HSAr^{iPr4} (Ar^{iPr4} = -C₆H₃-2,6-(C₆H₃-2,6-iPr₂)₂) with mesitylcopper as shown in *Scheme 1.2*.^[31]



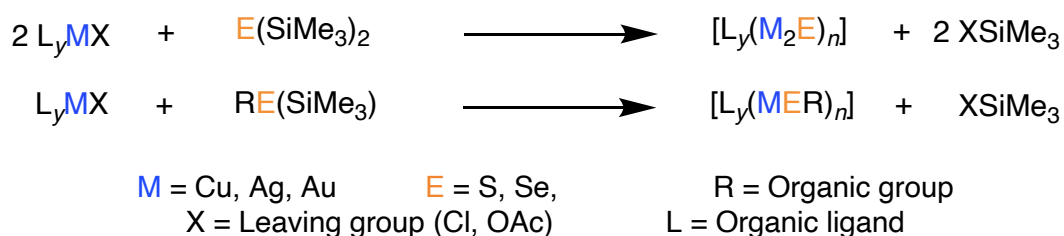
*Scheme 1.2: Reaction scheme for the synthesis of [CuSAr^{iPr4}]₂ (**I.X**) (Dipp = -C₆H₃-2,6-(C₆H₃-2,6-iPr₂)).^[31]*

This synthesis method is very convenient to produce metal chalcogenolate clusters but chalcogenols can be unstable and air sensitive (especially thiols and chalcogenols with smaller R groups). Another method used to synthesize metal chalcogenolate clusters is by using alkali metal analogues such as REA (A = alkali metal = Na, Li).^[32] The alkali metal analogues can provide selectivity and increased nucleophilic

reactivity due to the A-E bond.^[32] An example of a metal chalcogenolate complex produced through this synthesis method is $[\text{Cu}_3(\mu\text{-dppm})_3(\mu_3\text{-S}^t\text{Bu})_2]\text{BF}_4$ (**I.XI**) by *Yam and co-workers*.^[33]

1.2.1 Silylated Chalcogen Reagents for the Synthesis of Group 11 Metal Chalcogen Clusters

One of the most efficient ways to synthesize a metal chalcogen cluster today is by using trimethylsilylchalcogen reagents, $\text{E}(\text{SiMe}_3)_2$ and RESiMe_3 ($\text{E} = \text{S, Se, R} = \text{organic moiety}$).^{[3][34]} These are attractive reagents because they serve as soluble and easy to handle sources of chalcogens.^[35] These chalcogen reagents react readily with metal salts (MX_n) ($\text{X} = \text{leaving group}$) resulting in a M-E bond with the elimination of the silane (X-SiMe_3) as shown in *Scheme 1.3*.^{[1][2][34][36][37]}



Scheme 1.3: General reaction scheme for the synthesis of metal chalcogen clusters ($n = 1, 2, 3 \dots y = 1, 2, 3 \dots$) (Metal in the metal salts is also bonded to a ligand).^{[1][2][34][36][37]}

The reactivity of the metal salts (MX) with the trimethylsilyl chalcogen reagents can be controlled by changing the nature of X .^{[3][34][37]} The thermodynamic formation of the X-SiMe_3 drives the reaction forward which depends on the bond strength of the Si-X bond.^{[1][2][36]} The silyl reagents are also soluble in common organic solvents at low temperatures which allow for a controlled synthesis of the desired cluster while reducing the formation of the thermodynamically driven binary M_2E .^{[1]-[3][36]} The silane product is soluble in solvents and does not hinder the crystallization of the desired metal chalcogen cluster.^[38] Some metal chalcogenide clusters produced by this method of synthesis include $[\text{Cu}_{12}\text{S}_6(\text{dppo})_4]$ (**I.IV**) ($\text{dppo} = \text{diphenylphosphinoctane}$)^[18] (*Figure 1.4 (a)*), $[\text{Cu}_{26}\text{Se}_{13}(\text{PEt}_2\text{Ph})_{14}]$ (**I.XII**)^[39] and $[\text{Ag}_{188}\text{S}_{94}(\text{PnPr}_3)_{30}]$ (**I.VI**)^[24] reported by *Fenske et al.* Examples of the metal chalcogenolate clusters synthesized by using trimethylsilyl chalcogen reagents include $[\text{Cu}_2(\text{S-C}_6\text{H}_4\text{-OMe})_2(\text{dpppt})_2]$ (**I.I**) ($\text{dpppt} = \text{diphenylphosphinopentane}$)^[9] (shown in *Figure 1.1*), $[\text{Cu}_2(\text{SePh})_2(\text{dpppt})_2]$ (**I.XIII**)^[9] (*Figure 1.6*), $[\text{Ag}_7(\text{SPh})_7(\text{dppm})_3]$ (**I.XIV**) ($\text{dppm} = \text{diphenylphosphinomethane}$)^[2] and $[\text{Ag}_4(\text{SeiPr})_4(\text{dppm})_2]$ (**I.XV**).^[2]

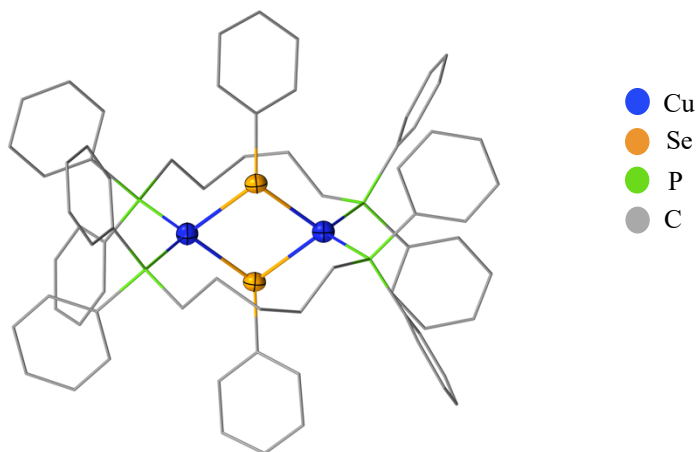
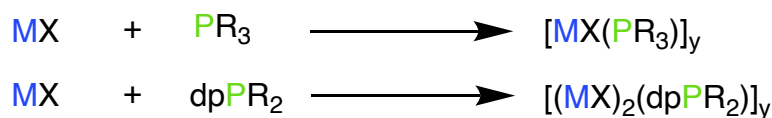


Figure 1.6: Molecular structure of $[Cu_2(SePh)_2(dpppt)_2]$ (**I.XIII**) (H atoms are omitted for clarity).^[9]

1.3 Phosphine Stabilized Group 11 Metal Chalcogen Clusters

Metal chalcogen clusters have a tendency to form the thermodynamic stable binary phases (M_2E) .^{[1]-[3][36]} Protective ligands are used to prevent their decomposition and stabilize the kinetic product of interest.^{[1]-[3][36]} One of the most common ligands used are monodentate / bidentate phosphines.^{[1][3][36]} Some examples of metal chalcogen clusters with phosphine ligands are $[Cu_{146}Se_{73}(PPh_3)_{30}]$ (**I.XVI**)^[40], $[Ag_{188}S_{94}(PnPr_3)_{20}]$ (**I.VI**)^[24], $[Cu_2(SePh)_2(PPh_3)_3]$ (**I.XVII**)^[2] and $[Ag_7(SPh)_7dppm]$ (**I.XIV**)^[2] reported by *Fenske et al.* In terms of metal chalcogenolate clusters, the organic moiety bonded to the chalcogen provides kinetic stability, but the incorporation of phosphine ligands can be used to change the structural and electronic properties of these clusters to control properties such as luminescence.

The synthesis of the cluster depends on the thermodynamic driving force of the Si-X bond and also more importantly, it also depends on the phosphine ligand used.^{[2][3][37][39]} The sterics of the phosphine play a big role in stabilizing as well as the size and the shape of the metal chalcogenide core.^{[1]-[3][34]} The very first step in synthesizing a phosphine stabilized metal chalcogen cluster is to form the reactive species using the phosphine to solubilize the metal salt as shown in *Scheme 1.4*.^{[1][3][39]} Once the phosphine stabilized metal salt complex is synthesized, it serves as an excellent entry point for the insertion of the chalcogen by using trimethylsilylchalcogen reagents as shown in *Scheme 1.3*.^{[1]-[3]} This results in polynuclear metal chalcogen complexes which can have luminescent properties in the solid state.^{[2][37]} These polynuclear complexes have the potential to be used in organic light emitting diodes (OLEDs) due to their high rigidity which results in high photostability and quantum yields of emission.^[18]



M = Cu, Ag, Au dpP = diphenylphosphine R = Organic group X = Leaving group (Cl, OAc)

Scheme 1.4: General reaction scheme for the synthesis of phosphine stabilized metal complexes (x = 1,2,3... y = 1,2,3...).^{[1][3][39]}

1.4 Luminescence, Photoluminescence: Fluorescence, Phosphorescence, Thermally Activated Delayed Fluorescence and Photoluminescence Quantum Yields

The definition of luminescence is “a spontaneous emission of radiation from an electronically excited species (or from a vibrationally excited species) not in thermal equilibrium with its environment”.^[41] There are different types of luminescence and each one depends on a different type of excitation (for example: chemiluminescence, electroluminescence, bioluminescence). Photoluminescence is the emission of light and is described as “the direct photoexcitation of the emitting species”.^[41] Photoluminescence arises from the absorption of photons (the wavelength is inversely proportional to the energy difference between the ground and the excited state of the electron) that can lead to the excitation of an electron; the molecule then emits light as it returns to its ground state.^[42] The absorption of photons results in LMCT (ligand to metal charge transfer, where the ligand is the donor and the metal is the acceptor) or MLCT (metal to ligand charge transfer, where the metal is the donor and the ligand is the acceptor). Charge transfer can occur between ligands and metal centres where one of them is an electron donor (Lewis base) and the other is an electron acceptor (Lewis acid). The absorption of light results in an electron transition from the donor to the acceptor.^[43] These transitions have high molar absorptivity values and can often be observed in the visible region.^[43]

Two principal types of photoluminescence exist: fluorescence and phosphorescence.^[44] One of the main differences between the two types is the time it takes for the electron to return to its ground state.^[45] For fluorescence, the emission of light can last from picoseconds to nanoseconds whereas in phosphorescence, the emission can last for microseconds or longer.^[41] Phosphorescence is longer lived because of the spin forbidden transition resulting in a different spin state multiplicity due to inter system crossing^[42] as shown in *Figure 1.7*.

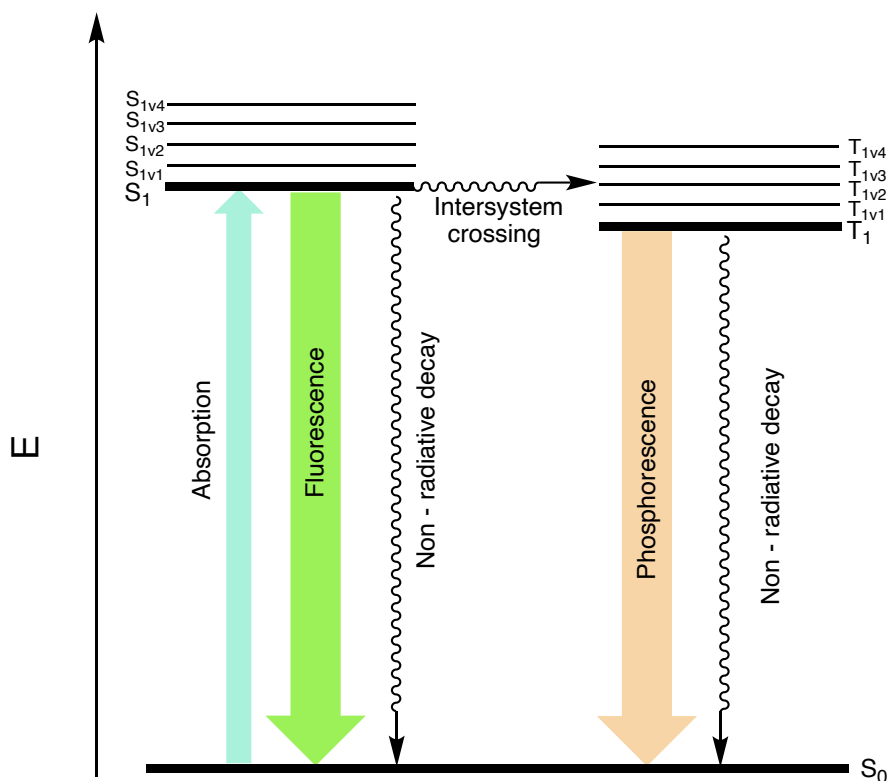


Figure 1.7: Simplified version of emission from the singlet state showing fluorescence and triplet state showing phosphorescence (figure adapted from literature).^[41]

Intersystem crossing ($S_1 \rightarrow T_1$) is a spin forbidden process because of the lack of effective spin orbit coupling (SOC - arises from the electron repulsion effect)^[46] and thus, the rate for phosphorescence is slower. Transition metal complexes have a central metal that has significant spin orbit coupling and results in efficient intersystem crossing and phosphorescence.^[47] The process of intersystem crossing makes photoluminescent transition metal complexes suitable candidates for organic light emitting diodes (OLEDs) through mechanisms such as thermally activated delayed fluorescence (TADF) and phosphorescence (PH).^{[47][48]}

TADF involves using thermal energy to undergo reverse intersystem crossing to re-populate S_1 (due to the small $\Delta E(S_1-T_1)$ gap), so that there is efficient light emission from the singlet state giving rise to adequate photoluminescence quantum yields (PLQYs) as shown in Figure 1.8.^[47] Whereas PH arises from intersystem crossing and has efficient light emission from the triplet state with high PLQYs.^[48] PLQYs are calculated by using the ratio between the number of photons emitted (N_{em}) to the number of photons absorbed (N_{abs}). Therefore, this calculation gives a measurement of photoluminescence efficiency whether it be by fluorescence or phosphorescence pathways.^[49]

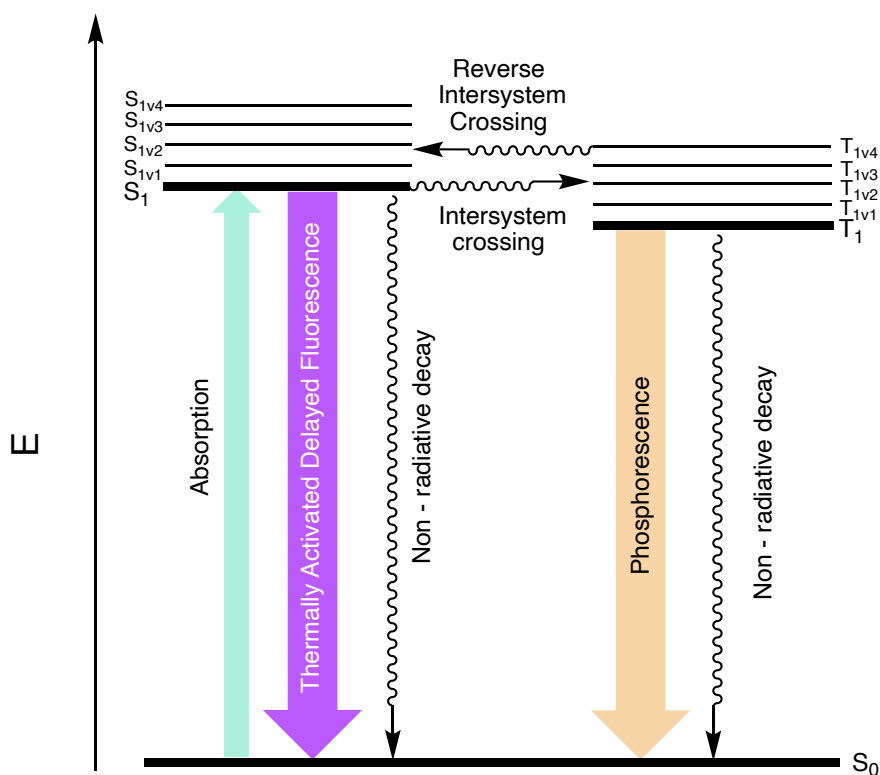


Figure 1.8: Simplified version of emission shown as thermally activated delayed fluorescence (TADF) and phosphorescence (figure adapted from literature).^{[41][47]}

When incorporating emissive compounds in light emitting materials such as OLEDs, the theoretical efficiency of fluorescence is only 25 % whereas the maximum theoretical efficiency of phosphorescence and TADF is 100 %.^[47] When electrons are excited, they have four different exciton states (one singlet and three triplets due to statistics and degeneracy).^[47] Singlet states populate the S_1 while triplet states populate the T_1 . Therefore, 25 % of the emission takes place from S_1 via fluorescence and 75 % takes place from T_1 by phosphorescence.^[47] With the process of SOC, theoretically all of the excitons from the S_1 state can be transferred into the T_1 state, resulting in a 100 % emission efficiency from the triplet state (phosphorescence). Similar to phosphorescence, the fast process of reverse intersystem crossing can result in a 100 % transfer of excitons from $T_1 \rightarrow S_1$ resulting in a maximum 100 % efficiency via TADF.^[47]

1.5 Luminescent Group 11 Metal Chalcogen Complexes incorporating Phosphine Ligands

In 1993, Yam and co-workers reported the first phosphine stabilized luminescent copper sulfide and silver sulfide complexes: $[\text{Cu}_4(\mu\text{-dppm})_4(\mu_4\text{-S})](\text{PF}_6)_2$ (I.VIII) and $[\text{Ag}_4(\mu\text{-dppm})_4(\mu_4\text{-S})](\text{PF}_6)_2$ (I.XVIII).^[20] The photophysical and photochemical properties of the $M^{(I)}$ tetramers were investigated and it was concluded that the long-lived excited state was due to the ligand to metal charge transfer process LMCT ($E^{2-} \rightarrow M_4$) ($E = \text{S}, M = \text{Cu}$) with some mixing of sd and pd orbitals of the metals.^[27] Since then, there has

been a significant amount of research that has been conducted in phosphine stabilized luminescent metal chalcogen clusters. Recently, *Eichhöfer* and *co-workers* have examined the use of σ donating phosphine ligands in stabilizing copper (I) chalcogenide clusters and how these affect the photophysical properties. Various copper chalcogenide clusters were synthesized where some had different phosphine ligands but the same core structure while others had the same phosphine ligand but different core structures.^[21] General structures of these clusters are shown in *Figure 1.9*.

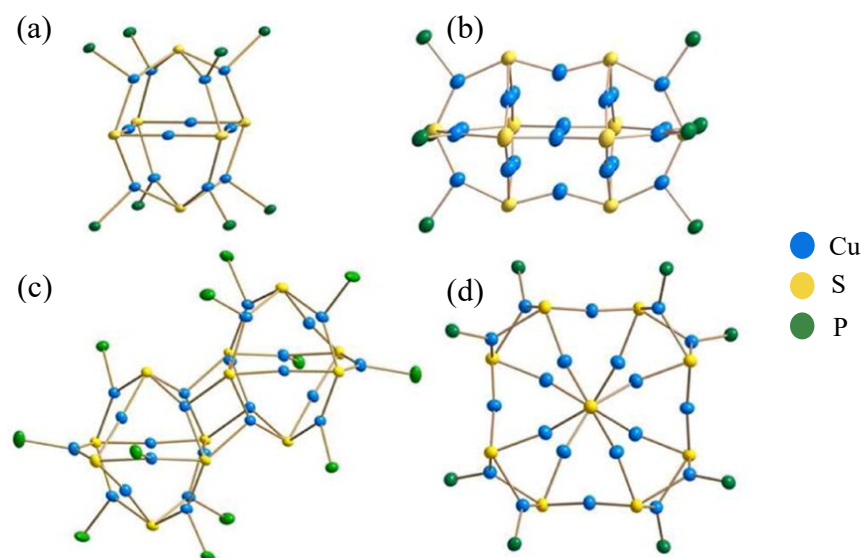


*Figure 1.9: General core structures of copper (I) sulfide clusters with phosphine ligands (a) $[Cu_{12}S_6(dpppt)_4]$ (I.XIX) (b) $[Cu_{20}S_{10}(PPh_3)_8]$ (I.XX) (c) $[Cu_{24}S_{12}(PEt_3Ph)_{12}]$ (I.XXI) (d) $[Cu_{20}S_{10}(P^tBu_3)_8]$ (I.XXII) (C and H atoms are omitted for clarity) (adapted with permission from A. Eichhöfer, G. Buth, S. Lebedkin, M. Kühn, F. Weigend, *Inorg. Chem.* **2015**, 54, 9413–9422. Copyright 2022 American Chemical Society).^[21]*

Bright red phosphorescent emission was observed at ambient temperature for complexes containing $Cu_{12}E_6P_8$ (E = S, Se) cores. These complexes showed high PLQYs between 21 % - 63 %.^[21] Through these observations, it was noted that the type of phosphine ligand as well as, surprisingly the crystal packing (triclinic vs. tetragonal) can affect the PLQYs. It was reported that all transitions below 495 nm involved electron donation from the cluster core to the phosphine ligand.^[21] The phosphine ligands used all had phenyl rings and thus low lying empty π^* orbitals; the complexes displayed electron transitions from the orbitals of the copper chalcogenide core to these ligand - based orbitals.^[21] Clusters that had phosphine ligands devoid of aromatic rings had transitions exclusively within the copper chalcogenide core. In these cases, electronic transitions involved HOMOs, HOMO - 1, HOMO - 2 (mostly comprising of d(Cu) and p(S) orbitals) and LUMOs (mostly comprising of Cu orbitals). For some complexes,

decreasing temperature resulted in increased intensity of emission while other complexes showed decreased intensity.^[21]

For luminescent metal chalcogenolates, one example is $[\text{Cu}_2(\mu\text{-S-C}_6\text{H}_4\text{-OMe})_2(\text{dpppt})_2]$ (**I.I**) (Figure 1.10) that displays solid state emission at room temperature ($\lambda_{\text{em}} = 465 \text{ nm}$).^[9] Another example of a luminescent copper chalcogenolate complex is $[\text{Cu}_{13}(\text{SePh})_{13}(\text{PPh}_3)_4]$ (**I.XXIII**) reported by Zhu and co-workers which exhibits red luminescence with $\lambda_{\text{em}} = 727 \text{ nm}$ in the solid state. This cluster does not display high emission intensity at room temperature but decreasing the temperature to 80 K increases the efficiency by 4-fold while also resulting in a hypsochromic shift ($\lambda_{\text{em}} = 680 \text{ nm}$).^[50] Both (**I.I**) and (**I.XXIII**) exhibit LMCT where the HOMO is localized over the copper chalcogenolate core and the LUMO is localized over the phosphine ligands.

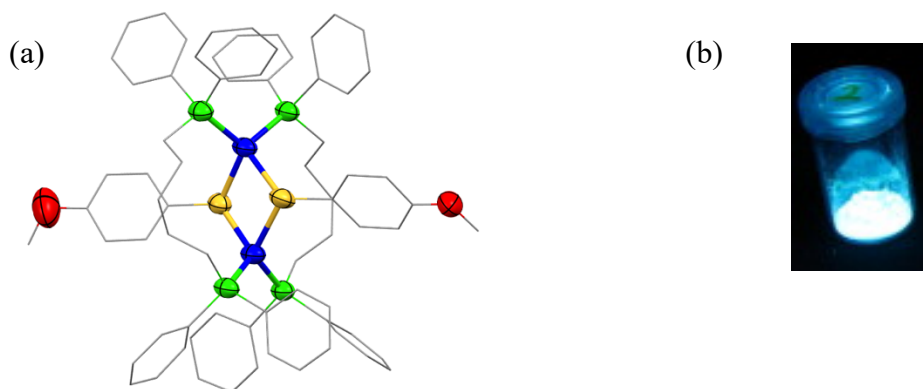


Figure 1.10: (a) Molecular structure of $[\text{Cu}_2(\text{S-C}_6\text{H}_4\text{-OMe})_2(\text{dpppt})_2]$ (**I.I**) (H atoms are omitted for clarity) (b) Emission of $[\text{Cu}_2(\text{S-C}_6\text{H}_4\text{-OMe})_2(\text{dpppt})_2]$ (**I.I**) (adapted from B. Hu, C. Y. Su, D. Fenske, O. Fuhr, *Inorg. Chim. Acta* **2014**, 419, 118–123. Copyright 2022 Elsevier).^[9]

Silver chalcogenolate clusters also have potential to be used as photofunctional materials but a major obstacle with using these compounds is that they are unstable and have poor luminescence at room temperature.^[51] One example of a luminescent silver chalcogenolate cluster is $[\text{Ag}_{14}(\text{SC}_6\text{H}_3\text{F}_2)_{12}(\text{PPh}_3)_8]$ (**I.XXIV**). This cluster has an Ag_6^{4+} core that is enclosed by a cube of $[\text{Ag}^+(\text{SC}_6\text{H}_3\text{F}_2)_3\text{PPh}_3]$ which share one corner ($\text{SC}_6\text{H}_3\text{F}_2$)⁻ between them. It is important to note that the central Ag atoms have the oxidation state $\text{Ag}^{(I)}/\text{Ag}^0$ which result in an octahedral Ag_6^{4+} core which is very rare in thiolate protected Ag clusters. Another feature of this cluster is that all the thiolates adopt a μ_3 coordination and bond to three Ag atoms. The transitions inside the cluster results in yellow luminescence at room temperature.^[52] Compound (**I.XXIV**) emits yellow in solid state and in solution as shown in Figure 1.11 and has $\lambda_{\text{em}} = 536 \text{ nm}$. While

it displays emission at RT, the photoluminescence quantum yield is only 0.1 %. It is also unstable in solution for long periods of time and loses luminescence in the presence of oxygen or light.^[52]

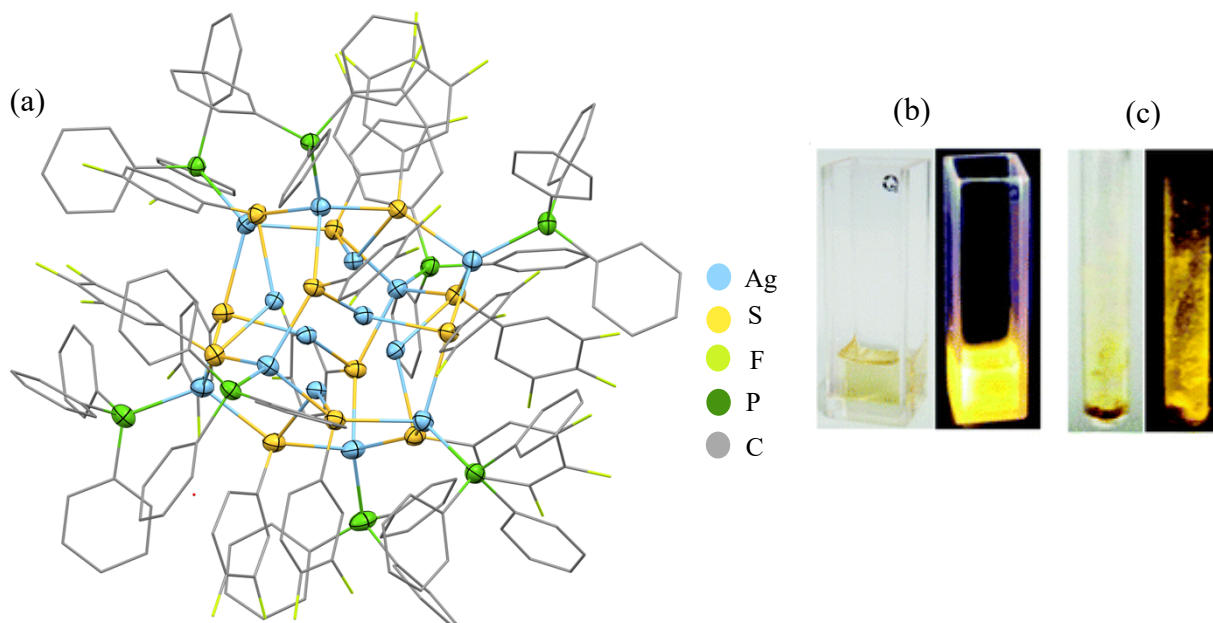


Figure 1.11: (a) Molecular structure of $[Ag_{14}(SC_6H_3F_2)_{12}(PPh_3)_8]$ (**I.XXIV**) (*H atoms are omitted for clarity*) (b) Emission of $[Ag_{14}(SC_6H_3F_2)_{12}(PPh_3)_8]$ (**I.XXIV**) in DCM (c) Emission of $[Ag_{14}(SC_6H_3F_2)_{12}(PPh_3)_8]$ (**I.XXIV**) in the solid state (adapted with permission from H. Yang, J. Lei, B. Wu, Y. Wang, M. Zhou, A. Xia, L. Zheng, N. Zheng, *Chem. Commun.* **2013**, 49, 300–302. Copyright 2022 Royal Society of Chemistry).^[52]

1.6 A Better Phosphine Ligand: 4,6 - bis(diphenylphosphino)dibenzofuran (DBFDP)

Copper (I) iodide clusters have yet to be incorporated as OLEDs due to their general poor processability and weak electroactivity. However, in a recent article the use of 4,6 - bis(diphenylphosphino)dibenzofuran (DBFDP) has shown to promote strong luminescence behaviour in stable copper (I) iodide clusters.^[53] The use of this ligand resulted in improved solution processability and electroactivity of the clusters compared to mononuclear / dinuclear copper complexes and other copper iodide clusters (for example: TTPPCuI (**I.XXV**) (TTPP = 2,2' - (phenylphosphinediyl)bis(2,1 - phenylene)bis(diphenylphosphine) (*Figure 1.12*))^{[53][54]} as well as dual emission characteristics. Dual emission here is described as two MLCT excited states existing together caused by a specific substitution pattern on the bridging phosphine ligand.^[55]

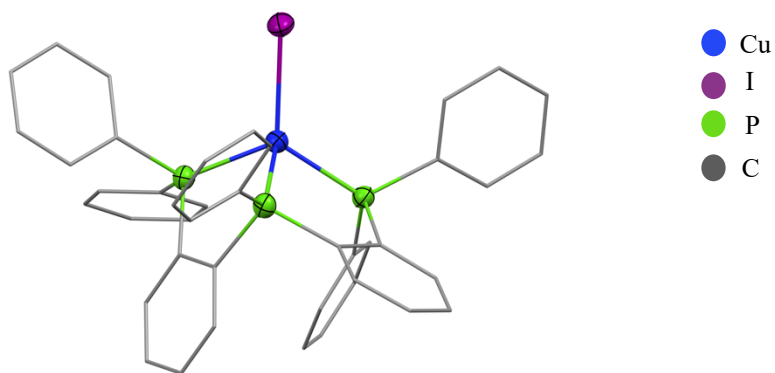


Figure 1.12: Molecular structure of $[\text{CuITTPP}]$ (**I.XXV**) (*H atoms are omitted for clarity*).^[54]

The emission decay of $[\text{Cu}_4(\mu_3\text{-I})_4(\mu_2\text{-dbfdp})_2]$ (**I.XXVI**) is temperature dependent as the lifetime of TADF decreases as the temperature increases (milliseconds to microseconds). The fraction curves of PH and TADF also show a strong temperature dependent relationship due to dual emissive character. As shown in Figure 1.13, (**I.XXVI**) shows strong temperature dependent luminescence as TADF increases as temperature increases while PH increases as temperature decreases. Interestingly, (**I.XXVI**) shows dual emissive behaviour (TADF and PH) at room temperature as the ratio between TADF and PH at room temperature is 1:1.

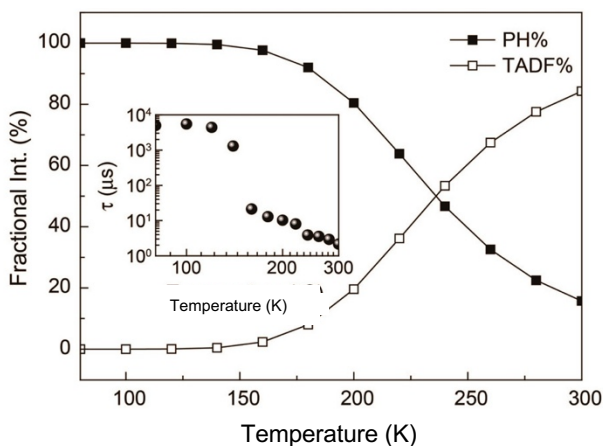


Figure 1.13: Temperature dependent TADF and PH emission of $[(\text{Cu}_4\text{I}_4)(\text{dbfdp})_2]$ (**I.XXVI**) with lifetime decays (figure adapted from M. Xie, C. Han, J. Zhang, G. Xie, H. Xu, *Chem. Mater.* **2017**, 29, 6606–6610. Copyright 2022 American Chemical Society).^[53]

DBFDP was selected while keeping two ideas in mind^[53]:

- 1) The distance between the two P atoms
- 2) The rigidity promoted by the phosphine ligand

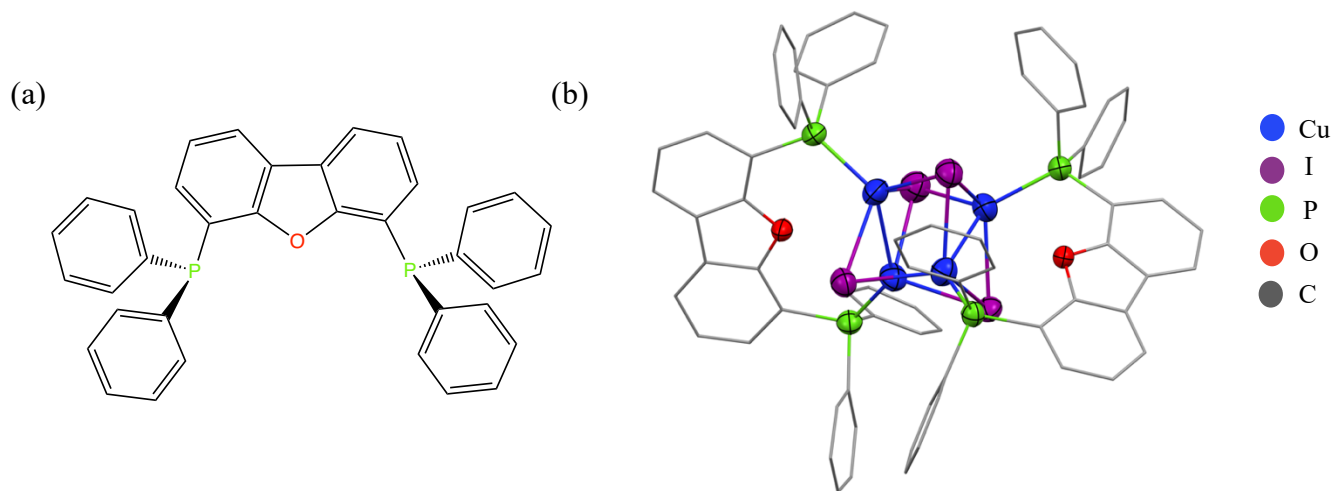


Figure 1.14: (a) 4,6 - bis(diphenylphosphino)dibenzofuran (DBFDP) (b) Molecular structure of $[(\text{Cu}_4\text{I}_4)(\text{dbfdp})_2]$ (**I.XXVI**) in the crystal (H atoms are omitted for clarity).^[53]

The distance between the two P atoms gives this ligand the ability to bridge two metal centres. Moreover, the energy gap between the HOMO and the LUMO is large and that results in a high - energy - gap chromophore.^[53] The two properties of this ligand allow it to be able to coordinate with CuI to result in the desired Cu_4I_4 cluster with a PLQY of $\sim 5\%$.^[53] Density functional theory (DFT) calculations of (**I.XXVI**) show the HOMO and the LUMO in the ground state. The HOMO of this complex is located on the Cu_4I_4 unit while the LUMO mainly consists of the dibenzofuran group and phosphorus coordination sites as shown in *Figure 1.15* which results in (M+X)LCT (metal + halide to ligand charge transfer).

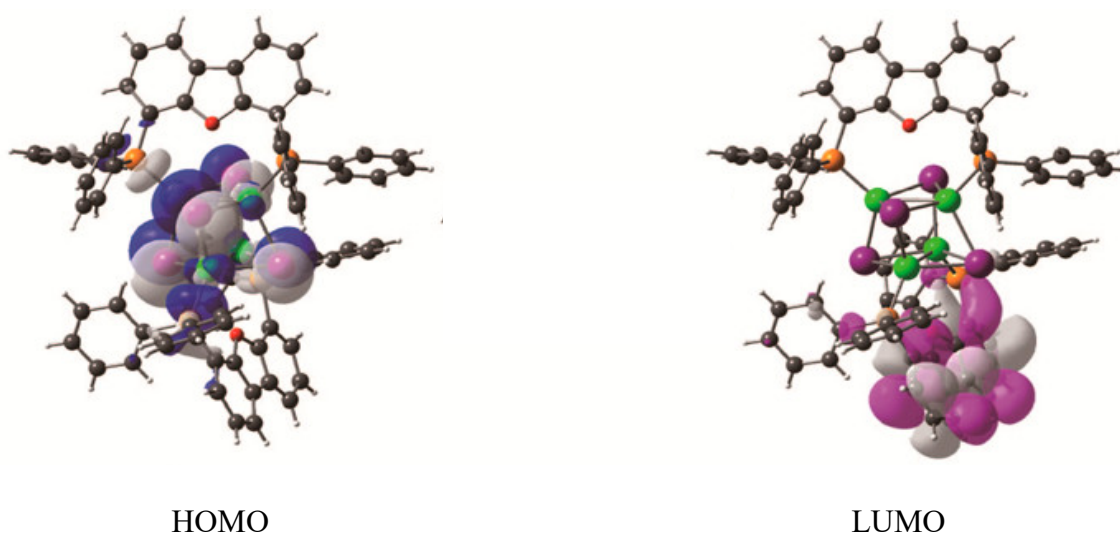


Figure 1.15: DFT Calculations for $[(\text{Cu}_4\text{I}_4)(\text{dbfdp})_2]$ (**I.XXVI**) (figure adapted from M. Xie, C. Han, J. Zhang, G. Xie, H. Xu, *Chem. Mater.* **2017**, *29*, 6606–6610. Copyright 2022 American Chemical Society).^[53]

1.7 Scope of Thesis

This thesis focuses on incorporating the 4,6 - *bis*(diphenylphosphino)dibenzofuran (DBFDP) and related ligands in group 11 metal chalcogen clusters to examine how these phosphine ligands affect the structural, electronic and photophysical properties of these complexes. Chapter 2 focuses on incorporating the bidentate DFBDP ligand in group 11 metal chalcogenolate clusters with an analysis of their molecular, electronic and luminescent properties. It also discusses how the nature of the chalcogen, and the group 11 metal can be used to change the structural and photophysical properties. Chapter 3 focuses on synthesizing a custom DBFDP ligand which is incorporated in copper chalcogenide clusters to determine how this ligand effects the molecular and photophysical properties. Chapter 4 summarizes the results from Chapter 2 and 3 and suggests future directions for projects involving the DBFDP ligands.

1.8 References

- [1] S. Dehnen, A. Eichhöfer, J. F. Corrigan, D. Fenske, 2004 Synthesis and characterization of Ib–VI nanoclusters. In *Nanoparticles* (ed. G. Schmid), pp. 107–185. Weinheim, Germany: Wiley-VCH.
- [2] O. Fuhr, S. Dehnen, D. Fenske, *Chem. Soc. Rev.* **2013**, *42*, 1871–1906.
- [3] S. Dehnen, A. Eichhöfer, D. Fenske, *Eur. J. Inorg. Chem.* **2002**, *2002*, 279.
- [4] V. W. W. Yam, *Pure Appl. Chem.* **2001**, *73*, 543–548.
- [5] V. W. W. Yam, E. C. C. Cheng, N. Zhu, *Angew. Chem. - Int. Ed.*, **2001**, 1763–1765.
- [6] V. W. W. Yam, K. K. W. Lo, W. Kit-Mai Fung, C.-R. Wang, *Coord. Chem. Rev.* **1998**, *171*, 17–41.
- [7] V. W. W. Yam, K. K. W. Lo, *Chem. Soc. Rev.* **1999**, *28*, 323–334.
- [8] R. S. Laitinen, R. Oilunkaniemi, *Selenium Tellurium Reagents Chem. Mater. Sci.* **2019**, V–VI.
- [9] B. Hu, C. Y. Su, D. Fenske, O. Fuhr, *Inorg. Chim. Acta* **2014**, *419*, 118–123.
- [10] O. Veselska, A. Demessence, *Coord. Chem. Rev.* **2018**, *355*, 240–270.
- [11] R. Langer, M. Yadav, B. Weinert, D. Fenske, O. Fuhr, *Eur. J. Inorg. Chem.* **2013**, 3623–3631.
- [12] N. V. S. Harisomayajula, S. Makovetskyi, Y. C. Tsai, *Chem. - A Eur. J.* **2019**, *25*, 8936–8954.
- [13] J. Wang, Y. L. Li, Z. Y. Wang, S. Q. Zang, *Cryst. Eng. Comm.* **2019**, *21*, 2264–2267.
- [14] Y. M. Wang, J. W. Zhang, Q. Y. Wang, H. Y. Li, X. Y. Dong, S. Wang, S. Q. Zang, *Chem. Commun.* **2019**, *55*, 14677–14680.
- [15] Y. H. Li, Z. Y. Wang, B. Ma, H. Xu, S. Q. Zang, T. C. W. Mak, *Nanoscale* **2020**, *12*, 10944–10948.
- [16] Y. L. Li, W. M. Zhang, J. Wang, Y. Tian, Z. Y. Wang, C. X. Du, S. Q. Zang, T. C. W. Mak, *Dalton Trans.* **2018**, *47*, 14884–14888.
- [17] H. Schmidbaur, A. Schier, *Angew. Chem. - Int. Ed.* **2015**, *54*, 746–784.
- [18] X. X. Yang, I. Issac, S. Lebedkin, M. Kühn, F. Weigend, D. Fenske, O. Fuhr, A. Eichhöfer, *Chem. Commun.* **2014**, *50*, 11043–11045.
- [19] S. Bestgen, X. Yang, I. Issac, O. Fuhr, P. W. Roesky, D. Fenske, *Chem. - A Eur. J.* **2016**, *22*, 9933–9937.
- [20] S. Bestgen, O. Fuhr, B. Breitung, V. S. Kiran Chakravadhanula, G. Guthausen, F. Hennrich, W. Yu, M. M. Kappes, P. W. Roesky, D. Fenske, *Chem. Sci.* **2017**, *8*, 2235–2240.
- [21] A. Eichhöfer, G. Buth, S. Lebedkin, M. Kühn, F. Weigend, *Inorg. Chem.* **2015**, *54*, 9413–9422.
- [22] D. Fenske, N. Zhu, T. Langtepe, *Angew. Chem. - Int. Ed.* **1998**, *37*, 2639–2644.
- [23] Y. P. Xie, J. L. Jin, G. X. Duan, X. Lu, T. C. W. Mak, *Coord. Chem. Rev.* **2017**, *331*, 54–72.

- [24] X. J. Wang, T. Langetepe, C. Persau, B.-S. Kang, G. M. Sheldrick, D. Fenske, D. Fenske, X. Wang, T. Langetepe, C. Persau, B. Kang, G. M. Sheldrick, *Angew. Chem. - Int. Ed.*, **2002**, *41*, 3818–3822.
- [25] L. C. Roof, J. W. Kolis, *Chem. Rev.* **1993**, *93*, 1037–1080.
- [26] M. S. Legator, D. L. Morris, D. L. Philips, C. R. Singleton, *Arch. Environ. Health* **2001**, *56*, 123–131.
- [27] V. W. W. Yam, K. K. W. Lo, *Comments Inorg. Chem.* **1997**, *19*, 209–229.
- [28] V. P. Ananikov, N. V Orlov, I. P. Beletskaya, *Organometallics* **2007**, *26*, *3*, 740–750.
- [29] A. L. Seligson, J. Arnold, *J. Am. Chem. Soc.*, **1993**, *115*, 8214–8220.
- [30] M. Bochmann, A. P. Coleman, K. J. Webb, M. B. Hursthouse, M. Mazid, *Angew. Chem. - Int. Ed. Eng.* **1991**, *30*, 973–975.
- [31] W. Zou, Q. Zhu, J. C. Fettinger, P. P. Power, *Inorg. Chem.* **2021**, *60*, 17641–17648.
- [32] D. Liotta, U. Sunay, H. Santiesteban, W. Markiewicz, *J. Org. React* **1977**, 187.
- [33] V. V. W. Yam, C. H. Lo, W. K. Fung, K. K. Cheung, *Inorg. Chem.* **2001**, *40*, 3435–3442.
- [34] M. W. DeGroot, J. F. Corrigan, *Organometallics* **2005**, *24*, 3378–3385.
- [35] M. W. Degroot, J. F. Corrigan, *Dalton Trans.* **2000**, 1235–1236.
- [36] D. G. MacDonald, J. F. Corrigan, *Philos. Trans. R. Soc. A Math. Phys. Eng. Sci.* **2010**, *368*, 1455–1472.
- [37] T. Duan, X. Z. Zhang, Q. F. Zhang, *Zeitschrift fur Naturforsch. - Sect. B J. Chem. Sci.* **2008**, *63*, 941–944.
- [38] M. W. DeGroot, J. F. Corrigan, *Zeitschrift fur Anorg. und Allg. Chemie* **2006**, *632*, 19–29.
- [39] A. Deveson, S. Dehnen, D. Fenske, *Dalton Trans.* **1997**, 4491–4497.
- [40] H. Krautscheid, D. Fenske, G. Baum, M. Semmelmann, *Angew. Chem. - Int. Ed. Eng.* **1993**, *32*, 1303–1305.
- [41] B. Valeur, M. N. Berberan-Santos, *J. Chem. Educ.* **2011**, *88*, 731–738.
- [42] C. A. Munson, J. L. Gottfried, F. C. De Lucia, K. L. Mcnesby, A. W. Miziolek, Army Research Laboratory-ARL-TR-4279: Laser-Based Detection Methods for Explosives, **2007**.
- [43] G. G. Moraga, **1993**, Concepts in Modern Chemistry. In Cluster Chemistry (e.d. G.G. Moraga), pp. 1–53. Berlin, Heidelberg: Springer Berlin Heidelberg.
- [44] A. S. Review, *Rev. Boliv. Química* **2018**, *35*, 108–116.
- [45] A. L. Powell, *J. Chem. Educ.* **1947**, *24*, 423–428.
- [46] N. S. Hosmane, *Adv. Inorg. Chem.* **2017**, 3–13.
- [47] L. P. Ravaro, K. P. S. Zanoni, A. S. S. de Camargo, *Energy Reports* **2020**, *6*, 37–45.

- [48] T. Takahashi, S. Seo, H. Nowatari, S. Hosoumi, T. Ishisone, T. Watabe, S. Mitsumori, N. Ohsawa, S. Yamazaki, *J. Soc. Inf. Disp.* **2016**, *24*, 360–370.
- [49] U. Resch-Genger, K. Rurack, *Pure Appl. Chem.* **2013**, *85*, 2005–2026.
- [50] F. Ke, Y. Song, H. Li, C. Zhou, Y. Du, M. Zhu, *Dalton Trans.* **2019**, *48*, 13921–13924.
- [51] R. W. Huang, Y. S. Wei, X. Y. Dong, X. H. Wu, C. X. Du, S. Q. Zang, T. C. W. Mak, *Nat. Chem.* **2017**, *9*, 689–697.
- [52] H. Yang, J. Lei, B. Wu, Y. Wang, M. Zhou, A. Xia, L. Zheng, N. Zheng, *Chem. Commun.* **2013**, *49*, 300–302.
- [53] M. Xie, C. Han, J. Zhang, G. Xie, H. Xu, *Chem. Mater.* **2017**, *29*, 6606–6610.
- [54] J. Zhang, C. Duan, C. Han, H. Yang, Y. Wei, H. Xu, J. Zhang, C. Duan, C. Han, H. Yang, Y. Wei, H. Xu, *Adv. Mater.* **2016**, *28*, 5975–5979.
- [55] E. C. Glazer, D. Magde, Y. Tor, *J. Am. Chem. Soc.* **2005**, *127*, 4190–4192.

Chapter 2

2.0 Luminescent Group 11 Metal Chalcogenolate Clusters with Conjugated Diphosphine Ligands

2.1 Introduction

Polynuclear metal chalcogenolate complexes are researched extensively due to their wide range of structural, chemical and photophysical properties.^[1] Specifically, coinage metal elements (copper, silver and gold) in combination with chalcogenolates have been of interest due to their high potential as modifiable complexes in regard to the dimensionality of the structure and the functionality of the organic substituents to change the electronic and conductive properties.^{[2][3]} These complexes can be used as light emitting materials because of their rich photophysical properties (emission at room temperature).^{[2]-[4]}

These clusters can be easily synthesized using silylated chalcogen reagents (RESiMe_3 , R = organic moiety, E = S, Se) with metal salt complexes (LMX , L = organic ligand, M = Cu, Ag, X = leaving group: OAc, Cl) bonded to a ligand.^{[1][5]-[8]} The formation of X-SiMe_3 drives the reaction forward and results in the metal chalcogenolate core.^{[1][6][8]} The size and the structure of these clusters can vary depending on the organic ligand used as well as the sterics of the organic moiety bonded to the chalcogen.^{[1][9][10]} The presence of the R group bonded to the chalcogen provides kinetic stability and prevents the formation of the Cu_2S binary phases.^{[9][11][12]} Organic ligands can also be incorporated in order to control properties such as luminescence.^{[3][4][11][12]}

Two interesting examples are $[\text{Cu}_2(p\text{-S-C}_6\text{H}_4\text{-NMe}_2)_2(\text{dpppt})_2]$ (**II.I**)^[4] and $[\text{Cu}_2(p\text{-Se-C}_6\text{H}_4\text{-NMe}_2)_2(\text{dpppt})_2]$ (**II.II**) reported by *Fenske* and *co-workers* where the incorporation of diphosphine ligands resulted in dimeric species exhibiting photoluminescence ($\lambda_{\text{em}} = 480 \text{ nm}$).^[3] The emissions in these complexes arise from LMCT (ligand to metal charge transfer) where the HOMO is composed of the copper sulfur core and the LUMO is composed of the phosphine ligands.^[3] Compounds (**II.I**) and (**II.II**) are isostructural to each other with slight geometric differences. The bond lengths for Cu-S for (**II.I**) are 2.384(2) - 2.436(2) Å whereas the bond lengths for Cu-Se for (**II.II**) are 2.4867(4) - 2.5210(4) Å. The bond lengths for (**II.II**) are slightly longer which can be attributed to the larger covalent radii of Se (1.16 Å) compared to the covalent radii of S (1.03 Å).^{[3][4][13]} When comparing the emission for (**II.I**) and (**II.II**), both complexes emit at 480 nm at room temperature which shows that changing the chalcogen from S to Se can result in similar emission properties.

Another example to consider is $[\text{Cu}_4(\text{P}^{\wedge}\text{S})_4(\text{CH}_3\text{CN})_2]$ (**II.III**) ($\text{P}^{\wedge}\text{S}$ = 2-(diphenylphosphino)benzenethiolate) (Figure 2.1) which has emission at 526 nm with PLQYs (photoluminescent quantum yields) of 19 % at room temperature.^[14] These transitions arise from (M+X)LCT where the HOMO is composed of the d orbitals of Cu and p orbitals of S and the LUMO is composed of the phenyl rings.^[14] Complex (**II.III**) has a tetranuclear core with μ_2 and μ_3 bridging thiolates. The copper centres have a tetrahedral geometry and the short distances between the Cu centres (2.776(1) Å) indicate the presence of cuprophilic interactions.^[14]

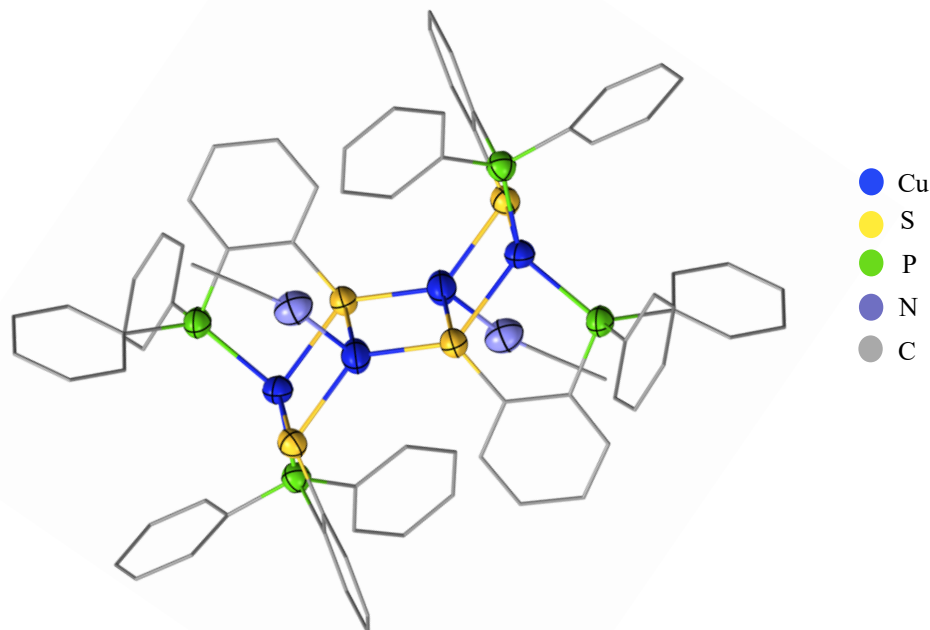


Figure 2.1: $[\text{Cu}_4(\text{P}^{\wedge}\text{S})_4(\text{CH}_3\text{CN})_2]$ ($\text{P}^{\wedge}\text{S}$ = 2-(diphenylphosphino)benzenethiolate) (**II.III**) (H atoms are omitted for clarity).^[14]

The bidentate 4,6 - bis(diphenylphosphino)dibenzofuran (DBFDP) was recently incorporated in copper iodide clusters to form the cubane $[\text{Cu}_4\text{I}_4(\text{dbfdp})_2]$ (**II.IV**).^[15] The use of this phosphine improved functions of the Cu_4I_4 (**II.IV**) such as solution processability as well as the electron transport and they now have the potential to be incorporated in organic light emitting diodes (OLEDs).^[15] Complex (**II.IV**) emits at 491 nm at room temperature with photoluminescence quantum yields (PLQYs) of ~5 %. The emission arises from the MLCT (metal to ligand charge transfer) where the HOMOs consist of the orbitals of the Cu_4I_4 core and the LUMOs are composed of the π^* system of the dibenzofuran backbone.^[15]

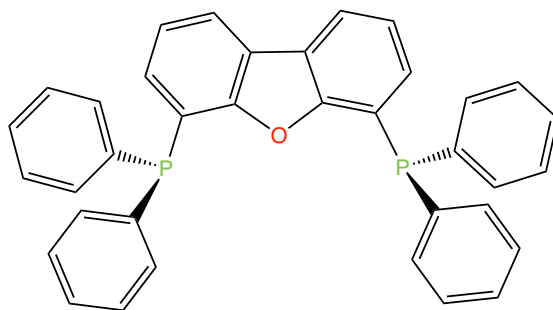


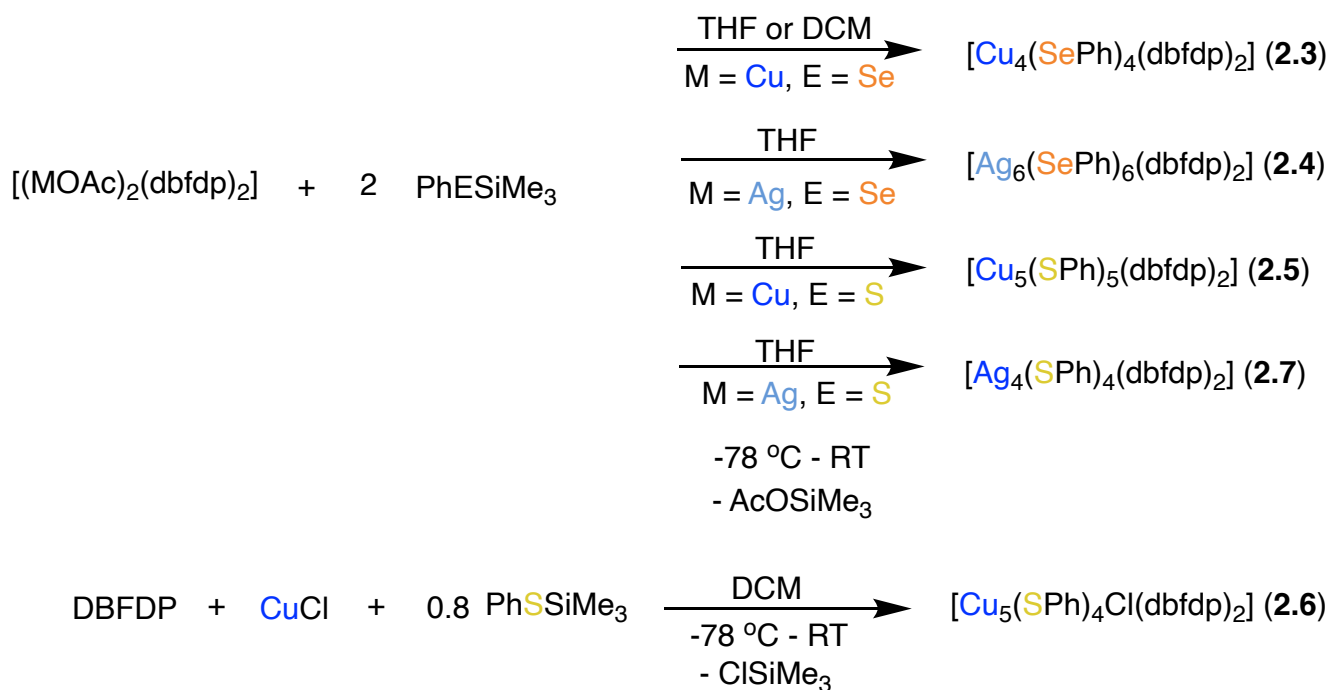
Figure 2.2: 4,6 - bis(diphenylphosphino)dibenzofuran (DBFDP).^[15]

Since the incorporation of DBFDP showed promising results with CuI clusters, this work reports on the synthesis of group 11 metal chalcogenolate clusters (M-ER, M = Cu, Ag, E = S, Se, R = Ph) with DBFDP. Five different clusters were synthesized by first reacting the CuOAc, AgOAc and CuCl with DBFDP resulting in [(CuOAc)₂(dbfdp)₂] (**2.1**)^[16], [(AgOAc)₂(dbfdp)₂] (**2.2**)^[17] and solutions of DBFDP with CuCl. These phosphine ligated metal complexes were then reacted with PhESiMe₃ (E = S, Se) at low temperatures to yield [Cu₄(SePh)₄(dbfdp)₂] (**2.3**), [Ag₆(SePh)₆(dbfdp)₂] (**2.4**), [Cu₅(SPh)₅(dbfdp)₂] (**2.5**), [Cu₅(SPh)₄Cl(dbfdp)₂] (**2.6**), [Ag₄(SPh)₄(dbfdp)₂] (**2.7**). As complexes (**2.3**) - (**2.7**) displayed luminescence at ambient temperature when irradiated with the UV lamp ($\lambda = 254$ nm and 365 nm), their photophysical properties were investigated in detail to determine how the bidentate phosphine ligand affects the structural and electronic properties of group 11 metal chalcogenolate clusters.

2.2 Results and Discussion

2.2.1 Synthesis and Characterization of [Cu₄($\mu_{2/3}$ -SePh)₄(μ -dbfdp)₂] (**2.3**), [Ag₆($\mu_{2/3}$ -SePh)₆(μ -dbfdp)₂] (**2.4**), [Cu₅($\mu_{2/3}$ -SPh)₅(μ -dbfdp)₂] (**2.5**), [Cu₅($\mu_{2/3}$ -SPh)₄Cl(μ -dbfdp)₂] (**2.6**), and [Ag₄($\mu_{2/3}$ -SPh)₄(μ -dbfdp)₂] (**2.7**)

It is well documented that phosphine ligated CuOAc, AgOAc and CuCl react with chalcogen reagents with -SiMe₃ moieties.^[18] [(CuOAc)₂(dbfdp)₂] (**2.1**), [(AgOAc)₂(dbfdp)₂] (**2.2**) and solutions of DBFDP with CuCl thus represented as a good entry point for the preparation of copper chalcogenolate and silver chalcogenolate complexes containing the DBFDP ligand. The synthesis of complexes (**2.3**) - (**2.5**) and (**2.7**) were carried out by adding 2 equivalents of PhESiMe₃ [E = S, Se] to solutions of [(MOAc)₂(dbfdp)₂] (M = Cu, Ag) in THF or DCM. The synthesis of complex (**2.6**) was carried out by adding 0.8 equivalents of PhSSiMe₃ to solutions of DBFDP with CuCl in DCM as shown in *Scheme 2.1*.



Scheme 2.1: Synthesis schemes of group 11 metal chalcogenolate complexes (2.3) - (2.7).

The addition of PhESiMe₃ at -78 °C to solutions of [(MOAc)₂(dbfdp)₂] and solutions of DBFDP with CuCl resulted in a reaction between OAc / Cl and SiMe₃, which further resulted in the formation of the metal chalcogenolate core and the elimination of the silane. The progression of the reactions was monitored by observing the change in luminescence using a handheld UV lamp as the temperature increased. The solutions of (2.1), (2.2) and solutions of DBFDP with CuCl only exhibited pale yellow luminescence. After adding the chalcogen, a significant change in the luminescence to bright yellow or orange was observed in the reaction solutions.

The addition of PhSeSiMe₃ to solutions of [(CuOAc)₂(dbfdp)₂] (2.1) in DCM resulted in changes to the colour of the solution from pale to intense yellow with no further change in colour observed from -78 °C to room temperature. The progression of the reaction can also be observed by the change in luminescence from pale yellow to orange. It was then layered with heptane as a counter solvent which resulted in the crystallization of yellow needles with green - yellow luminescence. The reaction can also be conducted in THF and proceeds the same way, but crystallization was more favourable in DCM than THF.

The ³¹P{¹H} NMR spectrum of [Cu₄(μ_{2/3}-SePh)₄(μ-dbfdp)₂] (2.3) showed a low frequency shift to -18 ppm compared to [(CuOAc)₂(dbfdp)₂] at -16 ppm.^[16] There is only one broad signal which suggested that the signal is an average of all the phosphorus environments. This low frequency shift could be due to the

presence of higher density of the electron cloud from the selenium versus OAc. Similar shifts for other PR_3 ligands have been reported in literature as a result of the coordination of copper to chalcogenolates.^{[19][20]} The broadening of the signal in complex **(2.3)** ($W_{1/2} = 66.0$ Hz) likely takes place because copper has two NMR active quadrupolar nuclei ^{63}Cu and ^{65}Cu ($I = 3/2$). This broadening has been reported with other PR_3 ligands.^[21]

The molecular structure of **(2.3)** was determined by single crystal X - ray diffraction. Complex **(2.3)** crystallizes in the triclinic space group $\text{P}\bar{1}$ and Z of 1. Molecules of **(2.3)** reside about a crystallographic inversion centre. Complex **(2.3)** has a Cu_4 core with μ_2 and μ_3 bridging selenolates with phosphine ligands present at the periphery. In **(2.3)**, two copper centres have a distorted tetrahedral coordination due to bonding with one phosphorus and three bridging selenium. The other two copper sites have a distorted trigonal planar coordination due to bonding with one phosphorus and two bridging selenium as shown in *Figure 2.3*. $[\text{Cu}_6(\mu\text{-dppm})_4(\mu_3\text{-SePh})_4](\text{BF}_4)_2$ (**II.V**)^[20] reported by *Yam and co-workers* has a similar arrangement to **(2.3)** for the selenolates and the Cu atoms. In **(II.V)**, each selenolate has μ_3 coordination and the Cu centres have trigonal planar and tetrahedral coordination geometries.^[20] The bond lengths reported for Cu-Se in **(II.V)** range between 2.369(1) - 2.579(4) Å.^[20] The bond lengths of **(2.3)** are well within the range of the ones reported for **(II.V)**.^[20]

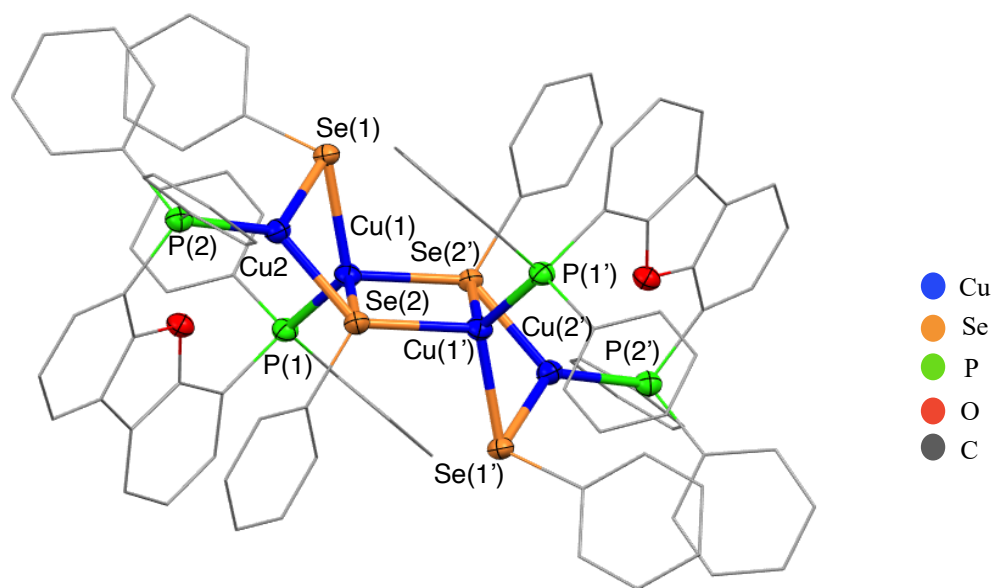


*Figure 2.3: Molecular structure of $[\text{Cu}_4(\text{SePh})_4(\text{dbfdp})_2]$ (**2.3**) in the crystal (Cu - Se: 2.3651(3) - 2.5797(3) Å, Cu - P: 2.2022(6) - 2.2412(5) Å, Cu(1) \cdots Cu(2): 2.6246(4) Å) (H atoms are omitted for clarity). The molecule resides about a crystallographic inversion centre.*

Complex **(2.3)** is very similar in structure to $[\text{Cu}_4(\text{P}^{\wedge}\text{S})_4(\text{CH}_3\text{CN})_2]$ (**II.III**)^[14] (*Figure 2.1*). The chalcogenolates in **(2.3)** and (**II.III**) differ in nature (Se vs. S) and in terms of their organic moiety but they both represent a tetranuclear core with μ_2 and μ_3 bridging chalcogenolates and tetrahedral / trigonal planar Cu centres.^[14] The short distance between the Cu centres (Cu(1) – Cu(2) 2.6246(4) Å) in **(2.3)** indicates the presence of cuprophilic interactions since the distance is within the range of 2.4 - 2.8 Å.^[22]

As complex **(2.3)** showed interesting results regarding the dimensionality of structure, Ag was incorporated to see how changing the metal affects the structure of group 11 metal chalcogenolates with bridging DBFDP. Similar to the preparation of **(2.3)**, 2 equivalents of PhSeSiMe₃ were added to solutions of $[(\text{AgOAc})_2(\text{dbfdp})_2]$ in THF at -78 °C which resulted in a change of the latter from a cloudy, and pale-yellow solution to a cloudy colourless solution until -30 °C. The progression of the reaction was also determined by using a handheld UV lamp as the addition of PhSeSiMe₃ resulted in a change from pale yellow to golden yellow luminescence. The solution became clear and was pale yellow in colour as it warmed to room temperature. The luminescence decreased as the solution warmed and at room temperature, there was no visible luminescence. The THF was then removed under vacuum and the crystalline powder was dissolved in toluene and layered with diethyl ether. This resulted in the crystallization of colourless blocks of $[\text{Ag}_6(\mu_{2/3}\text{-SePh})_6(\mu\text{-dbfdp})_2]$ (**2.4**).

The $^{31}\text{P}\{^1\text{H}\}$ NMR spectrum of the crystals of **(2.4)** showed a low frequency shift to -11 ppm ($W_{1/2} = 108.0$ Hz) when compared to $[(\text{AgOAc})_2(\text{dbfdp})_2]$ at -6 ppm. There is again only one broad signal which suggested an average of all the phosphorus environment. The change in chemical shift could be attributed to the Ag bonding to Se. Silver has two NMR active nuclei with a spin of $1/2$: ^{107}Ag and ^{109}Ag . Therefore, two doublets might be expected in the $^{31}\text{P}\{^1\text{H}\}$ NMR due to the splitting caused by the two NMR active nuclei of Ag. There is only one broad signal observed in the $^{31}\text{P}\{^1\text{H}\}$ NMR spectrum. A similar observation has been reported in literature where the $^{31}\text{P}\{^1\text{H}\}$ NMR spectrum for $[\text{Ag}_2(\mu\text{-R}_2\text{PCH}_2\text{PR}_2)_3]^{2+}$ (**II.VI**) (R = Me, Ph) shows only one broad peak at room temperature.^[23] The doublets due to coupling for **(II.VI)** are seen at low temperatures (< -35 °C) but the limited solubility of **(2.4)** prohibited a similar investigation.^{[23][24]}

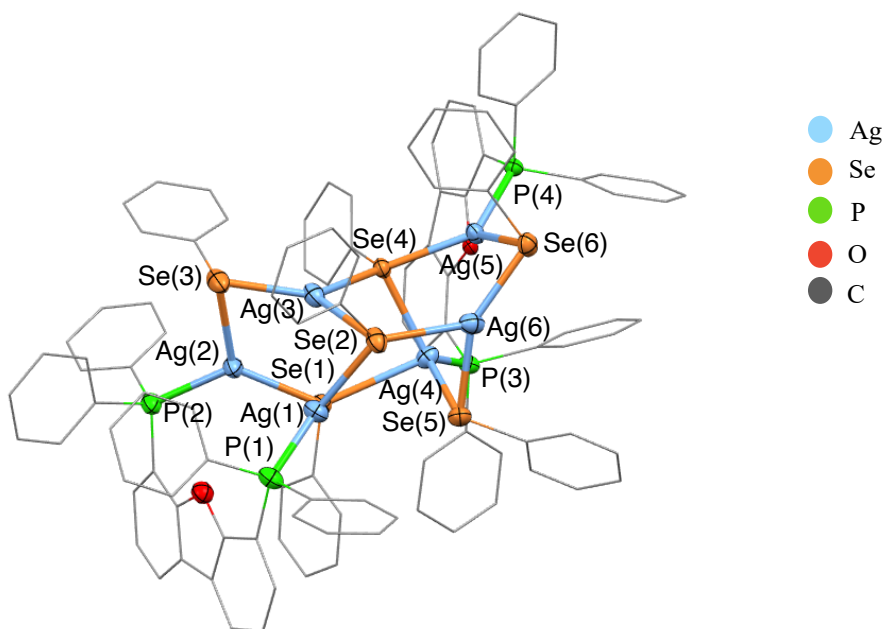


Figure 2.4: Molecular structure of $[Ag_6(SePh)_6(dfbdp)_2]$ (**2.4**) in the crystal (Ag - Se: 2.5145(9) - 3.0222(9) Å, Ag - P: 2.4371(18) - 2.4769(19) Å, Ag \cdots Ag: 2.9910(8) - 3.1320(8) Å) (H atoms are omitted for clarity).

Complex (**2.4**) crystallizes in the triclinic space group $P\bar{1}$ and Z of 2. Compound (**2.4**) has a hexanuclear core with μ_2 and μ_3 bridging selenolates and protective phosphine ligands at the edges. The core for (**2.4**) can also be considered as a dimer of $[Ag_3(SePh)_3]$. In (**2.4**), Ag(1), Ag(2), Ag(5) have a trigonal planar coordination geometry due to bonding with one phosphorus and two bridging selenium. Ag(3) and Ag(6) also have a trigonal planar coordination due to bonding with three selenium while Ag(4) has a tetrahedral geometry due to bonding to one phosphine and three selenolates as shown in *Figure 2.4*. The reported silver selenolate cluster, $[Ag_4(SeiPr)_4(dppm)_2]$ (**II.VII**) by *Fenske* and *Langetepe* has selenium in two coordination modes (μ_2 and μ_3) with bond lengths of Ag-Se ranging from 2.509(4) - 2.847(3) Å.^[25] Although (**II.VII**) is structurally different from (**2.4**) as (**II.VII**) only consists of 4 Ag atoms whereas (**2.4**) consists of 6 Ag, the Se atoms in (**II.VII**) have the same coordination modes as (**2.4**) and all the Ag atoms in (**II.VII**) have a trigonal planar geometry. The bond lengths reported for (**2.4**) are within the range for literature values reported for (**II.VII**).^[25] As for (**2.3**), possible metallophilic interactions are observed in (**2.4**). Argentophilic interactions are similar in nature to cuprophilic interactions but instead they are between two silver atoms. Argentophilic interactions follow the same rule as cuprophilic interactions where the distance of the “bond” must be shorter than the van der Waals radii of two Ag atoms, with the former having a distance shorter than 3.4 Å.^[26]

$[\text{Cu}_4(\mu_{2/3}\text{-SePh})_4(\mu\text{-dbfdp})_2]$ (**2.3**) and $[\text{Ag}_6(\mu_{2/3}\text{-SePh})_6(\mu\text{-dbfdp})_2]$ (**2.4**) show significant structural changes when switching the group 11 metal from Cu to Ag. (**2.4**) is a bigger complex than (**2.3**) as (**2.4**) consists of 6 Ag atoms whereas (**2.3**) consists of 4 Cu atoms. Given that changing the group 11 metal shows interesting structural differences, altering the chalcogenolate (from Se to S) to determine if the incorporation of a different chalcogen (S) would result in similar conformations (as observed for (**2.3**) and (**2.4**)) was the next progression in this vein of research.

Similar to the preparation of (**2.3**) and (**2.4**), the addition of 2.0 equivalents of PhSSiMe_3 to solutions of $[(\text{CuOAc})_2(\text{dbfdp})_2]$ in THF at $-78\text{ }^\circ\text{C}$ resulted in a change from a cloudy pale - yellow solution to a cloudy yellow solution with orange - yellow luminescence (reaction progression was determined by the change in colour of solution and the change in the colour of emission). The solution became clear and was yellow in colour as it warmed from $-10\text{ }^\circ\text{C}$ to RT with orange - yellow luminescence. The THF was then removed and the resultant crystalline powder was dissolved in toluene and layered with ether which resulted in the crystallization of yellow needles of $[\text{Cu}_5(\mu_{2/3}\text{-SPh})_5(\mu\text{-dbfdp})_2]$ (**2.5**) that exhibited green luminescence.

The $^{31}\text{P}\{^1\text{H}\}$ NMR spectrum of (**2.5**) showed a low frequency shift to -17 ppm compared to $[(\text{CuOAc})_2(\text{dbfdp})_2]$ at -16 ppm .^[16] This low frequency shift is explained by the coordination of copper to chalcogenolates and the broadening of the signal in complex (**2.5**) ($W_{1/2} = 86.0\text{ Hz}$) takes place because of the two quadrupolar active nuclei of $\text{Cu}^{[21]}$ as mentioned for $[\text{Cu}_4(\mu_{2/3}\text{-SePh})_4(\mu\text{-dbfdp})_2]$ (**2.3**).

Complex (**2.5**) crystallizes in the monoclinic space group $C2/c$ and Z of 4. Molecules of (**2.5**) reside about a 2 - fold rotation axis with a glide plane. Compound (**2.5**) has a pentanuclear core made of 5 Cu atoms with μ_2 and μ_3 bridging thiolates with the phosphine ligands present at the periphery. In (**2.5**), Cu(1), Cu(3), Cu(4) and Cu(5) have a trigonal planar coordination. Cu(1), Cu(3) and Cu(4) are bonded to one phosphorus and two bridging sulfur. Cu(5) has a trigonal planar geometry but is only bonded to three thiolates. Cu(2) has a tetrahedral geometry as it is bonded to three thiolate ligands and one phosphorus as shown in *Figure 2.5*. When comparing this to the structure of (**2.3**), (**2.5**) is a slightly larger cluster as (**2.5**) has 5 Cu atoms compared to 4 Cu atoms for (**2.3**). The selenolates in (**2.3**) and the thiolates in (**2.5**) both exhibit μ_2 and μ_3 coordination modes. An interesting difference between (**2.3**) and (**2.5**) is the fifth copper atom in (**2.5**) which is only bonded to thiolates.

Compound (**2.5**) can be compared to the previously reported cluster $[\text{Cu}_4(\text{P}^{\wedge}\text{S})_4(\text{CH}_3\text{CN})_2]$ (**II.III**) (*Figure 2.1*) which has the same chalcogen (S) and coordination modes of both μ_2 and μ_3 with Cu-S distances

between 2.272(2) - 2.578(2) Å.^[14] Compound (**II.III**) is structurally different than (**2.5**) as (**II.III**) has 4 Cu atoms with a different organic moiety on the chalcogen. Nevertheless, the thiolates in (**2.5**) show both coordination modes with the bond lengths such as in the cluster reported.^[14] (**2.5**) can also be compared to a slightly larger cluster [Cu₈(SPh)₈(PPh₃)₄] (**II.VIII**) that has μ₂ and μ₃ bridging thiolates with Cu-S distances between 2.228(2) - 2.342(1) Å.^[27] This cluster although larger than (**2.5**) has the same chalcogenolate and coordination modes and only differs in the number of Cu atoms. When comparing bond lengths of (**2.5**) to the bond lengths of (**II.III**) and (**II.VIII**), the bond lengths are well within the reported distances.^{[14][27]} The Cu-Cu distances also suggest the presence of cuprophilic interactions. The evidence of cuprophilic interactions is again observed in (**2.5**) as the distance between two Cu atoms are within 2.4 - 2.8 Å.^[22]

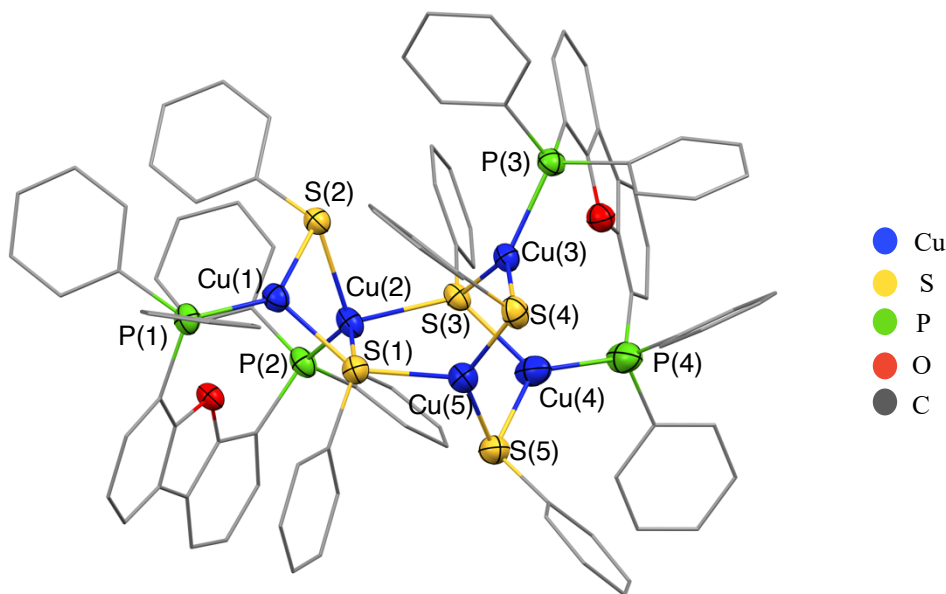


*Figure 2.5: Molecular structure of [Cu₅(SPh)₅(dbfdp)₂] (**2.5**) in the crystal (Cu - S: 2.2111(10) - 2.4494(10) Å, Cu - P: 2.1816(10) - 2.2617(10) Å, Cu ... Cu: 2.6942(6) - 2.8223(6) Å) (H atoms are omitted for clarity).*

An interesting observation is that when (**2.5**) is recrystallized from DCM, it results in colourless needles of [Cu₅(μ_{2/3}-SPh)₄Cl(μ-dbfdp)₂] (**2.6**). The crystals formed in DCM (**2.6**) transform and have a chloride functionality. A more efficient way of obtaining (**2.6**) was by adding 0.8 equivalents of PhSSiMe₃ to solutions of DBFDP with CuCl in DCM at -78 °C and warming to room temperature. The solution had yellow luminescence at cold temperatures which became orange as it warmed to room temperature. It was then layered with heptane as a counter solvent and resulted in the crystallization of colourless needles of (**2.6**) with teal luminescence.

The $^{31}\text{P}\{^1\text{H}\}$ NMR spectrum of the crystals of **(2.6)** showed a high frequency shift to -15 ppm ($W_{1/2} = 22.5$ Hz) compared to $[(\text{CuOAc})_2(\text{dbfdp})_2]$.^[16] As mentioned for **(2.3)** and **(2.5)**^{[19][20]}, the trend in shift for **(2.6)** is expected to be towards low frequency but the high frequency shift could be explained by the presence of the electron rich chloride.^[28]

Complex **(2.6)** crystallizes in the monoclinic space group $P2_1/m$ and Z of 2. Molecules of **(2.6)** reside about a mirror plane. **(2.6)** has a pentanuclear core similar to **(2.5)** with μ_2 and μ_3 bridging thiolates with a terminal chloride functionality. The core for **(2.6)** can also be viewed as a distorted square pyramid formed from the 5 Cu atoms. In **(2.6)**, four copper centres have a trigonal planar coordination due to bonding with one phosphorus and two bridging sulfur. The unique copper also has a trigonal planar coordination due to the bonding with one chlorine and two bridging thiolates as shown in *Figure 2.6*. The previously reported cluster $[\text{Cu}_8(\text{SPh})_8(\text{PPh}_3)_4]$ (**II.VIII**), has coordination modes of both μ_2 and μ_3 with distances between 2.228(2) - 2.342(1) Å.^[27] The thiolates in **(2.6)** show both coordination modes with the bond lengths such as in the cluster reported. No evidence for cuprophilic interactions were observed in **(2.6)** as the distances between two copper atoms are all greater than 2.8 Å.^[22]

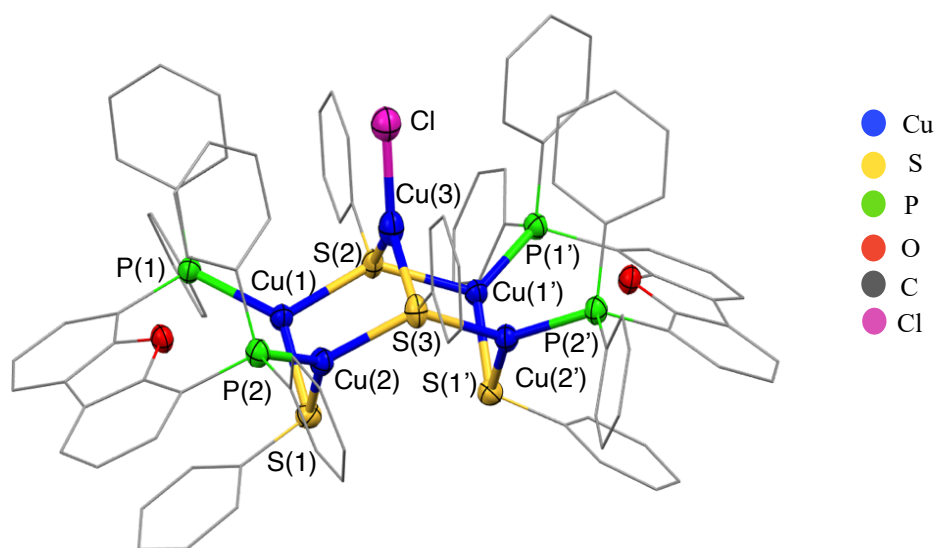


*Figure 2.6: Molecular structure of $[\text{Cu}_5(\text{SPh})_4\text{Cl}(\text{dbfdp})_2]$ (**2.6**) in the crystal (Cu - S: 2.2371(10) - 2.3050(7) Å, Cu - P: 2.2253(9) - 2.2369(9) Å, Cu - Cl: 2.2429(15) Å) (H atoms are omitted for clarity). The molecule resides about a mirror plane bisecting Cu(3)/S(2)/S(3)/Cl.*

Changing the group 11 metal from Cu to Ag when using PhSSiMe_3 resulted in $[\text{Ag}_4(\mu_2/\mu_3\text{-SPh})_4(\mu\text{-dbfdp})_2]$ (**2.7**). **(2.7)** was synthesized in a similar way as **(2.5)** by adding 2 equivalents of PhSSiMe_3 at -78 °C to solutions of $[(\text{AgOAc})_2(\text{dbfdp})_2]$ in THF. The addition of PhSSiMe_3 resulted in no observable change as

the solution remained cloudy and pale yellow from -78 °C to -40 °C with green - yellow luminescence. The solution started to become clear and turned orange as it warmed to room temperature. As the solution warmed to room temperature, the luminescence decreased and at room temperature, there was no visible luminescence. The THF was removed under vacuum and the resultant crystalline powder was dissolved in toluene and layered with ether. This resulted in the crystallization of orange plates with green - yellow luminescence.

The $^{31}\text{P}\{^1\text{H}\}$ NMR spectrum showed a low frequency shift to -11 ppm ($W_{1/2} = 177.6$ Hz) when compared to $[(\text{AgOAc})_2(\text{dbfdp})_2]$ at -6 ppm. The low frequency shift can again be due to the presence of sulfur as mentioned for **(2.5)**.^{[23][24][29]} No P-Ag coupling was observed.

Complex **(2.7)** crystallizes in the triclinic space group $\text{P}\bar{1}$ and Z of 1. Molecules of **(2.7)** reside about a crystallographic inversion centre. **(2.7)** has a tetranuclear cluster core (similar to $[\text{Cu}_4(\mu_{2/3}\text{-SePh})_4(\mu\text{-dbfdp})_2]$ **(2.3)**) with μ_2 and μ_3 bridging thiolates with DBFDP ligands present at the periphery. In **(2.7)**, two silver centres have a distorted tetrahedral coordination due to the bonding with one phosphorus and three bridging thiolates. The other two metals have a trigonal planar coordination due to the bonding with one phosphorus and two bridging thiolates as shown in *Figure 2.7*. A very similar cluster to **(2.7)** has been reported in literature. $[\text{Ag}_4(\text{SPh})_4(\text{PPh}_3)_4]$ **(II.IX)** displays both μ_2 and μ_3 coordination modes for the thiolate ligands with the Ag-S distances of 2.497(4) - 3.0006(8) Å.^[30] Compound **(II.IX)** is structurally similar to **(2.7)** as both these compounds have 4 Ag atoms and the same thiolate. Interestingly, **(2.7)** is also very structurally similar to $[\text{Cu}_4(\mu_{2/3}\text{-SePh})_4(\mu\text{-dbfdp})_2]$ **(2.3)** and $[\text{Cu}_4(\text{P}^{\wedge}\text{S})_4(\text{CH}_3\text{CN})_2]$ **(II.III)**.^[14] Complexes **(2.3)** and **(2.7)** have a different group 11 metal and chalcogenolate but form a similar tetranuclear core with μ_2 and μ_3 bridging chalcogenolates. Compound **(II.III)** also has a tetranuclear core formed from 4 Cu atoms with μ_2 and μ_3 bridging thiolates^[14] which is similar to the Ag tetranuclear core and thiolates for **(2.7)**.

When comparing the bond lengths of **(2.7)** to **(II.IX)**^[30], the bond lengths of **(2.7)** are within this range but some are even shorter (Ag(1)-S(1) and Ag(1)-S(2)). This could be due to using the more rigid phosphine which pinches the two Ag centres together resulting in the thiolates to be closer with shorter bond distances. No argentophilic interactions were observed as the distance between two silver atoms was greater than 3.4 Å.^[26] It is important to also note that although crystals of **(2.7)** were good enough to obtain crystal data, the quality of the data was poor as the crystals were small and weakly diffracting. The

molecule is also disordered and therefore has two different fractions. The bond lengths listed in *Figure 2.7* refer to fraction 1.

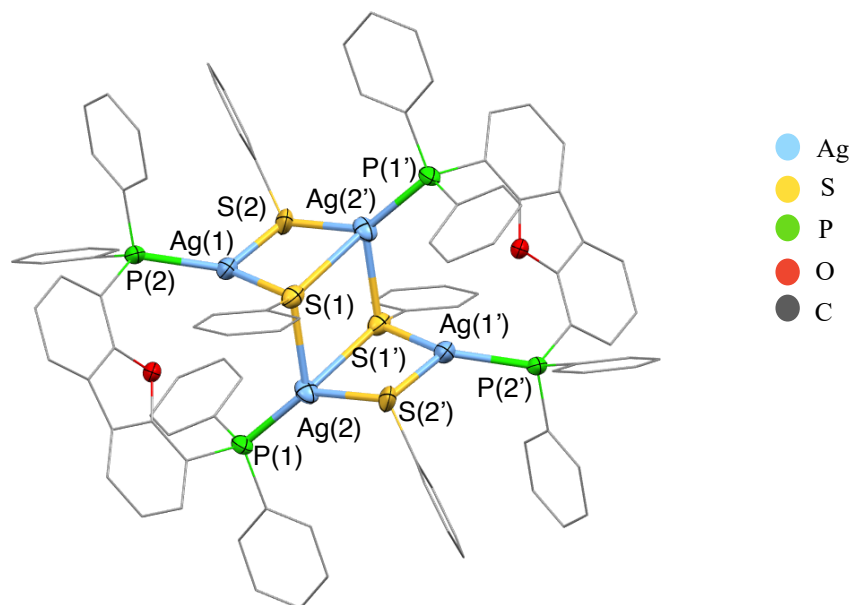


*Figure 2.7: Molecular structure of $[Ag_4(SPh)_4(dbfdp)_2]$ (**2.7**) in the crystal (Ag - S: 2.442(8) - 2.897(16) Å, Ag - P: 2.414(8) - 2.442(8) Å) (H atoms are omitted for clarity). (The molecule resides about a crystallographic inversion centre).*

2.2.2 Photophysical properties of Metal Chalcogenolate Complexes (**2.3**) - (**2.7**)

It has been previously reported that the use of DBFDP results in strong luminescence behaviour in stable copper (I) iodide clusters. The ability of DBFDP to bridge two Cu atoms and the rigidity due to the ligand results in efficient PLQY's of $[Cu_4I_4(dbfdp)_2]$.^[15] The incorporation of DBFDP could result in luminescence of the complexes prepared. When crystals of (**2.3**) - (**2.7**) were irradiated with a handheld UV lamp ($\lambda = 254$ nm and 365 nm), it was observed that (**2.3**) - (**2.7**) were similarly emissive in colour when irradiated with either wavelength. The luminescence of crystals of (**2.3**) - (**2.7**) is shown in *Figure 2.8*.

An interesting observation was that the crystals of (**2.3**) had very different luminescence features when suspended in DCM and after the removal of DCM. When (**2.3**) was crystallized in DCM, the crystals exhibited neon green emission in the reaction solution (DCM and heptane) when irradiated with the UV lamp (365 nm) (*Figure 2.9 (a)*). After isolating the crystals and drying them under vacuum, (**2.3**) turned into a powder which exhibited orange luminescence when irradiated with the UV lamp (365 nm) (*Figure 2.9 (b)*). This property of (**2.3**) may arise due to the potential luminescence vapochromism (also known as vapoluminescence) which is a common phenomenon for organometallic compounds.^{[31][32]}

Vapochromism refers to the change in colour and / or emission of a compound depending on the absorption or desorption of gas and / or vapour.^{[31][32]} The incorporation of vapours and / or gases can change the intermolecular interactions in the crystal lattice. For example, the changes in weak metal-metal interactions, π stacking, hydrogen bonding, and van der Waals forces could result in a different colour of emission.^{[31][32]} Although structurally different, $[\text{Cu}_4\text{I}_4(\text{TMP})_4]$ (**II.X**) (TMP = *tris*(3-methylphenyl)phosphine) exhibits vapochromic behaviour with MeCN.^[33] The emission spectrum of (**II.X**) showed significant changes depending on MeCN adsorption / desorption.^[33] Compound (**II.X**) has a $\lambda_{\text{em}} = 583 \text{ nm}$ with MeCN absorption and a $\lambda_{\text{em}} = 533 \text{ nm}$ with MeCN desorption.^[33] Complex (**2.3**) also exhibits potential vapochromism as the desorption of DCM resulted in a qualitative observation of a bathochromic shift in emission compared to the green emission of crystals of (**2.3**) in the reaction solution.

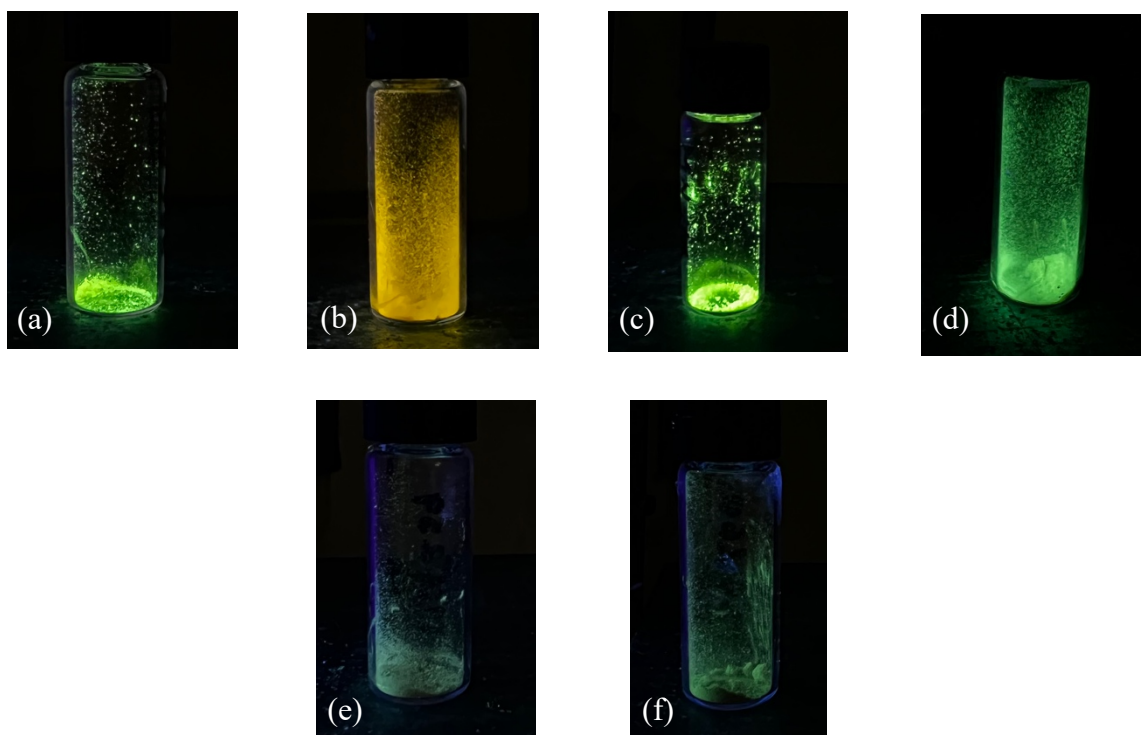


Figure 2.8: (a) Emission of $[\text{Cu}_4(\text{SePh})_4(\text{dbfdp})_2] \cdot (\text{2.3}) \cdot \text{THF}$ (b) Emission of $[\text{Cu}_4(\text{SePh})_4(\text{dbfdp})_2]$ (**2.3**) (c) Emission of $[\text{Ag}_6(\text{SePh})_6(\text{dbfdp})_2]$ (**2.4**) (d) Emission of $[\text{Cu}_5(\text{SPh})_5(\text{dbfdp})_2]$ (**2.5**) (e) Emission of $[\text{Cu}_5(\text{SPh})_4\text{Cl}(\text{dbfdp})_2]$ (**2.6**) (f) Emission of $[\text{Ag}_4(\text{SPh})_4(\text{dbfdp})_2]$ (**2.7**). (Qualitative observation of the emission of solid - state samples at room temperature when irradiated at 365 nm).

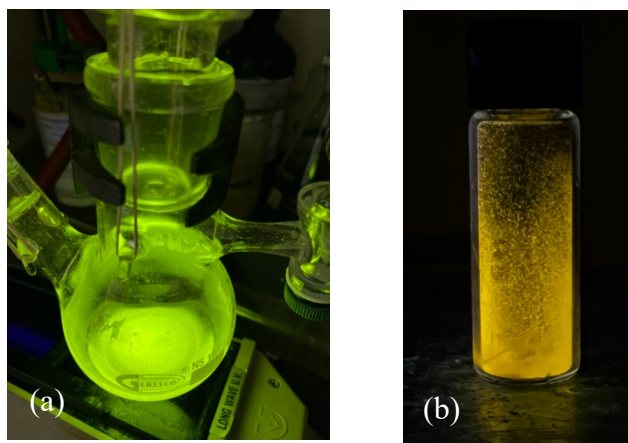


Figure 2.9: (a) Emission of $[\text{Cu}_4(\text{SePh})_4(\text{dbfdp})_2]$ (**2.3**) (in DCM and heptane) (b) Emission of $[\text{Cu}_4(\text{SePh})_4(\text{dbfdp})_2]$ (**(2.3)·DCM**) after isolation and removal of DCM under vacuum. (Qualitative observation of the emission of solid - state samples at room temperature when irradiated at 365 nm).

The emission and excitation spectra of (**2.3**) - (**2.7**) were obtained in the solid state. When comparing the clusters to each other, a notable difference in the λ_{exc} and λ_{em} can be seen. The change from copper to silver affects the intensity of the luminescence and results in a hypsochromic shift whereas, the change from selenium to sulfur only shifts the emission hypsochromically. The emission and excitation spectra are shown in *Figure 2.10* and *2.11*. DFT calculations have been done for the model complex (**2.3**) and reported in section **2.2.3 Theoretical Calculations for $[\text{Cu}_4(\mu_{2/3}\text{-SePh})_4(\mu\text{-dbfdp})_2]$ (**2.3**)**

For (**(2.3)·THF**), λ_{exc} was determined to be 470 nm and λ_{em} was observed at 560 nm with a PLQY of 34 %. The λ_{em} is in the green - yellow region which is also seen visually in *Figure 2.8*. For (**2.3**), $\lambda_{\text{exc}} = 475$ nm with $\lambda_{\text{em}} = 570$ nm. Comparing (**(2.3)·THF**) to (**2.3**), (**2.3**) has a slight bathochromic shift in terms of λ_{exc} and λ_{em} . When making the comparison to the emission of $[\text{Cu}_4(\text{P}^{\wedge}\text{S})_4(\text{CH}_3\text{CN})_2]$ (**(II.III)**) at 526 nm^[14] which is similar in structure but different in the chalcogen, the emission of (**(2.3)·THF**) and (**2.3**) both have bathochromic shifts. Interestingly, the PLQY of (**(2.3)·THF**) and (**2.3**) at room temperature are 34 % and 30 %, respectively which are up to 1.8 times higher than the PLQY reported for (**(II.III)**) at room temperature (PLQY = 19 %).^[14] Compound (**2.3**) therefore, shows an improved PLQY which could be due to the presence of a different chalcogen, the different phosphine ligand or a combination of both.

Changing the metal from Cu to Ag resulted in $[\text{Ag}_6(\text{SePh})_6(\text{dbfdp})_2]$ (**2.4**). The λ_{exc} for (**2.4**) was determined to be 400 nm with λ_{em} at 530 nm with a PLQY of 5 %. The difference between complex (**2.3**) and (**2.4**) is the transition metal used which causes a change in the structure from a tetranuclear core for

(2.3) to a hexanuclear core for (2.4). The changes in structure and nuclearity for (2.4) could be the reason for a slight hypsochromic shift for the emission as well as the PLQY. This can also be seen visually as the colour of emission of (2.4) is more blue - green compared to (2.3).

Changing the chalcogen to S when using Cu resulted in $[\text{Cu}_5(\text{SPh})_5(\text{dbfdp})_2]$ (2.5). The λ_{exc} and λ_{em} for (2.5) were determined to be at 465 nm and 530 nm respectively with a PLQY of 73 %. The difference between (2.3) and (2.5) is the chalcogen (from Se to S) with a change in 4 Cu atoms for (2.3) to 5 Cu atoms for (2.5). Comparing this to the λ_{em} (560 nm) and PLQYs (34 %) of complex (2.3), (2.5) has a hypsochromic shift with a PLQY that is 2.2 times higher. Comparing this to the λ_{em} (530 nm) (2.4), the λ_{em} of (2.5) is the same but there is a drastic difference between the PLQYs. (2.4) has a PLQY of 5 % whereas, the PLQY of (2.5) is 14.3 times higher which could be attributed to the differences in nuclearity and chalcogen. Moreover, when comparing to the already reported $[\text{Cu}_4(\text{P}^{\wedge}\text{S})_4(\text{CH}_3\text{CN})_2]$ (II.III) with λ_{em} at 526 nm with PLQYs of 19 % at room temperature^[14], (2.5) shows a similar λ_{em} with 3.8 times higher PLQYs. Although, (II.III) and (2.5) are structurally different from each other due to the number of Cu atoms and the chalcogenolate, (2.5) shows impressive PLQYs at room temperature.

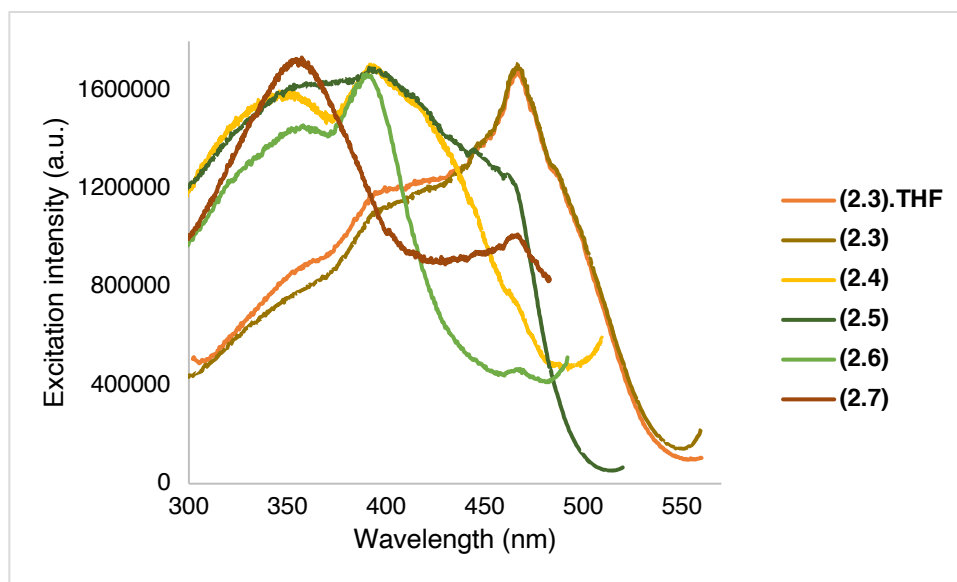


Figure 2.10: Excitation spectra of (2.3) - (2.7) in the solid state at room temperature. The selected $\lambda_{\text{exc(max)}}$ for these complexes range between 360 nm - 470 nm.

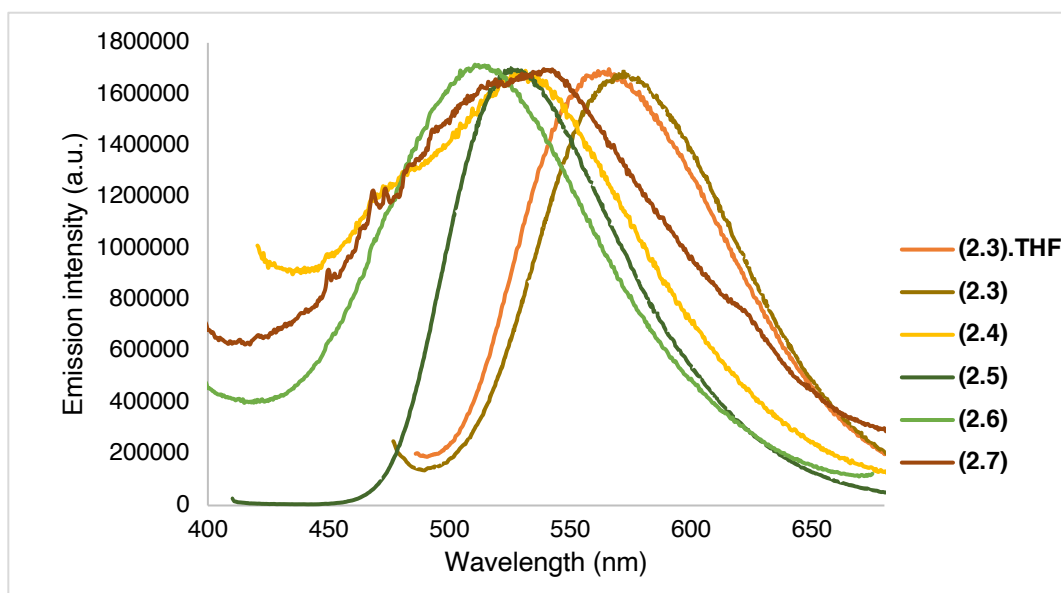


Figure 2.11: Emission spectra of (2.3) - (2.7) in the solid state at room temperature. ($\lambda_{exc} = 470$ nm ((2.3).THF)), $\lambda_{exc} = 475$ nm (2.3), $\lambda_{exc} = 400$ nm (2.4), $\lambda_{exc} = 465$ nm (2.5), $\lambda_{exc} = 390$ nm (2.6), $\lambda_{exc} = 360$ nm (2.7)) The λ_{em} for these complexes range between 510 nm - 570 nm. (The noise seen in (2.4) and (2.7) is due to the low emission intensity of the compounds).

While compound $[\text{Cu}_5(\text{SPh})_4\text{Cl}(\text{dbfdp})_2]$ (2.6) is very different from (2.3) - (2.5) and (2.7) due to its chloride functionality, it still exhibited emission at room temperature. λ_{exc} and λ_{em} for (2.6) were determined to be at 390 nm and 510 nm, respectively with PLQYs of 10 %. The different crystal packing and the chloride in (2.6) compared to (2.5) may be the reason for the hypsochromic shift in emission as well as the drastic decrease in PLQYs (10 % for (2.6) compared to 73 % for (2.5)).

Interestingly, $[\text{Ag}_4(\text{SPh})_4(\text{dbfdp})_2]$ (2.7) is structurally similar to (2.3) as both complexes have 4 metal atoms in the core with μ_2 and μ_3 bridging chalcogenolates. While their molecular structures are similar, (2.7) incorporates Ag atoms and thiolates which results in a λ_{exc} at 360 nm and λ_{em} at 540 nm with a PLQY of 9 %. The λ_{em} of (2.7) has a slight hypsochromic shift with lower PLQYs compared to (2.3) (560 nm with 34 % PLQYs). Another comparison to be made is to complex (2.5) where changing the group 11 metal from Cu (2.5) to Ag (2.7) resulted in a difference of the number of metal atoms in the core. This difference of the nature of the metal as well as the nuclearity in (2.5) and (2.7) does not result in a significant change in the λ_{em} as the λ_{em} are 530 nm and 540 nm, respectively but it may be the reason for a large difference in PLQYs of (2.5) (PLQY = 73 %) and (2.7) (PLQY = 9 %).

2.2.3 Theoretical Calculations for $[\text{Cu}_4(\mu_{2/3}\text{-SePh})_4(\mu\text{-dbfdp})_2]$ (2.3)

Calculations were carried out with TURBOMOLE employing Perdew-Burke-Ernzerhof (PBE) exchange energy and Hartree-Fock exchange energy in 3:1 ratio and polarized triple zeta valence basis set (def2-TZVP) (F. Weigend, personal communication). The density functional theory (DFT) simulations show that the electronic transitions in the cluster arise from HOMO, HOMO - 1, HOMO - 2, HOMO - 3 to LUMO and LUMO + 1. The major contribution for the HOMO region is from the p orbitals of selenium while the minor donation is from the d orbitals of copper. The LUMO region is mostly comprised of the π^* orbitals of the furan ring shown in *Figure 2.12*. Complex (2.3) exhibits (M+X)LCT which is the same transition type reported for $[\text{Cu}_4(\text{P}^{\wedge}\text{S})_4(\text{CH}_3\text{CN})_2]$ (II.III) and $[\text{Cu}_4\text{I}_4(\text{dbfdp})_2]$ (II.IV).^{[14][15]} The observation made for the DFT calculations for (2.3) is also consistent with the DFT calculations reported in literature for (II.III) and (II.IV).^{[14][15]} Compound (II.IV) has HOMO comprised of the Cu_4I_4 core with major donations from both elements while the LUMO consists of the π^* system of the dibenzofuran ring.^[15] It was observed that HOMO - 1, HOMO - 2 and HOMO - 3 for (2.3) have major donations from the p orbitals of selenium with minor donation from the d orbitals of copper while the LUMO + 1 is comprised of the dibenzofuran ring. The observations for the HOMO - 3s and LUMO + 1 are also consistent with the DFT calculations reported for $[\text{Cu}_4\text{I}_4(\text{dbfdp})_2]$ (II.IV) where the HOMO - 3s are composed of the Cu_4I_4 core while the LUMO consists of the dibenzofuran ring.^[15]

The transitions taking place from the HOMO's to LUMO's have a $\Delta E(\text{S}_1\text{-T}_1)$ ranging from 0.010 - 0.086 eV. Due to the small $\Delta E(\text{S}_1\text{-T}_1)$, it can be hypothesized that (2.3) can repopulate the S_1 state (due to intersystem crossing) resulting in TADF.^[34] Thermal re - population to the S_1 state occurs when the $\Delta E(\text{S}_1\text{-T}_1) \leq 100$ meV which results in TADF. When comparing to other group 11 metal complexes such as $[\text{Cu}_4(\text{P}^{\wedge}\text{S})_4(\text{CH}_3\text{CN})_2]$ ($\text{P}^{\wedge}\text{S} = 2\text{-}(\text{diphenylphosphino})\text{benzenethiolate}$) (II.III) which has a $\Delta E(\text{S}_1\text{-T}_1) = 0.096$ eV^[14] and specifically the $\Delta E(\text{S}_1\text{-T}_1) = 0.04$ eV of $[\text{Cu}_4\text{I}_4(\text{dbfdp})_2]$ (II.IV)^[15], the $\Delta E(\text{S}_1\text{-T}_1)$ values for (2.3) have an acceptable range. Variable temperature experiments will be required to investigate this.

The oscillator strength (f) of (2.3) ranges between 0.000 to 0.045. Oscillator strength is the probability of an emission taking place when electromagnetic radiation is applied.^{[35]-[37]} Therefore, the higher the (f), the higher the probability of an emission taking place.^{[35]-[37]} Comparing the (f) of (2.3) to the (f) reported in literature for (II.III) ($f = 0.0093$)^[14] and (II.IV) ($f = 0.009$)^[15], the (f) for (2.3) is up to 5 times higher. Therefore, it can be deduced that the probability of the emissive transitions taking place in (2.3) is high.

Since complexes (2.3) - (2.5) and (2.7) all have the same basic structure (at least two metal atoms bonded two phosphines and 2/3 chalcogenolates), it can be hypothesized that the transitions in the other compounds may also arise from the ME core to the dibenzofuran ring.

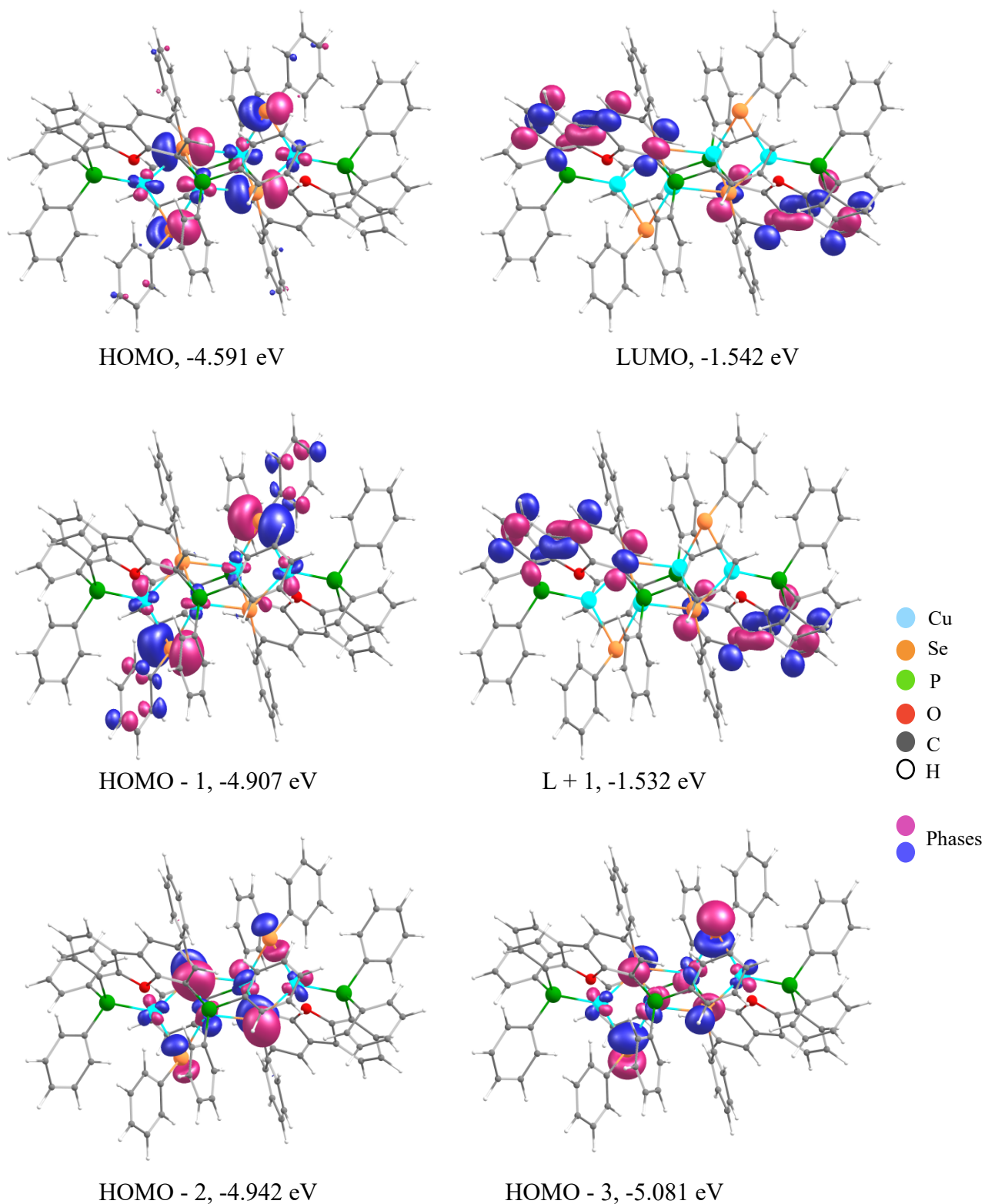


Figure 2.12: DFT Calculations for $[Cu_4(SePh)_4(dbfdp)_2]$ (2.3) displaying the HOMOs and LUMOs

2.3 Experimental

2.3.1 General Considerations

All experiments were carried out under an inert atmosphere of high purity, dried nitrogen using standard Schlenk line techniques on a double manifold vacuum line. All solvents used were either distilled over the appropriate desiccant under nitrogen or were dried by using a commercial Mbraun MB - SP series solvent purification system.

Dibenzofuran (TCI America), silver acetate (Fisher chemicals), chlorodiphenylphosphine (TCI America) and *n* - butyllithium (Acros Organics) were purchased and used without further purification. CuCl was purchased from Sigma Aldrich and purified by literature procedures.^[38]

Tetramethylethylenediamine (TMEDA) was refluxed over KOH pellets for three hours and distilled under nitrogen according to the literature procedure.^[39] Copper (I) acetate, phenyl(trimethylsilyl)sulfide and phenyl(trimethylsilyl)selenide were synthesized by a colleague using literature procedures and were used without further purification.^{[40][41][42]} 4,6 - bis(diphenylphosphino)dibenzofuran (DBFDP) was synthesized by incorporating two literature procedures with a few modifications (all steps were conducted under an inert system).^{[43][44]} [(MOAc)₂(dbfdp)₂] (M = Cu, Ag) were generated *in situ* as previously reported.^{[16][17]} A signal at $\delta_P = -6$ was observed for the ³¹P{¹H} NMR spectrum of [(AgOAc)₂(dbfdp)₂].

¹H and ³¹P{¹H} NMR spectra were recorded on the Bruker AvanceIII HD 400 (B400) with frequencies of 400.130 MHz and 161.976 MHz, respectively. The ¹H NMR spectra were referenced to the residual proton solvent in CDCl₃. The ³¹P{¹H} NMR spectra were referenced to the 85 % H₃PO₄. Attenuated Total Reflectance Infrared (ATR - IR) spectra of samples of (2.3) - (2.7) were obtained using Bruker Alpha II Spectrometer. The data were analyzed using the OPUS - Operator Default Software. The peaks in the IR spectrum of each compound are ranked according to their relative intensity and the ranks are shown in brackets (1 → 12, strongest to weakest intensity). Melting points of samples of (2.3) - (2.7) were recorded on a Gallenkamp melting point apparatus under N₂ atmosphere. Samples of (2.3) - (2.7) were also prepared for elemental analysis under N₂ atmosphere. Elemental Analysis was performed at the Centre for Environmental Analysis and Remediation by Patricia Granados at Saint Marys University in Halifax, Nova Scotia.

Single crystal X - ray data were completed by Dr. John F. Corrigan on a Bruker Kappa Axis Apex2 diffractometer at a temperature of 110 K. The sample was placed on a MiTeGen polyimide micromount

with a small amount of Paratone - N oil. The raw data were scaled, and absorption corrected using SADABS and the frame integration was done by SAINT.^{[45][46]} SHELXT program was used to solve the structure.^[47] All hydrogen atoms were obtained from the initial solution, introduced at idealized positions and were allowed to ride on the parent atom. The structural model was fit to the data by full matrix least squares based on F^2 . The structure was further refined using the SHELXL program from the SHELXTL suite of crystallographic software.^[48]

In the collection of the solid photoluminescence, crystalline powders of **(2.3)** - **(2.7)** were adhered to 2-sided Scotch tape (410B, 3M, Saint Paul, MN) on a custom-made platform with a 45-degree angle between the excitation beam and emission collection. The emission and excitation slit widths were optimized for the signal strength. The 2-sided tape was chosen from many brands to have a very low PL signal. The crystalline powder was spread over the tape to prevent the excitation beam from exciting the tape. The data were analyzed by using FelixGX version 2 software made by Photon Technology International (PTI).

PLQY were measured with crystalline powders of **(2.3)** - **(2.7)** that were placed in the sample holder of a Hamamatsu C11347-11 Quanrurus Absolute PL Quantum Yield Spectrometer. The emission spectra were recorded and analyzed using the default software and quantum yields were corrected using average 50 scans. No correction for possible sample reabsorption was accounted for.

2.3.2 Synthesis of $[Cu_4(SePh)_4(dbfdp)_2]$ (**2.3**)

$[Cu_2(OAc)_2(dbfdp)_2]$ was prepared with DBFDP (0.106 g, 0.200 mmol, 1.00 equiv.) and CuOAc (0.024 g, 0.20 mmol, 1.00 equiv.) by stirring for an hour in 20 mL of DCM. PhSeSiMe₃ (0.080 mL, 0.400 mmol, 2.00 equiv.) was added at -78 °C. The solution was warmed slowly to room temperature. The solution was layered with heptane and yellow crystals of **(2.3)** were observed after 3 days. The resulting crystals were isolated and washed twice with 20 mL of pentane and dried under vacuum for 5 - 6 hours (0.045 g, 46 % yield based on CuOAc). ¹H NMR (400 MHz, CDCl₃, 23.5 °C): δ = 7.96 (s, 4H), 7.74-7.46 (m, 72H), 7.03-6.93 (m, 20H). ³¹P {¹H} NMR (161 MHz, THF, 23.5 °C): δ = -18 ppm. ATR IR (cm⁻¹): 3048 w(Ph-H stretch) (12), 1571 (9), 1469 (10), 1433 (4), 1410 (7), 1389 (8), 1175 (3), 1093 (5), 1066 (11), 1019 (6), 723 (2), 686 (1). m.p. > 224 °C_{decomp.} Elemental analysis: $[Cu_4(SePh)_4(dbfdp)_2]$: Calcd: 59.08 % C and 3.72 % H, Found: 59.01 % C, and 3.97 % H. λ_{exc} = 470 nm, λ_{em} = 560 nm, PLQY = 34 %. Crystal structure data, bond angles and bond lengths are attached in the **Appendix** in *Tables S2.1, S2.2 and S2.3*. ¹H NMR and ³¹P {¹H} NMR are attached in the **Appendix** in *Figures S2.1 and S2.2*.

2.3.3 Synthesis of $[Ag_6(SePh)_6(dbfdp)_2]$ (2.4)

$[Ag_2(OAc)_2(dbfdp)_2]$ was prepared with DBFDP (0.103 g, 0.190 mmol, 1.00 equiv.) and AgOAc (0.032 g, 0.190 mmol, 1.00 equiv.) by stirring for one hour in 20 mL of THF. PhSeSiMe₃ (0.08 mL, 0.40 mmol, 2.00 equiv.) was added with stirring at -78 °C. The solution was slowly warmed to room temperature. The THF was removed under vacuum and the crystalline powder was dissolved in toluene and layered with ether. Colourless crystals of (2.4) were observed after 3 days. The resulting crystals were isolated and washed twice with 20 mL of pentane and dried under vacuum for 5 - 6 hours (0.038 g, 45 % yield based on AgOAc). ¹H NMR (400 MHz, CDCl₃, 23.5 °C): δ = 7.98-7.96 (d, 4H, *J* = 8.2 Hz), 7.34-7.17 (m, 81H), 6.82-6.74 (m, 12H), 6.59 (s, 11H). ³¹P {¹H} NMR (161 MHz, CDCl₃, 23.5 °C): δ = -11 ppm. ATR IR (cm⁻¹): 3047 w(Ph-H stretch) (12), 1570 (9), 1469 (10), 1433 (4), 1410 (7), 1391 (8), 1182 (3), 1093 (5), 1065 (11), 1019 (6), 730 (2), 687 (1). m.p. = 140 °C_{decomp.} Elemental analysis: {[Ag₆(SePh)₆(dbfdp)₂]}·C₇H₈: Calcd: 50.25 % C and 3.30 % H, Found: 53.51 % C and 3.47 % H (The ¹H NMR spectrum shows only one NMR active product. The elemental analysis was conducted twice at separate facilities and results in the same elemental analysis values which did not match the calculated values. Additional analysis is needed to check for compound homogeneity). λ_{exc} = 390 nm, λ_{em} = 530 nm, PLQY = 5 %. Crystal structure data, bond angles and bond lengths are attached in the **Appendix** in *Tables S2.4, S2.5 and S2.6*. ¹H NMR and ³¹P {¹H} NMR are attached in the **Appendix** in *Figures S2.3 and S2.4*.

2.3.4 Synthesis of $[Cu_5(SPh)_5(dbfdp)_2]$ (2.5)

$[Cu_2(OAc)_2(dbfdp)_2]$ was prepared with DBFDP (0.113 g, 0.210 mmol, 1.00 equiv.) and CuOAc (0.026 g, 0.210 mmol, 1.00 equiv.) by stirring for an hour in 20 mL of THF. PhSSiMe₃ (0.080 mL, 0.420 mmol, 2.00 equiv.) was added at -78 °C. The solution was warmed slowly to room temperature. The solution was layered with heptane and yellow crystals of (2.5) were observed after 3 days. The resulting crystals were isolated and washed twice with 20 mL of pentane and dried under vacuum for 5 - 6 hours (0.042 g, 51 % yield based on CuOAc). ¹H NMR (400 MHz, CDCl₃, 23.5 °C): δ = 7.84 (s, 4H), 7.24-7.12 (m, 82H), 6.76-6.58 (m, 16H). ³¹P {¹H} NMR (161 MHz, THF, 23.5 °C): δ = -17 ppm. ATR IR (cm⁻¹): 3071 w(Ph-H stretch) (12), 1575 (9), 1469 (10), 1434 (4), 1408 (7), 1393 (8), 1173 (3), 1094 (5), 1080 (11), 1019 (6), 735 (2), 684 (1). m.p. > 260 °C_{decomp.} Elemental analysis: {[Cu₅(SPh)₅(dbfdp)₂]}·1.5 C₇H₈: Calcd: 65.12 % C and 4.32 % H, Found: 65.14 % C, 4.35 % H. λ_{exc} = 465 nm, λ_{em} = 530 nm, PLQY = 73 %. Crystal structure data, bond angles and bond lengths are attached in the **Appendix** in *Tables S2.7, S2.8 and S2.9*. ¹H NMR and ³¹P {¹H} NMR are attached in the **Appendix** in *Figures S2.5 and S2.6*.

2.3.5 Synthesis of $[Cu_5(SPh)_4Cl(dbfdp)_2]$ (2.6)

DBFDP (0.140 g, 0.26 mmol, 1 equiv.) with CuCl (0.026 g, 0.260 mmol, 1.00 equiv.) was stirred for one hour in 20 mL of DCM. PhSSiMe₃ (0.080 mL, 0.420 mmol, 1.80 equiv.) was added while stirring at -78 °C. The solution was warmed slowly to room temperature. The solution was layered with heptane and colourless crystals of (2.6) were observed after 3 days. The resulting crystals were isolated and washed twice with 20 mL of pentane and dried under vacuum for 5 - 6 hours (0.053 g, 54 % yield based on CuCl). ¹H NMR (400 MHz, CDCl₃, 23.5 °C): δ = 7.60-7.58 (d, 4H, *J* = 8.2 Hz), 7.33-7.06 (m, 78H), 6.60-6.56 (t, 4H, *J* = 8.2 Hz), 6.27-6.23 (t, 4H, *J* = 7.6 Hz), 6.04-6.00 (t, 6H, *J* = 8.2 Hz). ³¹P {¹H} NMR (161 MHz, CDCl₃, 23.5 °C): δ = -15 ppm. ATR IR (cm⁻¹): 3053 w(Ph-H stretch) (12), 1573 (9), 1471 (10), 1434 (4), 1412 (7), 1395 (8), 1189 (3), 1094 (5), 1022 (11), 1014 (6), 738 (2), 690 (1). m.p. = 192 °C_{decomp}. Elemental analysis: {[Cu₅(SPh)₄Cl(dbfdp)₂]}·0.25 C₇H₁₆: Calcd: 62.10 % C and 4.02 % H, Found: 59.62 % C and 3.89 % H. λ_{exc} = 390 nm, λ_{em} = 510 nm, PLQY = 10 %. Crystal structure data, bond angles and bond lengths are attached in the **Appendix** in *Tables S2.10, S2.11 and S2.12*. ¹H NMR and ³¹P {¹H} NMR are attached in the **Appendix** in *Figures S2.7 and S2.8*.

2.3.6 Synthesis of $[Ag_4(SPh)_4(dbfdp)_2]$ (2.7)

[Ag₂(OAc)₂(dbfdp)₂] was prepared with DBFDP (0.113 g, 0.210 mmol, 1.00 equiv.) and AgOAc (0.035 g, 0.210 mmol, 1.00 equiv.) by stirring for an hour in 20 mL of THF (cloudy yellow solution). PhSSiMe₃ (0.080 mL, 0.420 mmol, 2.00 equiv.) was added while stirring at -78 °C. The solution was slowly warmed to room temperature. The THF was removed under vacuum and the crystalline powder was dissolved in toluene and layered with ether. Orange crystals of (2.7) were observed after 2 days. The resulting crystals were washed twice with 20 mL of pentane and dried under vacuum for 5 - 6 hours (0.032 g, 31 % yield based on AgOAc). ¹H NMR (400 MHz, CDCl₃, 23.5 °C): δ = 8.00-7.98 (d, 4H, *J* = 8.2 Hz), 7.24-7.19 (m, 72H), 6.76 (s, 10H), 6.65 (s, 10H). ³¹P {¹H} NMR (161 MHz, CDCl₃, 23.5 °C): δ = -11 ppm. ATR IR (cm⁻¹): 3050 w(Ph-H stretch) (12), 1571 (9), 1467 (10), 1433 (4), 1408 (7), 1388 (8), 1170 (3), 1082 (5), 1076 (11), 1022 (6), 732 (2), 688 (1). m.p. = 133 °C_{decomp}. Elemental analysis: {[Ag₄(SPh)₄(dbfdp)₂]}·0.5 C₇H₈: Calcd: 60.14 % C, and 3.85 % H, Found: 58.28 % C and 3.89 % H. λ_{exc} = 360 nm, λ_{em} = 540 nm, PLQY = 9 %. Crystal structure data, bond angles and bond lengths are attached in the **Appendix** in *Tables S2.13, S2.14 and S2.15*. ¹H NMR and ³¹P {¹H} NMR are attached in the **Appendix** in *Figures S2.9 and S2.10*.

2.4 Conclusions

The addition of PhESiMe₃ (E = S, Se) to [(MOAc)₂(dbfdp)₂] (M = Cu, Ag)^{[16][17]} resulted in metal chalcogenolate complexes with (CuSe), (AgSe), (CuS) and (AgS) core and bridging DBFDP. [Cu₄(SePh)₄(dbfdp)₂] ((**2.3**)·THF), [Cu₅(SPh)₅(dbfdp)₂] (**2.5**) and [Ag₄(SPh)₄(dbfdp)₂] (**2.7**) displayed green - yellow emission in the solid state at room temperature, with a PLQY of 34 % ((**2.3**)·THF), 73 % (**2.5**) and 9 % (**2.7**). [Ag₆(SePh)₆(dbfdp)₂] (**2.4**) and [Cu₅(SPh)₄Cl(dbfdp)₂] (**2.6**) displayed teal coloured emission in the solid state at room temperature, with a PLQY of 5 % and 10 % respectively. Compound (**2.3**) also exhibited potential vapochromism behaviour with green - yellow emission of crystals when in the reaction solution (DCM and heptane) and orange emission after removal of DCM. (**2.3**) had PLQYs of 30 %. It was also observed that the reaction solutions of (**2.3**) had orange luminescence but green - yellow luminescence in the solid state, while the reaction solutions of (**2.5**) and (**2.6**) had yellow luminescence but green - yellow and blue - green luminescence in the solid state, respectively. The solutions of (**2.4**) and (**2.7**) displayed no visible luminescence in solution at room temperature but when crystallized, they had blue - green and green - yellow emission, respectively. The differences in luminescence and PLQYs can be attributed to the nature of the metal (Cu vs. Ag), chalcogen (S vs. Se), and the number of metal atoms present in the complexes as the number of metals forming the core can vary from 4 - 6. Due to these complexes having efficient PLQYs of up to 73 %, (**2.3**) - (**2.7**) as luminescent metal chalcogenolate clusters incorporating the DBFDP ligand could have potential application in OLEDs. Future work will be to obtain emission and excitation data for complexes (**2.3**), (**2.5**) and (**2.6**) in solution.

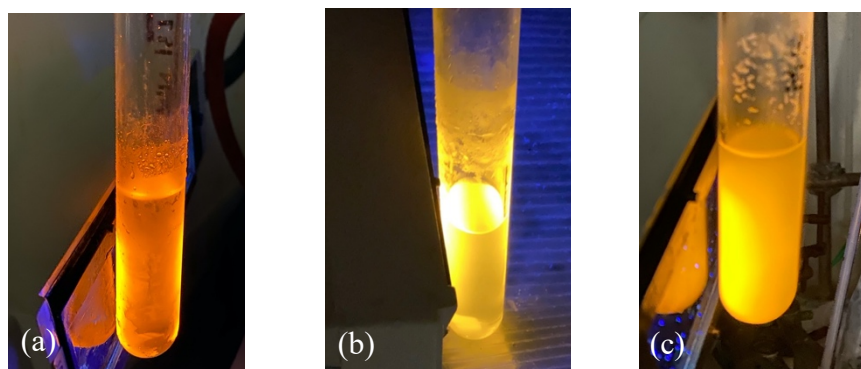


Figure 2.13: (a) Emission of the reaction mixture of [Cu₄(SePh)₄(dbfdp)₂] (**2.3**) (b) [Cu₅(SPh)₅(dbfdp)₂] (**2.5**) and (c) [Cu₅(SPh)₄Cl(dbfdp)₂] (**2.6**) at room temperature when irradiated at 365 nm. (Qualitative observation of the emission of solution - state samples at room temperature when irradiated at 365 nm).

2.5 References

- [1] O. Fuhr, S. Dehnen, D. Fenske, *Chem. Soc. Rev.* **2013**, *42*, 1871–1906.
- [2] O. Veselska, A. Demessence, *Coord. Chem. Rev.* **2018**, *355*, 240–270.
- [3] B. Hu, C. Y. Su, D. Fenske, O. Fuhr, *Inorg. Chim. Acta* **2014**, *419*, 118–123.
- [4] R. Langer, M. Yadav, B. Weinert, D. Fenske, O. Fuhr, *Eur. J. Inorg. Chem.* **2013**, 3623–3631.
- [5] M. W. DeGroot, J. F. Corrigan, *Organometallics* **2005**, *24*, 3378–3385.
- [6] D. G. MacDonald, J. F. Corrigan, *Philos. Trans. R. Soc. A Math. Phys. Eng. Sci.* **2010**, *368*, 1455–1472.
- [7] T. Duan, X. Z. Zhang, Q. F. Zhang, *Zeitschrift fur Naturforsch. - Sect. B J. Chem. Sci.* **2008**, *63*, 941–944.
- [8] S. Dehnen, A. Eichhöfer, J. F. Corrigan, D. Fenske, 2004 Synthesis and characterization of Ib–VI nanoclusters. In *Nanoparticles* (ed. G. Schmid), pp. 107–185. Weinheim, Germany: Wiley-VCH.
- [9] S. Dehnen, A. Eichhöfer, D. Fenske, *Eur. J. Inorg. Chem.* **2002**, *2002*, 279.
- [10] A. Deveson, S. Dehnen, D. Fenske, *Dalton Trans.* **1997**, 4491–4497.
- [11] S. Li, X. S. Du, B. Li, J. Y. Wang, G. P. Li, G. G. Gao, S. Q. Zang, *J. Am. Chem. Soc.* **2018**, *140*, 594–597.
- [12] X. Yang, I. Isaac, C. Persau, R. Ahlrichs, O. Fuhr, D. Fenske, *Inorg. Chim. Acta* **2014**, *421*, 233–245.
- [13] A. Eichhöfer, G. Buth, S. Lebedkin, M. Kühn, F. Weigend, *Inorg. Chem.* **2015**, *54*, 9413–9422.
- [14] K. Shimada, A. Kobayashi, Y. Ono, H. Ohara, T. Hasegawa, T. Taketsugu, E. Sakuda, S. Akagi, N. Kitamura, M. Kato, *J. Phys. Chem. C* **2016**, *120*, 16002–16011.
- [15] M. Xie, C. Han, J. Zhang, G. Xie, H. Xu, *Chem. Mater.* **2017**, *29*, 6606–6610.
- [16] M. Nayyar, Chem 4491E Thesis: Luminescent Copper Chalcogenide Clusters, The University of Western Ontario **2020**.
- [17] K. Y. Li, Chem 4491E Thesis: Ligand Controlled Luminescence in Silver and Gold Chalcogenide Clusters, The University of Western Ontario **2021**.
- [18] A. M. Polgar, A. Zhang, F. MacK, F. Weigend, S. Lebedkin, M. J. Stillman, J. F. Corrigan, *Inorg. Chem.* **2019**, *58*, 3338–3348.
- [19] T. H. Huang, M. H. Zhang, M. L. Tao, X. J. Wang, *Synth. React. Inorganic, Met. Nano-Metal Chem.* **2014**, *44*, 986–990.
- [20] V. W. W. Yam, C. H. Lam, K. M. Fung, K. K. Cheung, *Inorg. Chem.* **2001**, *40*, 3435–3442.
- [21] T. Arun Luiz, *Rasayan J. Chem.* **2015**, *8*, 13–17.
- [22] N. V. S. Harisomayajula, S. Makovetskyi, Y. C. Tsai, *Chem. - A Eur. J.* **2019**, *25*, 8936–8954.

- [23] A. Caballero-Muñoz, J. M. Guevara-Vela, A. Fernández-Alarcón, M. A. Valentín-Rodríguez, M. Flores-Álamo, T. Rocha-Rinza, H. Torrens, G. Moreno-Alcántar, *Eur. J. Inorg. Chem.* **2021**, 2021, 2702–2711.
- [24] J. McNulty, K. Keskar, *Eur. J. Org. Chem.* **2012**, 5462–5470.
- [25] D. Fenske, T. Langetepe, *Angew. Chem. - Int. Ed.* **2002**, 41, 300–784.
- [26] H. Schmidbaur, A. Schier, *Angew. Chem. - Int. Ed.* **2015**, 54, 746–784.
- [27] F. Ke, Y. Song, H. Li, C. Zhou, Y. Du, M. Zhu, *Dalton Trans.* **2019**, 48, 13921–13924.
- [28] J. V. Hanna, S. E. Boyd, P. C. Healy, G. A. Bowmaker, B. W. Skelton, A. H. White, *Dalton Trans.* **2005**, 2547–2556.
- [29] D. V Partyka, N. Deligonul, *Inorg. Chem* **2009**, 48, 9463.
- [30] L. S. Ahmed, J. R. Dilworth, J. R. Miller, N. Wheatley, *Inorg. Chim. Acta* **1998**, 278, 229–231.
- [31] O. S. Wenger, *Chem. Rev.* **2013**, 113, 3686–3733.
- [32] E. Li, K. Jie, M. Liu, X. Sheng, W. Zhu, F. Huang, *Chem. Soc. Rev.* **2020**, 49, 1517–1544.
- [33] K. Yang, S. L. Li, F. Q. Zhang, X. M. Zhang, *Inorg. Chem.* **2016**, 55, 7323–7325.
- [34] L. P. Ravaro, K. P. S. Zanoni, A. S. S. de Camargo, *Energy Reports* **2020**, 6, 37–45.
- [35] H. Appel, K. Burke, MSc. Thesis: Oscillator Strengths from Time Dependent Density Functional Theory, The State University of New Jersey **1999**.
- [36] W. Demtröder, 1996 Absorption and Emission of Light. In *Laser Spectroscopy* (ed. W. Demtröder), pp. 31. Berlin, Heidelberg: Springer.
- [37] J. W. Robinson, 1996, Comparison of Absorption and Emission. In *Atomic Spectroscopy* (ed. J. W. Robinson), pp. 21–26. Baton Rouge, Louisiana: Marcel Dekker.
- [38] S. Balter, PhD Thesis: Synthesis and Structure of Tellurium Bridged Iron, Cobalt and Copper Clusters, University of Karlsruhe **1994**.
- [39] W. L. F. Armarego, C. L. L. Chai, *Purification of Laboratory Chemicals*, **2013**.
- [40] D. A. Edwards, Roger Richards, *J. Chem. Soc. Dalton Trans.* **1973**, 0, 2463–2468.
- [41] C. A. Bruynes, T. K. Jurriens, *J. Org. Chem.* **2002**, 47, 3966–3969.
- [42] M. R. Detty, M. D. Seidler, *J. Org. Chem.* **2002**, 46, 1283–1292.
- [43] A. M. Kranenburg, Y. E. M. Van Der Burgt, P. C. J. Kamer, P. W. N. M. Van Leeuwen, J. H. Van't Hoff, K. Goubitz, J. Fraanje, *Organometallics* **1995**, 14, 3081–3089.
- [44] C. Han, G. Xie, J. Li, Z. Zhang, H. Xu, Z. Deng, Y. Zhao, P. Yan, S. Liu, *Chem. - A Eur. J.* **2011**, 17, 8947–8956.
- [45] Bruker-AXS, SADABS version 2012.1, **2012**, Bruker-AXS, Madison, WI 53711, USA
- [46] Bruker-AXS, SAINT version 2013.8, **2013**, Bruker-AXS, Madison, WI 53711, USA

[47] Sheldrick, G. M., *Acta Cryst.* **2015**, *A71*, 3-8

[48] Sheldrick, G. M., *Acta Cryst.* **2015**, *C71*, 3-8

Chapter 3

3.0 Luminescent Copper Chalcogenide Clusters with Conjugated Diphosphine Ligands

3.1 Introduction

Ligand stabilized group 11 metal chalcogenide clusters have been researched extensively in the past decade due to their diverse structures and photophysical properties which allow these complexes to have applications in fields of optoelectronics, bioimaging and photochemistry.^{[1]-[4]} These complexes are of interest because of their long - lived excited states and due to the ability to change the structure and the photophysical properties depending on the organic ligand used.^{[5][6]} The organic ligands can affect the electronic structure of these compounds leading to HOMO - LUMO energy gaps which can result in properties such as luminescence.^[7] The ability to modulate the electronic and optical properties through ligand engineering makes these complexes interesting candidates for organic light emitting diodes (OLEDs).^{[8][9]}

Phosphine ligands are one of the most common organic ligands that are incorporated in the shell of copper chalcogenide clusters in order to prevent the formation of the thermodynamically driven binary phase of bulk Cu_2E (E = S, Se).^{[5][6][8]-[10]} In 1993, the Yam group reported the first luminescent copper sulfide complex $[\text{Cu}_4(\mu\text{-dppm})_4(\mu_4\text{-S})](\text{PF}_6)_2$ (**III.I**) (dppm = *bis*(diphenylphosphino)methane).^[11] The photophysical and photochemical properties of the $\text{Cu}^{(I)}$ tetramer were investigated and it was concluded that the long lived excited state was due to the ligand to metal charge transfer process LMCT ($\text{E}^{2-} \rightarrow \text{M}_4$) (E = S, M = Cu).^[11]

These phosphine stabilized copper chalcogenide complexes tend to have a general formula of $(\text{Cu}_2\text{E})_x$ (E = S, Se) for their core with phosphine ligands present at the periphery.^[6] The synthesis of these compounds is first done by reacting the phosphine ligand with the metal salt (CuX , X = leaving group: OAc, Cl) to form a reactive species which is soluble in common organic solvents.^{[6][12][13]} Once the phosphine solubilized metal complex is synthesized, it serves as an excellent entry point for the insertion of the chalcogen by using trimethylsilylchalcogen reagents.^{[5][6][12]} The formation of X-SiMe_3 drives the reaction forward resulting in a copper chalcogenide core with protective phosphine ligands bonded to the copper.^[5]
[12][14]-[16]

Recently, *Eichhöfer* and *co-workers* demonstrated the effect of different phosphine ligands on the structure and the photoluminescence quantum yields (PLQYs) of copper chalcogenide clusters.^[17] They synthesized several copper sulfide clusters with different phosphine ligands. Some phosphine ligands resulted in a similar core structure whereas some resulted in completely different core structures.^[17] The common theme throughout was the maintenance of the 2:1 ratio between Cu:E (E = S, Se). Bright red emission was observed for complexes containing a $\text{Cu}_{12}\text{E}_6\text{P}_8$ (E = S, Se) core at ambient temperature. These clusters showed high PLQYs between 21 % - 63 % at ambient temperature.^[17] Through these observations, it was noted that the type of phosphine ligand as well as, surprisingly the crystal packing (triclinic vs. tetragonal) can affect the PLQYs.^[17] The lifetime studies showed that the emission corresponded to phosphorescence as the emission lasted a few microseconds at ambient temperature.^[17] The phosphine ligands had phenyl rings and thus low lying empty π^* orbitals; the complexes displayed electron transitions from the orbitals of the copper chalcogenide core to these ligand - based orbitals.^[17] Clusters that had phosphine devoid of aromatic rings had transitions exclusively within the Cu_2E core. Electronic transitions involved HOMOs (mostly comprising of d(Cu) and p(S) orbitals) and LUMOs (mostly comprising of Cu orbitals).^[17]

4,6 - *bis*(diphenylphosphino)dibenzofuran (DBFDP) has recently proven to be a good ligand for CuI cubane clusters resulting in frameworks with photoluminescence quantum yields (PLQYs) of ~5 % as shown by *Xie* and *co-workers*.^[18]

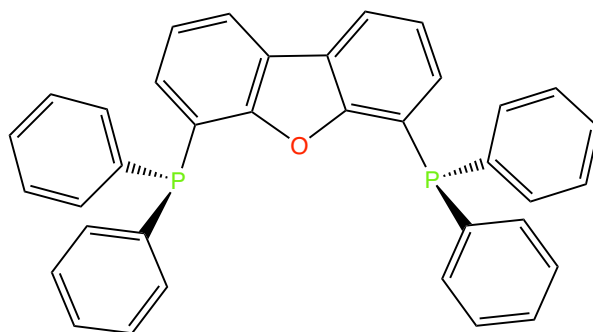


Figure 3.1: 4,6 - bis(diphenylphosphino)dibenzofuran (DBFDP).^[18]

The incorporation of this ligand onto Cu_4I_4 clusters raises the potential for these frameworks to be used in organic light emitting diodes (OLEDs).^[18] The emission arises from the metal + halide to ligand charge transfer (M+X LCT).^[18] The transition for the $[\text{Cu}_4\text{I}_4(\text{dbfdp})_2]$ (**III.11**) takes place from the HOMO and HOMO - 3s which are composed of the CuI units to the LUMO which is composed of the π^* system of the dibenzofuran moiety.^[18] Since phosphine stabilized copper chalcogenide clusters also display

photoluminescence, it was of interest to investigate if/ how the DBFDP ligand would affect their structural and electronic properties.^[19]

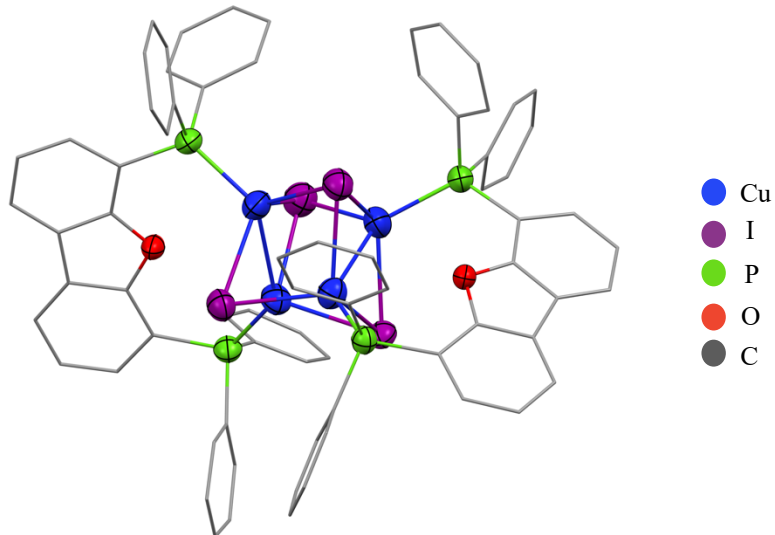


Figure 3.2: Molecular structure of $[(\text{Cu}_4\text{I}_4)(\text{dbfdp})_2]$ (**III.II**) (*H atoms are omitted for clarity*).^[18]

The incorporation of DBFDP in copper chalcogenide (Cu_2E , $\text{E} = \text{S}, \text{Se}$) clusters of undetermined structures was previously investigated. These complexes exhibited bright red luminescence with PLQYs of $\sim 4\%$ but suitable sized single crystals could not be obtained to determine their molecular structure.^[19] Elemental analysis indicated that the ratio of the Cu_2E core ($\text{E} = \text{S}, \text{Se}$) to DBFDP was $\sim 2:1$ but the low solubility of these complexes in organic solvents made it a challenge to recrystallize them.^[19] Therefore, the incorporation of a substituted DBFDP was explored.

In a recent article, *Xie and co-workers* showed how introducing donating groups on the backbone of the dibenzofuran affects the electronic structure and the PLQYs of CuI clusters.^[20] The donating groups DCz (carbazole) and DtBCz (*tert* butyl carbazole) were first incorporated on the 2,8 positions of the dibenzofuran resulting in DCzDBF (**III.III**) and DtBCzDBF (**III.IV**). Compound (**III.III**) and (**III.IV**) were used to synthesize the substituted phosphines DCzDBFDP (**III.V**) (DCz = carbazole on 2,8 positions) and DtBCzDBFDP (**III.VI**) (DtBCz = *tert* butyl carbazole on 2,8 positions) as shown in *Figure 3.3*.^[20] The CuI cubane clusters formed were $[\text{Cu}_4\text{I}_4(\text{DCzdbfdp})_2]$ (**III.VII**) and $[\text{Cu}_4\text{I}_4(\text{DtBCzdbfdp})_2]$ (**III.VIII**). The PLQYs of these complexes increased up to 65 % and resulted in less cluster centered (CC) transitions.^[20] Cluster centered (CC) transitions result in the loss of energy due to irradiative transitions as the transitions involve metal to halide charge transfer (MXCT) ($\text{X} = \text{Halide}$) and serve as a quenching site of excited energy.^{[20][21]} CC transitions result in the distortion of the excited states and due to the destabilization of the excited state, this results in the loss of energy (for example: heat) and the inhibition

of radiative transitions (for example: emission).^[22] The incorporation of DCz and DtBCz on the backbone of the dibenzofuran decreases the gap between the HOMO and HOMO - 3 resulting in the suppression of CC transitions and an increase in radiative transitions.^[20] These donating groups result in more ligand centered transitions as the HOMO and HOMO - 3s are mostly comprised of the donating groups while the LUMO consists of the dibenzofuran ring.^[20] Compared to the HOMO and HOMO - 3s of [Cu₄I₄(dbfdp)₂] (**III.II**), the orbitals of (**III.VII**) and (**III.VIII**) have minimal donation from the Cu₄I₄ units and result in less CC transitions and more ligand centered transitions with high PLQYs (up to 15 times higher than (**III.II**)).

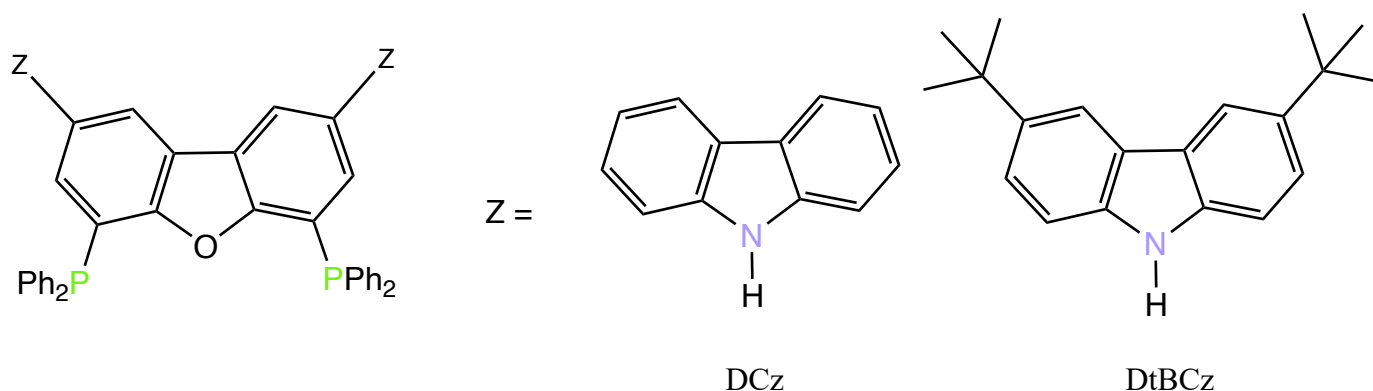


Figure 3.3: Substituted 4,6 - bis(diphenylphosphino)dibenzofuran.^[20]

The incorporation of the DCz and DtBCz substituted phosphine was therefore an attractive route to synthesize and characterize the molecular structure of copper chalcogenide clusters while improving their PLQYs. However, attempts to prepare the substituted dibenzofuran (**III.III**) and (**III.IV**) could not be achieved in high purity or yield, so another donor group (ethyl) was incorporated into the backbone of the dibenzofuran.

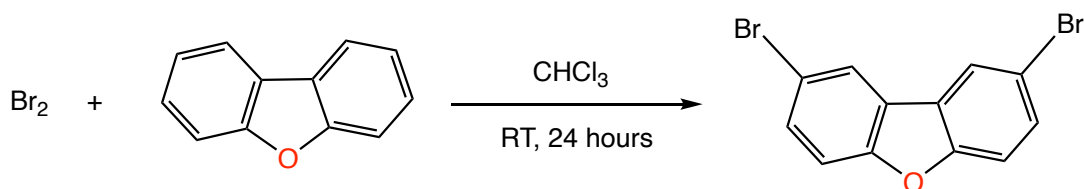
Herein, the preparation and the incorporation of the bidentate phosphine 2,8 - diethyl(4,6 - bis - (diphenylphosphino))dibenzofuran (EtDBFDP) in copper chalcogenide clusters is reported. EtDBF (2,8 - diethyldibenzofuran) (**3.1**) was first synthesized by reacting 2,8 - dibromodibenzofuran with ^tBuLi using air sensitive techniques. Then, the substituted dibenzofuran phosphine was synthesized using literature procedures resulting in EtDBFDP (**3.2**).^[18] Ligand (**3.2**) was then further reacted with CuOAc to form the reactive and soluble metal acetate phosphine complex. Bis(trimethylsilyl)selenide and Bis(trimethylsilyl)sulfide were then introduced to solutions of the phosphine solubilized CuOAc resulting in [(Cu₁₂Se₆)(etdfbdp)₄] (**3.3**) and [(Cu₁₂S₆)(etdfbdp)₄] (**3.4**). Crystals of (**3.3**) and (**3.4**) displayed

luminescence at ambient temperature when irradiated with a UV lamp. A full analysis of their molecular structure and their photophysical properties will be conducted.

3.2 Results and Discussion

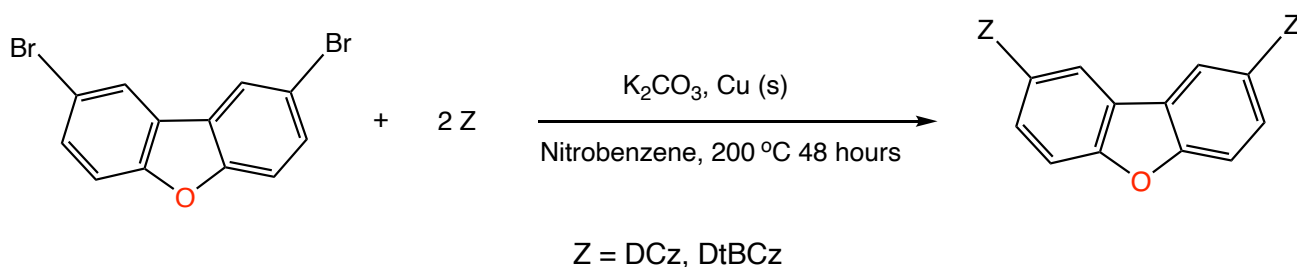
3.2.1 Synthesis and Characterization of EtDBF (3.1) and EtDBFDP (3.2)

The molecular structure of the previously prepared $[(Cu_2E)_x(dbfdp)_y]$ complexes by the *Corrigan* group could not be obtained as the single crystals were micrometer in size and could not be measured.^[19] These compounds had low solubility in organic solvents and so recrystallization attempts to grow bigger crystals was not successful. Therefore, the incorporation of the substituted phosphine presented as an attractive route to synthesize (Cu_2E) clusters. It was hypothesized that the substitution in the backbone of the dibenzofuran (DBF) would result in changes in solubility and / or different crystal packing which could possibly result in single crystals of suitable size to determine the molecular structure. Multiple attempts were made to synthesize the substituted dibenzofuran DCzDBF (**III.III**) and DtBCzDBF (**III.IV**) reported by *Xie* and *co-workers*^[20] in order to incorporate these into the previously prepared $(Cu_2E)_x(dbfdp)_y$ clusters. The first step was to brominate the 2 and 8 positions on the dibenzofuran ring as shown in *Scheme 3.1*.^[20]



Scheme 3.1: Synthesis of 2,8 - dibromo - dibenzofuran.^[20]

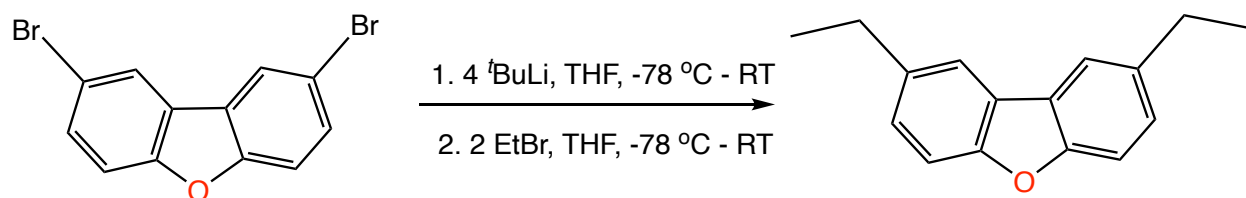
Once the dibenzofuran ring was brominated, the carbazole / *tert*-butyl-carbazole was added in nitrobenzene with copper powder and potassium carbonate and refluxed for 48 hours as shown in *Scheme 3.2*.^[20]



Scheme 3.2: Synthesis of carbazole substituted dibenzofuran.^[20]

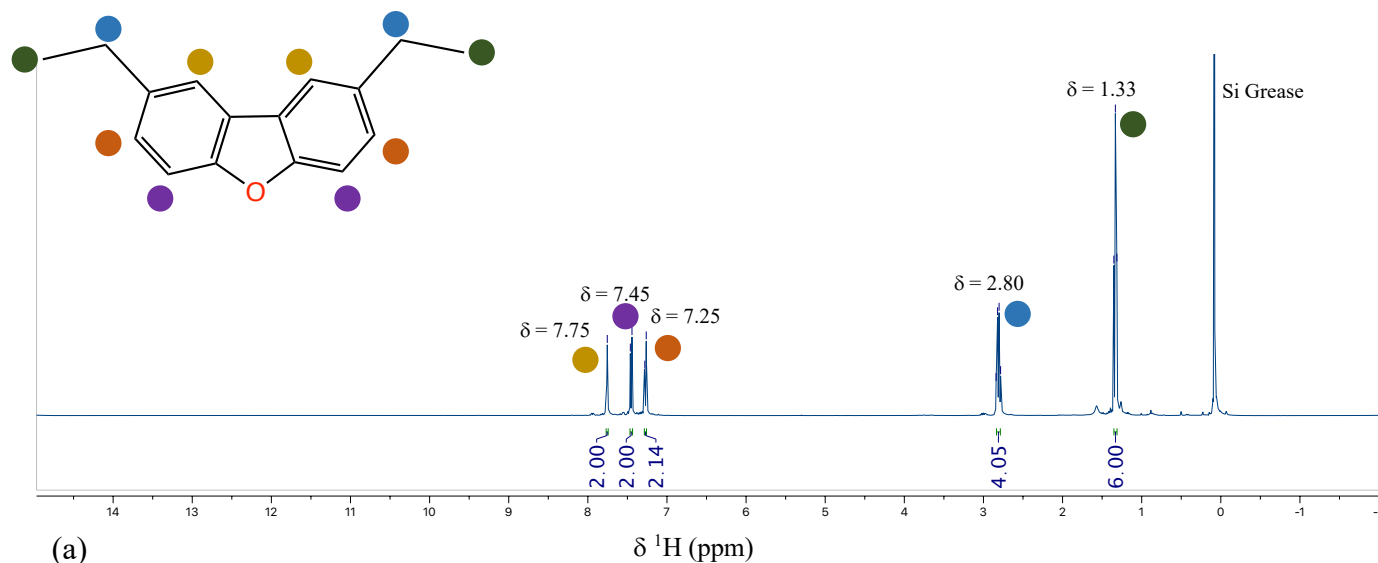
Once synthesized, multiple attempts were made to purify the product through precipitation, extraction and column chromatography, but (III.III) or (III.IV) could not be obtained in high purity or yields. Since (III.III) and (III.IV) could not be obtained in high purity, (III.V) and (III.VI) could also not be synthesized and therefore, (III.V) and (III.VI) could not be incorporated in Cu₂E clusters.

Since the substitution on the 2,8 positions of the dibenzofuran ring with carbazole / *tert*-butyl carbazole failed, an attempt was made to form a Grignard with the 2,8-dibromo-dibenzofuran to introduce a simple ethyl group. Unfortunately, 2,8-dibenzofuran would not form a Grignard. A Wurtz Fitting reaction with Na⁰ and a lithium halogen reaction with Li⁰ followed by the addition of bromoethane were also tried but did not result in a clean substitution. However, the organolithium reagent, ^tBuLi was used which resulted in a lithium halogen exchange under the conditions outlined in *Scheme 3.3*. This was then followed by the addition of EtBr and resulted in a clean substitution with good yields (93 %) of EtDBF (**3.1**) as shown in *Scheme 3.3*.



Scheme 3.3: Synthesis of 2,8-diethyl-dibenzofuran (EtDBF) (3.1).

The ¹H NMR spectrum of (**3.1**) confirmed the presence of the ethyl protons in the aliphatic region together with aromatic proton signals. A ¹³C{¹H} NMR spectrum is also attached in **Appendix 3.1** as *Figure S3.1*.



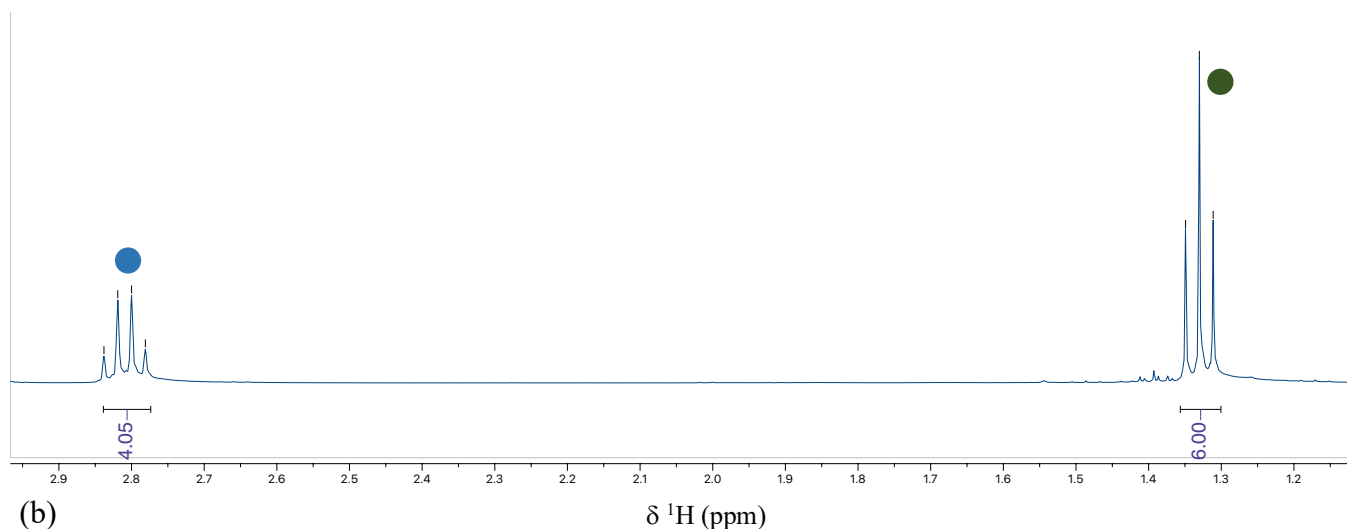
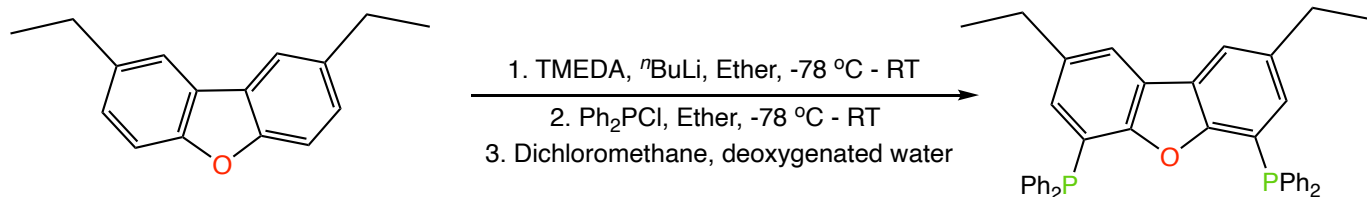


Figure 3.4: (a) ^1H NMR spectrum (CDCl_3): EtDBF (**3.1**) (b) Zoomed in aliphatic region of EtDBF (**3.1**) displaying the triplet and the quartet multiplicities of the ethyl group.

To prepare the substituted phosphine, $n\text{BuLi}$ with tetramethylethylenediamine (TMEDA) was added to the solution of (**3.1**) in order to deprotonate at the 4,6 positions. This was followed by the addition of the chlorodiphenylphosphine (PPh_2Cl) resulting in EtDBFDP (**3.2**) (shown in Scheme 3.4) with yields of 40 %.^[18]



Scheme 3.4: Synthesis of 2,8-diethyl(4,6 - bis-(diphenylphosphino))dibenzofuran (EtDBFDP) (**3.2**).^[18]

The $^{31}\text{P}\{^1\text{H}\}$ NMR spectrum of (**3.2**) showed a single peak at -16 ppm corresponding to one environment for the phosphorus centre (Figure 3.5). A similar chemical shift at -16 ppm was observed for the unsubstituted DBFDP.^[18] The ^1H , $^{13}\text{C}\{^1\text{H}\}$ and $^{31}\text{P}\{^1\text{H}\}$ spectra are attached in Appendix 3.1 as Figure S3.2, S3.3 and S3.4.

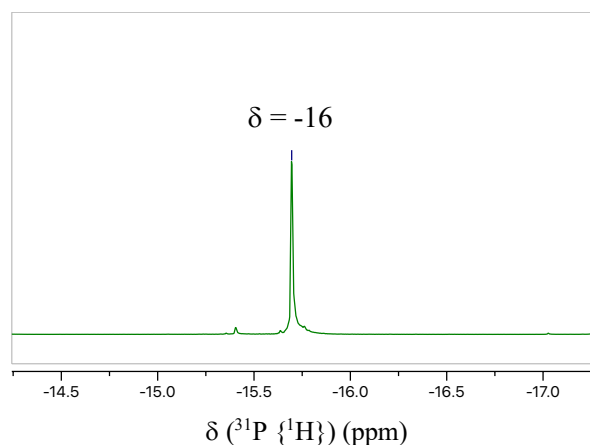


Figure 3.5: ^{31}P $\{^1\text{H}\}$ NMR spectrum (CDCl_3): EtDBFDP (**3.2**) δ : -16 ppm.

3.2.2 Synthesis and Characterization of $[\text{Cu}_{12}\text{Se}_6(\text{etdbfdp})_4]$ (**3.3**)

It has been shown recently that DBFDP acts as a bidentate phosphine ligand when reacted with CuOAc resulting in $[(\text{CuOAc})_2(\text{dfbdp})_2]$ (**III.IX**).^[19] The Cu centres have a distorted tetrahedral coordination due to the bonding with two P atoms and two bridging O from the acetate ligands, as shown in Figure 3.6.^[19] Since there are no structural changes made at the phosphorus atoms, EtDBFDP (**3.2**) should also behave in a similar way and should act as a bidentate phosphine ligand when reacted with CuOAc. Compound (**3.2**) in a similar fashion, was therefore reacted with one equivalent of CuOAc in THF to yield a clear and colourless solution. It is well documented that phosphine ligated CuOAc reacts with chalcogen reagents with $-\text{SiMe}_3$ moieties.^{[5][6][12][23]} The reaction between the AcO-SiMe_3 drives the reaction forward resulting in a Cu_2E core which phosphine ligands present at the periphery.

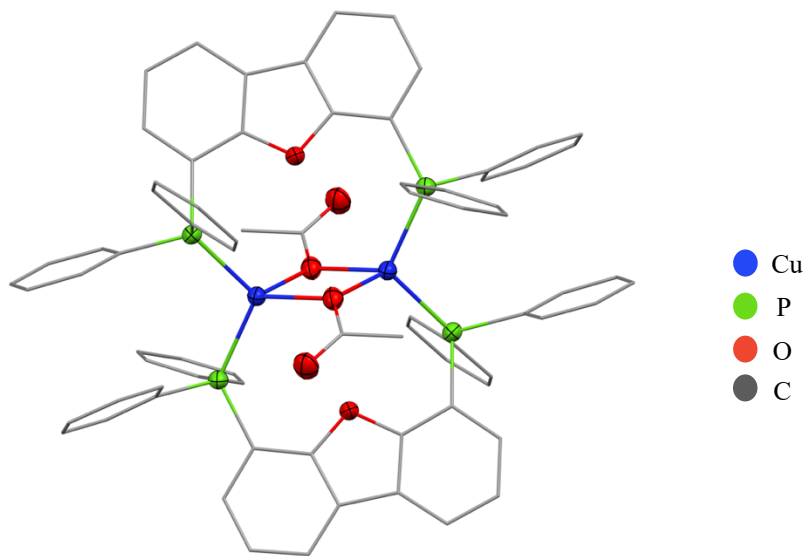
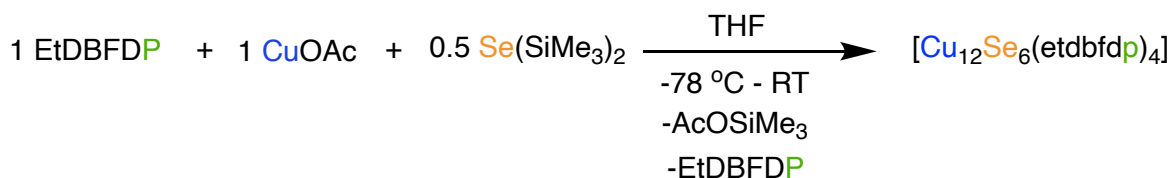


Figure 3.6: Molecular structure of $[(\text{CuOAc})_2(\text{dfbdp})_2]$ (**III.IX**) (H atoms are omitted for clarity).^[19]

This represented a good entry point for the preparation of copper chalcogenide complexes containing the EtDBFDP (**3.2**) ligand. The synthesis of complex (**3.3**) was done by adding 0.5 equivalents of Se(SiMe₃)₂ to solutions of (**3.2**) with CuOAc in THF, as shown in *Scheme 3.5*.



*Scheme 3.5: Synthesis of [Cu₁₂Se₆(etdbfdp)₄] (**3.3**).*

The colour of the solution changed from colourless to pale yellow to orange as the solution warmed to -20 °C. The reaction solution was then layered with heptane at this temperature. Red - orange crystals with red luminescence formed after 2 - 3 days. The warming of the reaction solution of (**3.3**) to room temperature resulted in a brown coloured solution with no luminescence which indicated the formation of bulk Cu₂Se which can be common for copper chalcogenide clusters left in solution at room temperature.^{[17][24][25]}

The molecular structure of (**3.3**) was determined by single crystal X - ray diffraction. Complex (**3.3**) crystallizes in the monoclinic space group P2₁/c and Z of 2. In (**3.3**), all Se atoms have a μ₄ coordination geometry and form a near to ideal octahedron with the Cu centres bridging at the edges. Eight Cu centres have a trigonal planar geometry due to bonding with one phosphorus and two bridging Se. The other four Cu centres in the middle of the core have a linear coordination geometry due to bonding to two bridging selenium as shown in *Figure 3.7*. Interestingly, the Cu₂E core for (**3.3**) is isostructural to [Cu₁₂Se₆(dppo)₄] (**III.X**) (*Figure 3.8*) (dppo = diphenylphosphinooctane) reported by *Eichhöfer* and *co - workers* with slightly different geometric parameters.^[17]

Compound (**III.X**) also has a near to ideal octahedron formed of the Se atoms with Cu bridging the edges.^[17] The bond lengths reported for the 8 Cu atom in the corners bonded to Se and P in [Cu₁₂Se₆(dppo)₄] (**III.X**) range between 2.355(2) - 2.458(2) Å while the Cu-Se distances in the middle of the core range between 2.295(1) - 2.307(2) Å.^[17] The bond lengths for the analogous Cu-Se bonds for (**3.3**) range between 2.3606(14) - 2.4632(16) Å while the Cu-Se bonds in the middle of the core range between 2.2705(14) - 2.3186(16) Å. All of the bond lengths for (**3.3**) are well within the range to the ones reported.

For **(3.3)**, the distances between pairs of Cu centres bonded to the same phosphine ligand, (Cu(1)-Cu(2) and Cu(3)-Cu(4)) are 2.9563(17) Å and 2.8771(17) Å. The distances between the other two Cu pairs, (Cu(1)-Cu(3) and Cu(2)-Cu(4)) are 2.9868(15) Å and 2.8484(15) Å. These distances show no presence of cuprophilic interactions. The analogous distances observed in **(III.X)**^[17], (2.8953(17) - 3.0412(19) Å) are on average longer than those observed for **(3.3)**. This may be due to incorporating the bidentate EtDBFDP **(3.2)** because it pinches the two adjacent metal centres closer together resulting in shorter distances. Whereas, the phosphine in **(III.X)**, bonds to metal centres on opposite ends (vertically) resulting in larger distances between adjacent Cu atoms.^[17] These shorter bond lengths within the cluster of **(3.3)** could result in more rigidity in the cluster. Cu...Cu distances of the central 4 Cu atoms and the adjacent 4 Cu atoms range between 2.5966(16) - 2.8477(16) Å indicating the presence of cuprophilic interactions.

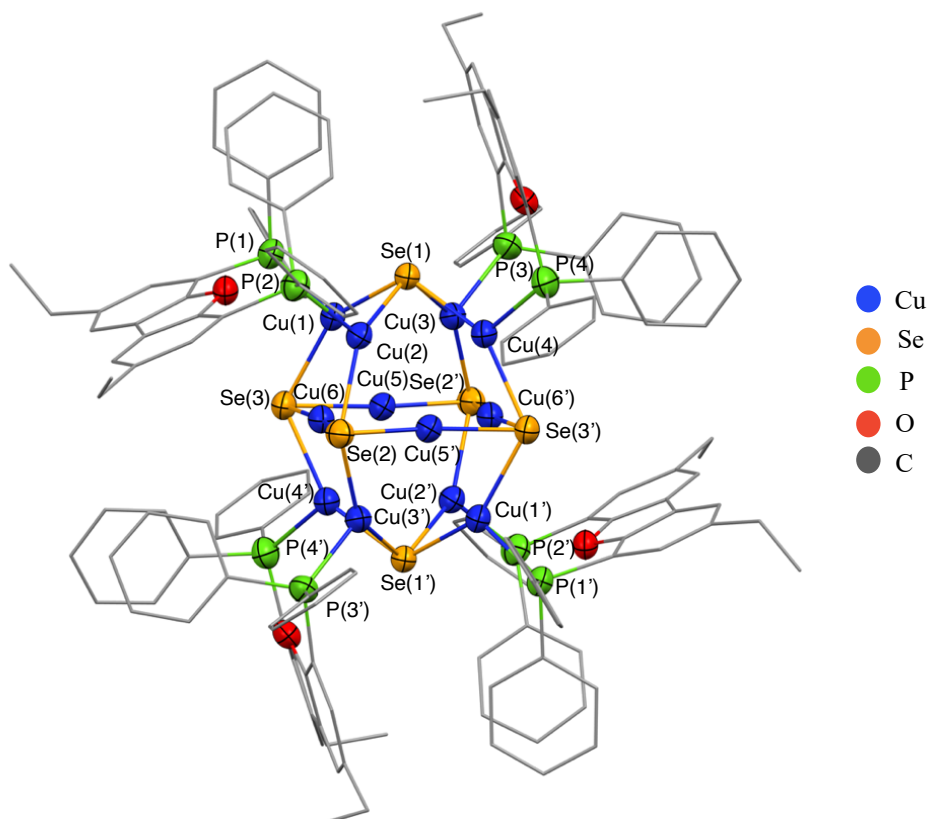


Figure 3.7: Molecular structure of $[\text{Cu}_{12}\text{Se}_6(\text{dbfdp})_4]$ (**3.3**) in the crystal (Cu - Se: 2.2705(14) - 2.4632(16) Å, Cu - P: 2.298(3) - 2.318(3) Å, Cu...Cu: 2.5966(16) - 2.9868(15) Å) (H atoms are omitted for clarity). (The molecule resides about a crystallographic inversion centre).

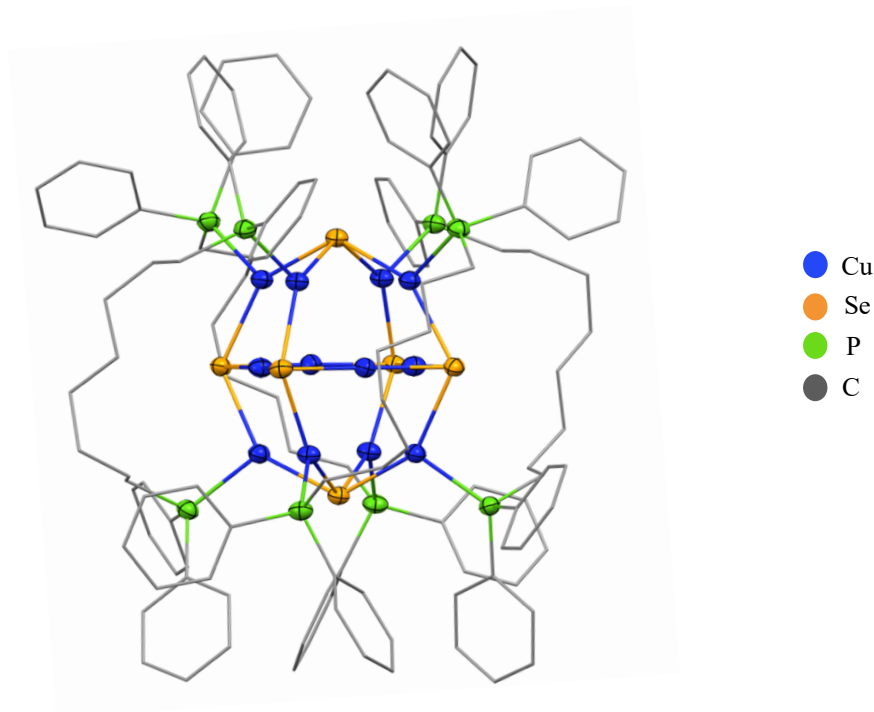
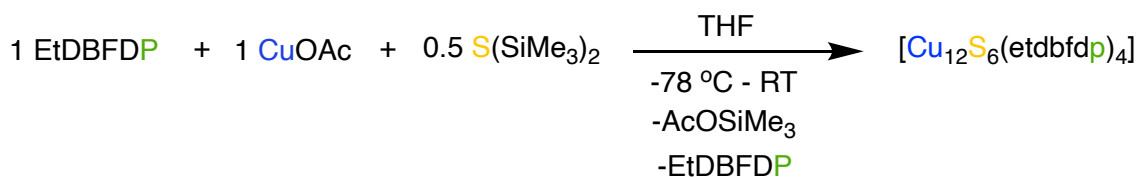


Figure 3.8: Molecular structure of $[Cu_{12}Se_6(dppo)_4]$ (**III.X**).^[17]

3.2.3 Synthesis and Characterization of $[Cu_{12}S_6(etdbfdp)_4]$ (**3.4**)

The synthesis of (**3.4**) was attempted by adding 0.5 equivalents of $S(SiMe_3)_2$ to solutions of (**3.2**) with $CuOAc$ in THF, as shown in *Scheme 3.6*.



*Scheme 3.6: Synthesis of $[Cu_{12}S_6(etdbfdp)_4]$ (**3.4**).*

The addition of $S(SiMe_3)_2$ at $-78 \text{ }^\circ\text{C}$ to solutions of (**3.2**) with $CuOAc$ results in a reaction between OAc and $SiMe_3$ resulting in the formation of a $(Cu_2S)_x$ core and the elimination of the silane. The colour of the solution changed from colourless to pale yellow to deep yellow as the solution warmed to $-20 \text{ }^\circ\text{C}$. The reaction solution was placed at $-20 \text{ }^\circ\text{C}$ overnight and layered with heptane at this temperature. Red - orange crystals exhibiting red luminescence formed after 3 - 4 days together with copious amounts of colourless precipitate. The precipitate likely indicates the presence of unreacted $CuOAc$ / phosphine which would mean that the complete reaction to form (**3.4**) requires further probing in terms of temperatures and time. The solution of (**3.2**) and $CuOAc$ with $S(SiMe_3)_2$ was also warmed to room temperature but only resulted in a brown coloured solution (similar to the reaction solution of $Se(SiMe_3)_2$) with no luminescence

indicating the formation of the bulk Cu₂S. This is common for copper chalcogenide clusters left in solution at room temperature.^{[17][24][25]}

A full analysis of the molecular structure of **(3.4)** is still required. X - ray diffraction data of poorly scattering crystals show that it is isostructural to [Cu₁₂Se₆(etdfdp)₄] **(3.3)**. The data are not reported in this thesis. However, the measured cell constants are reported in the experimental section. It has been previously shown that when using a different chalcogen with Cu and the same phosphine, it can result in isostructural molecular structures. Replacing Se with S in [Cu₁₂E₆(dppo)₄] results in [Cu₁₂S₆(dppo)₄] **(III.XI)** with slight geometric differences such as shorter Cu-E bond lengths due to the small covalent radii of S (1.03 Å) compared to Se (1.16 Å).^{[8][17]} A similar observation is made for **(3.4)** where the molecular structure of the sulfide analog is isostructural to **(3.3)** with the same cell constants.

3.2.4 Photophysical Properties of [Cu₁₂Se₆(etdbfdp)₄] (3.3) and [Cu₁₂S₆(etdbfdp)₄] (3.4)

It has been previously reported that the use of DFBDP results in strong luminescence behaviour in stable copper (I) iodide clusters.^[18] The ability of DBFDP to bridge to two Cu atoms and the rigidity of the cluster results in efficient luminescence of [Cu₄I₄(dbfdp)₂] **(III.II)**.^[18] DBFDP was also previously used to synthesize copper chalcogenide clusters [(Cu₂E)_x(dbfdp)_y] which resulted in orange crystals with bright red luminescence. These complexes had PLQYs of ~4 % but suitable sized crystals could not be obtained to determine their molecular structure.^[19] Therefore, **(3.2)** was used to synthesize copper chalcogenide clusters in an attempt to produce crystals of suitable size to determine the molecular structure of these complexes while also determining how the photophysical properties were affected.

It was observed that the reaction solution of **(3.2)** and CuOAc did not have significant luminescence. When Se(SiMe₃)₂ was added at cold (-78 °C) temperatures, it resulted in an instant change in luminescence. The appearance of luminescence in the reaction solutions as well as the change in luminescence with rising temperatures serves as an indication that a reaction is taking place. The reaction solution was similarly emissive for both wavelengths ($\lambda_{\text{exc}} = 254 \text{ nm}$ and 365 nm) when irradiated with the handheld UV lamp. The solution exhibited yellow luminescence between reaction temperatures of -70 °C and -20 °C (*Figure 3.9(a)*). As the reaction solution warmed, the luminescence became a brighter yellow - orange and at -20 °C, the luminescence of the solution was bright orange.

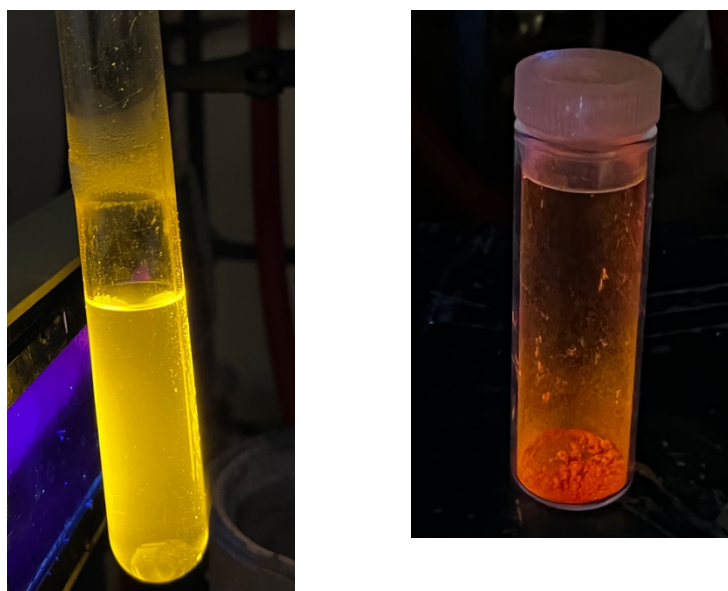


Figure 3.9: (a) Emission of the reaction mixture of EtDBFDP (**3.2**) with CuOAc and Se(SiMe₃)₂ in THF at -40 °C (b) Emission of crystals of [Cu₁₂Se₆(etdbfdp)₄] (**3.4**) (Qualitative observation of the emission of the reaction solution and solid - state samples at room temperature when irradiated at 365 nm).

The reaction solution was layered with heptane at -20 °C and resulted in red - orange crystals of (**3.3**) with red luminescence when irradiated with the UV lamp (254 nm and 365 nm) (Figure 3.9 (b)). The colour of the crystals as well as the qualitative observation of the luminescence is consistent with phosphine stabilized copper selenide crystals, as reported by Eichhöfer and co - workers.^[17] Compound (**III.X**) also form as red crystals with bright red luminescence. λ_{exc} for (**3.3**) were determined to be 425 nm, 475 nm, and 520 nm with $\lambda_{em} = 653$ nm as these excitation wavelengths resulted in the highest intensity of emission at 653 nm. Out of the three determined excitation wavelengths, $\lambda_{exc} = 475$ nm resulted in the highest intensity for $\lambda_{em} = 653$ nm. The excitation and the emission spectra for (**3.3**) are shown in Figure 3.10 and Figure 3.11, respectively. This contrasts to the $\lambda_{exc} = 350$ nm which results in the highest intensity λ_{em} at 638 nm for [Cu₁₂Se₆(dppo)₄] (**III.X**) (dppo = diphenylphosphinoctane) with PLQYs of 53 %.^[17] The drastic difference in the λ_{exc} resulting in a similar λ_{em} of (**3.3**) to (**III.X**) may be due to the incorporation of EtDBFDP (**3.2**) as the phosphine is the key difference between (**3.3**) (incorporates EtDBFDP (**3.2**)) and (**III.X**) (incorporates dppo). (**3.2**) has low lying empty π^* orbitals compared to dppo and therefore the transitions in (**3.3**) require less energy (longer wavelength) to result in a similar emission wavelength. A full analysis of the photophysical properties of (**3.3**) will be conducted.

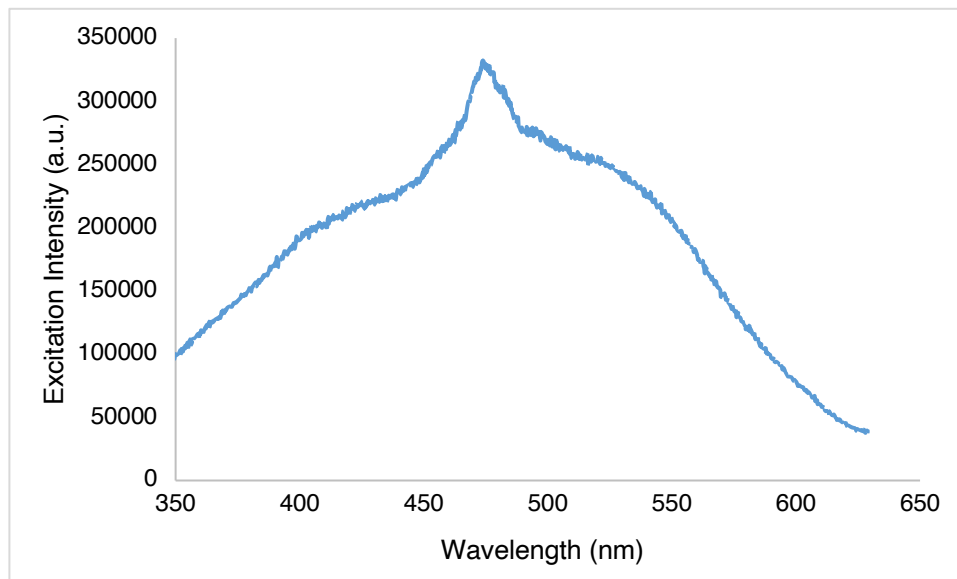


Figure 3.10: Excitation spectrum of $[Cu_{12}Se_6(etdbfdp)_4]$ (**3.3**) in the solid state at room temperature. The selected $\lambda_{exc(max)}$ for this complex is at 475 nm.

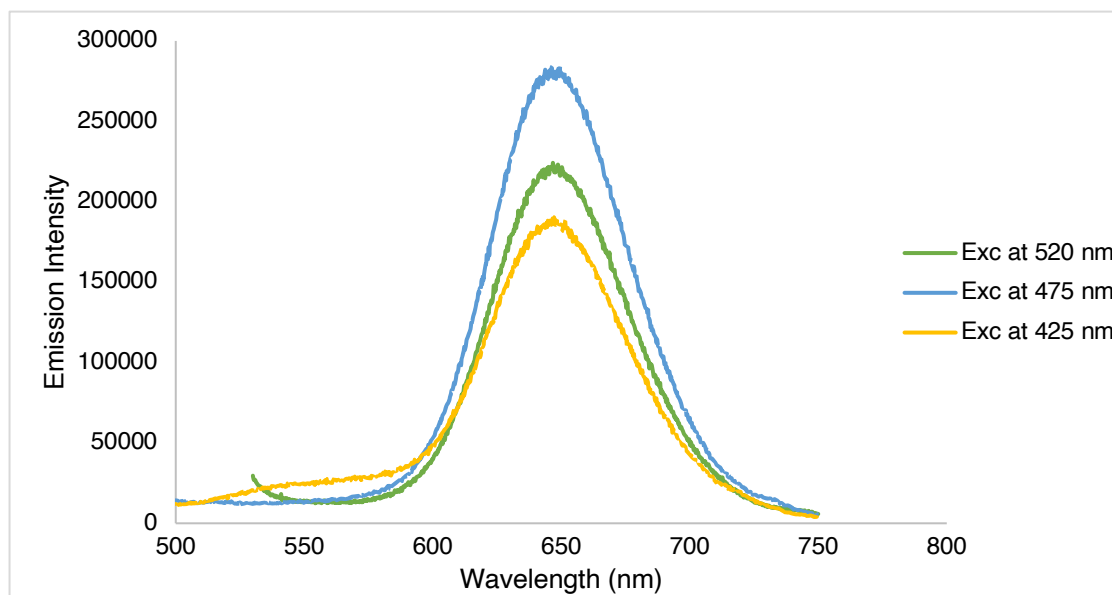


Figure 3.11: Emission spectra of $[Cu_{12}Se_6(etdbfdp)_4]$ (**3.3**) in the solid state at room temperature. The highest intensity for λ_{em} (653 nm) is when the sample is irradiated at 475 nm.

Similarly, the reaction solution of (**3.2**) and CuOAc with $S(SiMe_3)_2$ displayed luminescence as the chalcogen was added. The solution was emissive at both wavelengths ($\lambda = 254$ nm and 365 nm) when irradiated with the handheld UV lamp. The solution exhibited yellow luminescence between reaction

temperatures of $-70\text{ }^{\circ}\text{C}$ and $-20\text{ }^{\circ}\text{C}$ (Figure 3.12). Compared to the solution of (3.2) and CuOAc with $\text{Se}(\text{SiMe}_3)_2$, the luminescence for the solution of (3.2) and CuOAc with $\text{S}(\text{SiMe}_3)_2$ was more yellow in colour. As the reaction solution warmed to $-20\text{ }^{\circ}\text{C}$, the luminescence became a brighter yellow. This difference in luminescence between the reaction solutions of (3.3) and (3.4) could be due to the difference in the chalcogen used or due to an incomplete reaction as mentioned earlier.

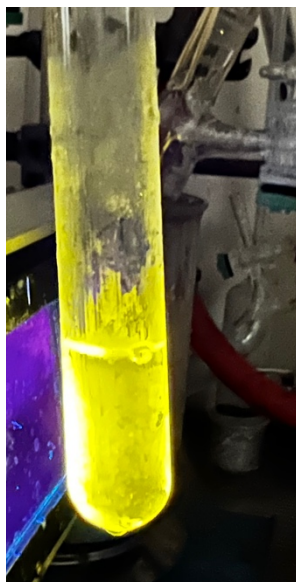


Figure 3.12: Emission of the reaction mixture solution of EtDBFDP (3.2) and CuOAc with $\text{S}(\text{SiMe}_3)_2$ in THF at $-40\text{ }^{\circ}\text{C}$ with a handheld UV lamp. (Qualitative observation of the emission of the reaction solution when irradiated at 365 nm).

Similar to (3.3), when reaction solutions of (3.2) and CuOAc with $\text{S}(\text{SiMe}_3)_2$ were warmed to room temperature, they also became brown in colour with no visible luminescence likely indicating the presence of copper sulfide. Since the solution was unstable at room temperatures, it was layered with heptane at $-20\text{ }^{\circ}\text{C}$ which resulted in red - orange crystals of with red luminescence when irradiated with the UV lamp (254 nm and 365 nm). A full X - ray structural and photophysical analysis on the crystals will be conducted. The colour of the crystals as well as the luminescence observed is again consistent with phosphine stabilized copper sulfide crystals reported by Eichhöfer and co - workers.^[17] For example, the complexes $[\text{Cu}_{12}\text{S}_6(\text{dpppt})_4]$ (III.XII) (dpppt = diphenylphosphinopentane) and $[\text{Cu}_{12}\text{S}_6(\text{dppo})_4]$ (III.XI) (dppo = diphenylphosphinoctane) also crystallize as red - orange crystals. These complexes also have bright red luminescence at ambient temperature with emissions at 648 nm and 665 nm, respectively.^[17] The reported complexes also had PLQYs of up to 48 % and 67 %, respectively.^[17]

3.3 Experimental

3.3.1 General Considerations

All experiments were carried out under an inert atmosphere of high purity, dried nitrogen using standard Schlenk line techniques on a double manifold vacuum line. All solvents used were either distilled over the appropriate desiccant under nitrogen or were dried by using a commercial Mbraun MB - SP series solvent purification system.

Dibenzofuran (TCI America), bromine (Alfa Aesar), *tert* - butyl - lithium (Sigma Aldrich), bromoethane (Sigma Aldrich), chlorodiphenylphosphine (TCI America) and *n* - butyllithium (Acros Organics) were purchased and used without further purification. Tetramethylethylenediamine (TMEDA) was refluxed over KOH pellets for three hours and distilled under nitrogen according to the literature procedure.^[27] Copper (I) acetate, *bis*(trimethylsilyl)sulfide and *bis*(trimethylsilyl)selenide were synthesized by a colleague using literature procedures and were used without further purification.^{[28][29]} 2,8 - dibromodibenzofuran was synthesized according to the literature procedure.^[20]

¹H, ³¹P{¹H}, ¹³C{¹H} NMR spectra were recorded on the Bruker AvanceIII HD 400 (B400) with frequencies of 400.130 MHz, 161.976 MHz and 100.613 MHz respectively. The ¹H NMR spectra were referenced to the residual proton solvent in CDCl₃. The ¹³C{¹H} NMR spectra were referenced to the carbon atoms in CDCl₃. The ³¹P{¹H} NMR spectra were referenced to the 85 % H₃PO₄.

Single crystal X - ray data collection were completed by Dr. John F. Corrigan on a Bruker Kappa Axis Apex2 diffractometer at a temperature of 110 K. The sample was placed on a Mitegen polyimide micromount with a small amount of Paratone N oil. The raw data were scaled, and absorption corrected using SADABS and the frame integration was done by SAINT.^{[30][31]} SHELXT program was used to solve the structure.^[32] All hydrogen atoms were obtained from the initial solution, introduced at idealized positions and were allowed to ride on the parent atom. The structural model was fit to the data by full matrix least squares based on F^2 . The structure was further refined using the SHELXL program from the SHELXTL suite of crystallographic software.^[33]

3.3.2 Synthesis of EtDBF (3.1)

2,8 - dibromodibenzofuran (1.24 g, 3.83 mmol, 1.00 equiv.) was dissolved in 150 mL of THF and stirred at room temperature for a few minutes. ^tBuLi (15.3 mL, 15.3 mmol, 4.00 equiv.) was then added dropwise to the cold (-78 °C) reaction solution which resulted in a yellow solution. As the reaction warmed to room

temperature, the colour of the solution turned brown - yellow with a colourless - beige precipitate. The solution was then cooled again to $-78\text{ }^{\circ}\text{C}$ and EtBr (0.850 mL, 11.5 mmol, 3.00 equiv.) was added dropwise while stirring. This resulted in an instant colour change to pale yellow with colourless precipitate. At room temperature, the solution was clear and yellow in colour. 50 mL of deoxygenated water was added to the reaction solution and the THF was removed under vacuum. The product was then extracted with DCM (3 x 30 mL) and further dried using MgSO_4 . Solvent was then removed which resulted in **(3.1)** as a yellow oil. (0.80 g, 93 % yield). ^1H NMR (400 MHz, CDCl_3 , $23.5\text{ }^{\circ}\text{C}$): $\delta = 7.75$ (s, 2H), 7.45 (d, 2H $J = 8.5$ Hz), 7.25 (d, 2H, $J = 9.1$ Hz), 2.80 (q, 4H, $J = 7.6$ Hz), 1.33 (t, 6H, $J = 7.6$ Hz). $^{13}\text{C}\{^1\text{H}\}$ NMR (400 MHz, CDCl_3 , $23.5\text{ }^{\circ}\text{C}$): $\delta = 155.1, 138.8, 127.1, 124.4, 119.5, 111.3, 29.0, 16.5$. ^1H , and $^{13}\text{C}\{^1\text{H}\}$ NMR spectra are attached in the Appendix. ^1H and $^{13}\text{C}\{^1\text{H}\}$ chemical shifts match the literature values.^[34]

3.3.3 Synthesis of EtDBFDP (3.2)

(3.2) was synthesized using similar literature procedures as used for DBFDP.^[18]

(3.1) (0.80 g, 3.50 mmol, 1.00 equiv.) was dissolved in 50 mL of diethyl ether and stirred at room temperature for a few minutes. TMEDA (1.58 mL, 10.6 mmol, 3.00 equiv.) was added to the stirring solution at room temperature. $n\text{BuLi}$ (6.93 mL, 10.6 mmol, 3.00 equiv.) was then added dropwise to the cold ($-78\text{ }^{\circ}\text{C}$) reaction solution which resulted in a yellow solution at cold temperatures. The solution was then warmed to room temperature and stirred overnight which resulted in a clear orange solution. PPh_2Cl (2.08 mL, 11.6 mmol, 3.30 equiv.) in 20 mL of diethyl ether was added dropwise to the cold ($-78\text{ }^{\circ}\text{C}$) reaction solution which resulted in a yellow solution with colourless precipitate. The solution was then warmed to room temperature and stirred overnight which resulted in an orange solution with colourless precipitate. The solvent was then removed under vacuum which resulted in a yellow oil with colourless precipitate. The oil and the precipitate were dissolved in DCM and the organic layer was extracted with DCM and water (3 x 30 mL). 50 mL of hexanes were added to the solution and the precipitate was filtered. The solvent was then removed under vacuum which resulted in a yellow oil. The yellow oil was purified by flash column chromatography (DCM) which resulted in a flaky white powder. (0.83 g, 40 % yield). ^1H NMR (400 MHz, CDCl_3 , $23.5\text{ }^{\circ}\text{C}$): $\delta = 7.72$ (s, 2H), 7.28-7.18 (m, 24H), 6.91 (d, 2H, $J = 7.2$ Hz), 2.65 (q, 4H, $J = 7.6$ Hz), 1.18 (t, 6H, $J = 7.6$ Hz). $^{13}\text{C}\{^1\text{H}\}$ NMR (400 MHz, CDCl_3 , $23.5\text{ }^{\circ}\text{C}$): $\delta = 157.0, 139.1, 136.1, 132.3, 128.7, 123.8, 120.5, 28.9, 16.3$. $^{31}\text{P}\{^1\text{H}\}$ NMR (400 MHz, CDCl_3 , $23.5\text{ }^{\circ}\text{C}$): $\delta = -16$ ppm

3.3.4 Synthesis of $[\text{Cu}_{12}\text{Se}_6(\text{etdbfdp})_4]$ (3.3)

EtDBFDP **(3.2)** (0.095 g, 0.160 mmol, 1.00 equiv.) and CuOAc (0.020 g, 0.160 mmol, 1.00 equiv.) were stirred together for one hour in 20 mL of THF to yield a clear and colourless solution. $\text{Se}(\text{SiMe}_3)_2$ (0.020

mL, 0.090 mmol, 0.500 equiv.) was added to a stirring solution at -78 °C. The solution was slowly warmed to -20 °C with noticeable colour change from colourless to orange. The solution was layered with 40 mL of heptane and left at -20 °C. Red - orange crystals were observed after 3 - 4 days. (0.028 g, 56 % yield based on CuOAc). Crystal structure data, bond angles and bond lengths are attached in the **Appendix** in *Tables S3.1, S3.2 and S3.3*. $^{31}\text{P}\{^1\text{H}\}$ NMR: TBD (to be determined). ^1H NMR: TBD. m.p. = TBD. ATR - IR: TBD. Elemental Analysis: TBD. $\lambda_{\text{exc}} = 475 \text{ nm}$, $\lambda_{\text{em}} = 653 \text{ nm}$, PLQY = TBD.

3.3.5 Synthesis of $[\text{Cu}_{12}\text{S}_6(\text{etdbfdp})_4]$ (3.4)

EtDBFDP (**3.2**) (0.112 g, 0.190 mmol, 1.00 equiv.) and CuOAc (0.023 g, 0.190 mmol, 1.00 equiv.) were stirred together for one hour in 20 mL of THF to yield a clear and colourless solution. $\text{S}(\text{SiMe}_3)_2$ (0.020 mL, 0.090 mmol, 0.500 equiv.) was added to a stirring solution at -78 °C. The solution was slowly warmed to -20 °C with noticeable colour change from colourless to yellow. The solution was left undisturbed overnight in a freezer at -20 °C. The solution was layered with 40 mL of heptane after 24 hours and left at -20 °C. A few red - orange crystals together with copious amounts of colourless precipitate were observed after 5 - 6 days. (Cell constants: $a = 0.71073 \text{ \AA}$, $b = 18.6948 \text{ \AA}$, $c = 24.3083 \text{ \AA}$, $\alpha = 17.2523^\circ$, $\beta = 90.000^\circ$, $\gamma = 108.576^\circ$). Additional analysis will be conducted. Yield = TBD. $^{31}\text{P}\{^1\text{H}\}$ NMR: TBD. ^1H NMR: TBD. m.p. = TBD. ATR-IR: TBD. Elemental Analysis: TBD. $\lambda_{\text{exc}} = \text{TBD}$, $\lambda_{\text{em}} = \text{TBD}$, PLQY = TBD.

3.4 Conclusions

In summary, a novel procedure was used to synthesize EtDBF (**3.1**) with good yields of up to 93 %. EtDBF (**3.1**) was used to synthesize EtDBFDP (**3.2**) which was further reacted with CuOAc followed by the addition of Se(SiMe₃)₂ and S(SiMe₃)₂ as the phosphine stabilized copper complexes are good entry points for the trimethylsilylchalcogenide reagents.^{[5][6][12][23]} The addition of E(SiMe₃)₂ (E = S, Se) to solutions of (**3.2**) with CuOAc resulted in [Cu₁₂Se₆(dbfdp)₄] (**3.3**) and [Cu₁₂S₆(dbfdp)₄] (**3.4**). The reaction solution of Se(SiMe₃)₂ and (**3.2**) with CuOAc was clear and yellow at low temperatures with bright yellow luminescence indicating reaction progression. At -20 °C, this reaction solution was orange in colour with orange luminescence. When crystallized at -20 °C, the crystals of (**3.3**) were red - orange in colour with red - orange luminescence. The full determination of the molecular structure of the complex synthesized by the addition of S(SiMe₃)₂ to solutions of (**3.2**) with CuOAc is still under progress but the preliminary data shows an isostructural compound of formula [Cu₁₂S₆(dbfdp)₄] (**3.4**). When compared, the reaction solution of S(SiMe₃)₂ and (**3.2**) with CuOAc was also clear and yellow at low temperatures with bright yellow luminescence. This reaction solution stayed yellow in colour with yellow luminescence at -20 °C. The difference in luminescence for (**3.3**) could be due to the incomplete reaction. When crystallized, it also resulted in a few red - orange crystals of (**3.4**) with red - orange luminescence with copious amounts of precipitate. The qualitative observations for the red crystals of (**3.3**) and (**3.4**) are consistent with the other phosphine ligated copper selenide / sulfide clusters reported in literature.^{[8][17]} Complexes such as reported [Cu₁₂Se₆(dppo)₄] (**III.X**), [Cu₁₂S₆(dpppt)₄] (**III.XII**) and [Cu₁₂S₆(dppo)₄] (**III.XI**) also crystallize as red crystals at low temperatures with bright red luminescence with PLQYs of up to 63 % at room temperature.^{[8][17]} Moreover, the DBFDP stabilized copper chalcogenide complexes previously prepared by the *Corrigan* group also crystallized as red - orange crystals with bright red luminescence with PLQYs of up to ~4 %, but due to their high insolubility, the molecular structures of these complexes could not be obtained.^[19] The incorporation of (**3.2**) in Cu₂E (E = S, Se) clusters shows very similar results as seen in the literature^{[8][17]} and the *Corrigan* lab.^[19] The $\lambda_{\text{exc}} = 475$ nm of (**3.3**) shows a drastic bathochromic shift compared to the $\lambda_{\text{exc}} = 350$ nm of (**III.X**).^[17] Since the key difference between the two compounds is the phosphine, this significant change may be due to using the custom / tailored rigid bidentate phosphine ligand (**3.2**). Complexes (**3.3**) and (**3.4**) show promising results as luminescent materials and a complete analysis of the photophysical properties (emission, excitation, PLQYs) of (**3.3**) and (**3.4**) will be conducted.

3.5 References

- [1] C. Latouche, C. W. Liu, J.Y. Saillard, *J. Clust. Sci.* **2014**, *25*, 147–171.
- [2] R. R. Arvizo, S. Bhattacharyya, R. A. Kudgus, K. Giri, R. Bhattacharya, P. Mukherjee, *Chem. Soc. Rev.* **2012**, *41*, 2943–2970.
- [3] H. W. Chang, R. Y. Shiu, C. S. Fang, J. H. Liao, P. V. V. N. Kishore, S. Kahlal, J. Y. Saillard, C. W. Liu, *J. Clust. Sci.* **2017**, *28*, 679–694.
- [4] R. S. Dhayal, J. H. Liao, Y. C. Liu, M. H. Chiang, S. Kahlal, J.Y. Saillard, C. W. Liu, *Angew. Chem. - Int. Ed.* **2015**, *54*, 1–6.
- [5] O. Fuhr, S. Dehnen, D. Fenske, *Chem. Soc. Rev.* **2013**, *42*, 1871–1906.
- [6] S. Dehnen, A. Eichhöfer, D. Fenske, *Eur. J. Inorg. Chem.* **2002**, *2002*, 279.
- [7] A. Chu, F. K. W. Hau, L. Y. Yao, V. W. W. Yam, *ACS Mater. Lett.* **2019**, *1*, 277–284.
- [8] X. X. Yang, I. Issac, S. Lebedkin, M. Kühn, F. Weigend, D. Fenske, O. Fuhr, A. Eichhöfer, *Chem. Commun.* **2014**, *50*, 11043–11045.
- [9] B. Hu, C. Y. Su, D. Fenske, O. Fuhr, *Inorg. Chim. Acta* **2014**, *419*, 118–123.
- [10] E. C. C. Cheng, W. Y. Lo, T. K. M. Lee, N. Zhu, V. W. W. Yam, *Inorg. Chem.* **2014**, *53*, 3854–3863.
- [11] V. W. W. Yam, K. K. W. Lo, *Comments Inorg. Chem.* **1997**, *19*, 209–229.
- [12] G. Schmid, *Nanoparticles: From Theory to Application*, **2004**, 109–112.
- [13] A. Deveson, S. Dehnen, D. Fenske, *Dalton Trans.* **1997**, 4491–4497.
- [14] M. W. DeGroot, J. F. Corrigan, *Organometallics* **2005**, *24*, 3378–3385.
- [15] D. G. MacDonald, J. F. Corrigan, *Philos. Trans. R. Soc. A Math. Phys. Eng. Sci.* **2010**, *368*, 1455–1472.
- [16] T. Duan, X. Z. Zhang, Q. F. Zhang, *Zeitschrift für Naturforsch. - Sect. B J. Chem. Sci.* **2008**, *63*, 941–944.
- [17] A. Eichhöfer, G. Buth, S. Lebedkin, M. Kühn, F. Weigend, *Inorg. Chem.* **2015**, *54*, 9413–9422.
- [18] M. Xie, C. Han, J. Zhang, G. Xie, H. Xu, *Chem. Mater.* **2017**, *29*, 6606–6610.
- [19] M. Nayyar, Chem 4491E Thesis: Luminescent Copper Chalcogenide Clusters, The University of Western Ontario **2020**.
- [20] M. Xie, C. Han, Q. Liang, J. Zhang, G. Xie, H. Xu, *Sci. Adv.* **2019**, *5*, 1–9.
- [21] K. K. R., *J. Am. Chem. Soc.* **1989**, *111*, 5005–5006.
- [22] M. Vitale, W. E. Palke, P. C. Ford, *J. Phys. Chem.* **1992**, *96*, 8329–8336.
- [23] A. M. Polgar, A. Zhang, F. Mack, F. Weigend, S. Lebedkin, M. J. Stillman, J. F. Corrigan, *Inorg.*

Chem. **2019**, *58*, 3338–3348.

- [24] M. L. Fu, I. Issac, D. Fenske, O. Fuhr, *Angew. Chem. - Int. Ed.* **2010**, *49*, 6899–6903.
- [25] S. Dehnen, *J. Clust. Sci.* **1996**, *7*, 351–369.
- [26] N. V. S. Harisomayajula, S. Makovetskyi, Y. C. Tsai, *Chem. - A Eur. J.* **2019**, *25*, 8936–8954.
- [27] W. L. F. Armarego, C. L. L. Chai, *Purification of Laboratory Chemicals*, **2013**.
- [28] D. A. Edwards, Roger Richards, *J. Chem. Soc. Dalton Trans.* **1973**, *22*, 2463–2468.
- [29] J. H. So, P. Boudjouk, *Synth.* **1989**, *1989*, 306–307.
- [30] Bruker-AXS, SADABS version 2012.1, **2012**, Bruker-AXS, Madison, WI 53711, USA
- [31] Bruker-AXS, SAINT version 2013.8, **2013**, Bruker-AXS, Madison, WI 53711, USA
- [32] Sheldrick, G. M., *Acta Cryst.* **2015**, *A71*, 3-8
- [33] Sheldrick, G. M., *Acta Cryst.* **2015**, *C71*, 3-8
- [34] L. Niu, H. Yang, Y. Jiang, H. Fu, *Adv. Synth. Catal.* **2013**, *355*, 3625–3632.

Chapter 4

4.0 Conclusions and Outlook

4.1 Summary and Conclusions

The work in this thesis discusses the preparation and analysis of Luminescent Group 11 Metal Chalcogen Clusters with Bidentate Phosphine Ligands.

Luminescent group 11 metal chalcogenolate clusters are synthesized by forming the precursors $[(\text{CuOAc})_2(\text{dbfdp})_2]^{[1]}$ (**2.1**), $[(\text{AgOAc})_2(\text{dbfdp})_2]^{[2]}$ (**2.2**) and solutions of DBFDP with CuCl. These precursors are further reacted with chalcogen reagents (PhESiMe_3) ($E = \text{S}, \text{Se}$) at low temperatures to form metal chalcogenolate clusters, $[\text{Cu}_4(\text{SePh})_4(\text{dbfdp})_2]$ (**2.3**), $[\text{Ag}_6(\text{SePh})_6(\text{dbfdp})_2]$ (**2.4**), $[\text{Cu}_5(\text{SPh})_5(\text{dbfdp})_2]$ (**2.5**), $[\text{Cu}_5(\text{SPh})_4\text{Cl}(\text{dbfdp})_2]$ (**2.6**), $[\text{Ag}_4(\text{SPh})_4(\text{dbfdp})_2]$ (**2.7**). Complexes (**2.3**) - (**2.7**) differ in structure from each other depending on the group 11 metal and the chalcogen. The number of metal atoms present in the clusters range from 4 - 6 while the chalcogenolates display μ_2 and μ_3 bridging modes (*Figure 4.1*). Interestingly, (**2.6**) has a chloride functionality that could be further reacted with chalcogen reagents to form mixed chalcogenolate / chalcogenide clusters.

The main theme seen throughout complexes (**2.3**) - (**2.7**) is the bonding of the phosphine to two metal centres which are bridged by the chalcogenolates. It was observed that the nuclearity and the dimensionality of these complexes depends heavily on the combination of the group 11 metal and the chalcogen used. As observed, compound $[\text{Cu}_4(\text{SePh})_4(\text{dbfdp})_2]$ (**2.3**) and $[\text{Ag}_6(\text{SePh})_6(\text{dbfdp})_2]$ (**2.4**) differ in the number of metal atoms (4 metal atoms for (**2.3**) and 6 metal atoms for (**2.4**)) when incorporating the same chalcogenolate (selenolate). This could be due to the larger size of the Ag atom which causes the Ag centres and the Se to spread out resulting in a bigger cluster. Comparing the core of (**2.3**) to the core of (**2.5**), the nuclearity of Cu increases (4 (**2.3**) vs. 5 (**2.5**)) when the chalcogen is changed from Se to S. As the size of S is smaller than Se, it could be possible that the incorporation of 5 metal atoms with 5 thiolates is needed in order to form a stable cluster core. Interestingly, when using thiolates with Ag, the number of Ag centres decreases to 4 as observed in (**2.7**) which may be due to the combination of the bigger sized Ag atom with the smaller sized bridging thiolate. In (**2.4**), the combination of larger sized Ag and Se resulted in a Ag_6 core, whereas in (**2.7**), the Ag with the smaller sized chalcogen (S) forms a Ag_4 core.

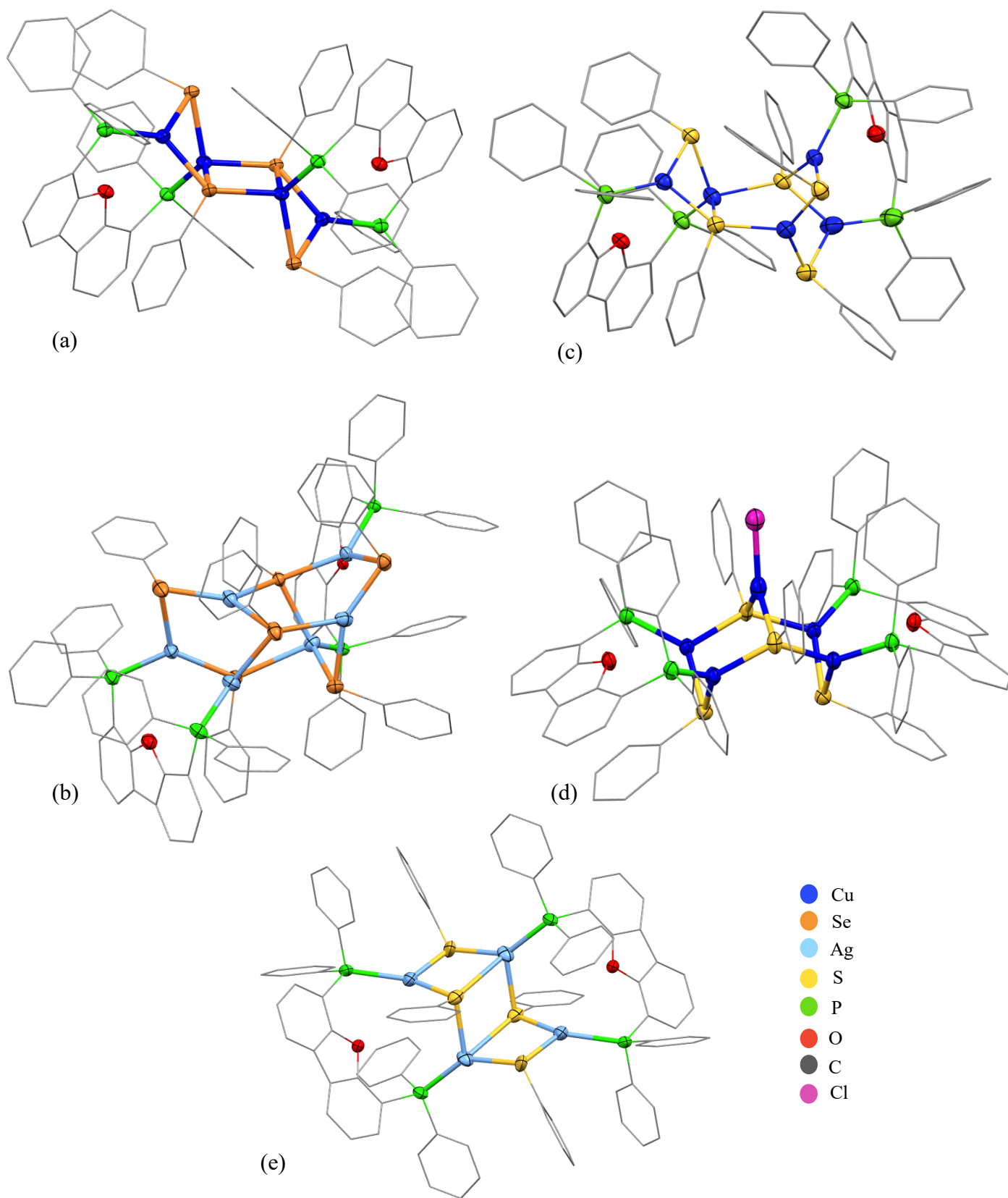


Figure 4.1: (a) Molecular structure $[\text{Cu}_4(\text{SePh})_4(\text{dbfdp})_2]$ (2.3), (b) $[\text{Ag}_6(\text{SePh})_6(\text{dbfdp})_2]$ (2.4), (c) $[\text{Cu}_5(\text{SPh})_5(\text{dbfdp})_2]$ (2.5), (d) $[\text{Cu}_5(\text{SPh})_4\text{Cl}(\text{dbfdp})_2]$ (2.6), (e) $[\text{Ag}_4(\text{SPh})_4(\text{dbfdp})_2]$ (2.7).

As observed with the reported compounds, the photophysical properties of **(2.3)** - **(2.7)** also depend on the combination of the metal and the chalcogen. Complexes containing Cu (**(2.3)** and **(2.5)**) have higher PLQYs compared to the ones with Ag (**(2.4)** and **(2.7)**). Compounds **(2.3)** and **(2.5)** have a PLQY of 34 % and 73 %, respectively whereas **(2.4)** and **(2.7)** have a PLQY of 5 % and 9 %, respectively. The chalcogen also affects the PLQYs significantly. The size of the cluster varies depending on the metal and the chalcogen. A trend for the chalcogen is seen. Compounds containing Se have lower PLQYs than the ones with S. **(2.3)** and **(2.5)** both incorporate Cu and differ in the chalcogen (Se for **(2.3)** and S for **(2.5)**), and this variation in incorporating S results in 2.15 times higher PLQYs. Comparing the PLQYs of **(2.4)** which consists of Se to **(2.7)** which comprises S, the PLQY of **(2.7)** is 1.76 times higher. It is observed that the core structure nuclearity as well as the PLQYs of these complexes depends on the group 11 metal and the chalcogen used.

Furthermore, the PLQYs of **(2.3)** and **(2.5)** show an excellent efficiency for such group 11 metal chalcogenolate clusters when compared to the PLQY of 19 % of the reported $[\text{Cu}_4(\text{P}^{\wedge}\text{S})_4(\text{CH}_3\text{CN})_2]$ (**IV.I**) ($\text{P}^{\wedge}\text{S} = 2\text{-(diphenylphosphino)benzenethiolate}$).^[3] The PLQYs of **(2.3)** and **(2.5)** are up to 3.8 times higher which could be due to a number of reasons such as the number of core Cu atoms, a different chalcogenolate and / or the phosphine (DBFDP) ligand used.

Previous attempts for synthesizing luminescent copper chalcogenide clusters with DBFDP were also made in the *Corrigan* lab, but the molecular structure of these complexes could not be determined by single crystal X - ray crystallography due to the μm size of the crystals.^[1] It was hypothesized that changing the backbone of the dibenzofuran ring (introducing alkyl groups) may result in a different crystal packing resulting in bigger single crystal sizes that could be analyzed. The incorporation of the tailored EtDBFDP (**3.2**) proved to be successful in synthesizing suitable sized crystals of $[\text{Cu}_{12}\text{Se}_6(\text{etdbfdp})_4]$ (**3.3**). It was observed that all Se atoms in **(3.3)** display μ_4 bridging coordination modes which form a close to ideal octahedron with Cu centres bridging at the edges. The phosphine ligands form a shell around the core by bonding to the Cu atoms in the corners. The core of **(3.3)** is isostructural to that reported for $[\text{Cu}_{12}\text{Se}_6(\text{dppo})_4]$ (**IV.II**) where all the Se atoms have μ_4 bridging modes with Cu atoms bridging at the edges.^[4] The incorporation of the bidentate phosphine (**3.2**) resulted in short bond distances between the pairs of Cu atoms when comparing to **(IV.II)** which could increase the overall rigidity of the cluster. Attempts to synthesize the analogous Cu_2S clusters with **(3.2)** were also made. The preliminary data shows the formation of an isostructural $[\text{Cu}_{12}\text{S}_6(\text{etdbfdp})_4]$ (**3.4**) with the same cell constants as **(3.3)**. A full structural data analysis of **(3.4)** will be conducted.

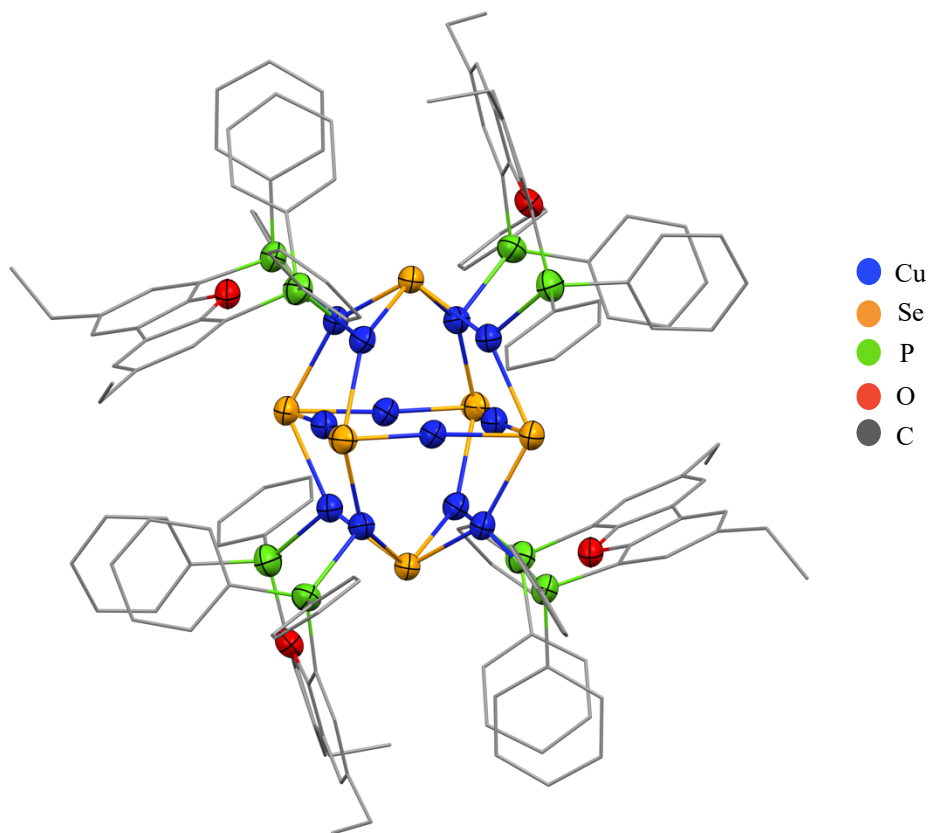


Figure 4.2: Molecular structure of $[\text{Cu}_{12}\text{Se}_6(\text{etdbfdp})_4]$ (**3.3**) in the crystal (H atoms are omitted for clarity). (The molecule resides about a crystallographic inversion centre).

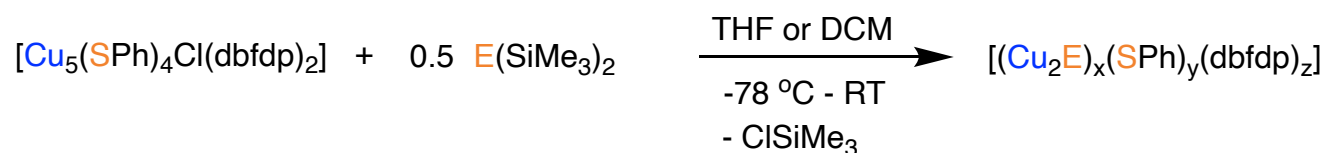
In terms of the luminescence properties, the crystals of (**3.3**) have red - orange emission at room temperature which is consistent with the qualitative observations of (**IV.II**) (red emission at room temperature).^[4] Although, qualitatively similar, (**3.3**) and (**IV.II**) differ in their λ_{exc} . λ_{exc} for (**3.3**) with the highest intensity has a bathochromic shift ($\lambda_{\text{exc}} = 475 \text{ nm}$) compared to the $\lambda_{\text{exc}} = 390 \text{ nm}$ for (**IV.II**)^[4] which could be due to the difference in the phosphine ligand used. While there is a significant variation in the λ_{exc} , the λ_{em} is quite similar for the two compounds as (**3.3**) has $\lambda_{\text{em}} = 653 \text{ nm}$ and (**IV.II**) has $\lambda_{\text{em}} = 638 \text{ nm}$. The next step is to determine how the incorporation of EtDBFDP (**3.2**) changes PLQY of (**3.3**) compared to the PLQY = 53 % for (**IV.II**).^[4] A full analysis of the photophysical studies of (**3.3**) will be conducted.

The incorporation of DBFDP and the related diphosphine EtDBFDP (**3.2**) resulted in highly luminescent group 11 metal chalcogen complexes with sufficient PLQYs for the metal chalcogenolate clusters. The molecular structure of the metal chalcogenolate (M-ER) (M = Cu, Ag, E = S, Se, R = organic moiety) complexes relies heavily on the combination of group 11 metal and the chalcogenolate used while the

molecular structure of copper chalcogenide (Cu_2E) compounds is isostructural when changing the chalcogen from S to Se. A key similarity between the two types of clusters is that the phosphine ligand bonds two metal centres and is present at the periphery forming a protective shell around the metal chalcogen core.

4.2 Outlook - Luminescent Group 11 Metal Chalcogenolate Clusters with Conjugated Diphosphine Ligands

Changing the metal to Au and / or changing the chalcogen to Te can be explored to see how this changes the emission properties of the group 11 metal chalcogenolate clusters. Additionally, due to the chloride functionality seen in complex $[\text{Cu}_5(\text{SPh})_4\text{Cl}(\text{dbfdp})_2]$ (**2.6**), it may be possible to synthesize metal chalcogenide / chalcogenolate clusters by adding a chalcogenide reagent to displace the chloride and potentially yield a more condensed cluster.



Scheme 4.1: Proposed scheme to synthesize metal chalcogenide / chalcogenolate clusters.

It has been previously shown that changing the organic moiety on copper chalcogenolate clusters can also change the colour of emission.^[5] This may be another interesting route to take to determine how the organic moieties on chalcogenolates affect the structural as well as the photophysical properties while still using DBFDP as the protective phosphine ligand.

Changing the substituents on the DBFDP ligand may result in different energy gaps which could change the wavelength of emission. It has been previously shown that incorporating electron donating groups on the dibenzofuran backbone results in increased PLQYs (from 5 % to 65 %) of Cu_4I_4 clusters.^[6] New substituted phosphines are currently being employed in copper chalcogenide clusters which show promising results (as mentioned in *Chapter 3*). Incorporating these substituted phosphines in group 11 metal chalcogenolate clusters would present an interesting outlook on how the electronic and optical properties can be affected.

4.3 Outlook - Luminescent Copper Chalcogenolate Clusters with Conjugated Diphosphine Ligands

Future work would include obtaining a full electronic and optical analysis of complex (3.4). This will include the crystal data information for (3.4), elemental analysis as well as UV - Vis (absorption, emission, excitation), lifetime and PLQYs studies. Due to the easy synthesis reported in this chapter of introducing donating groups onto the backbone, different groups could be incorporated onto the dibenzofuran ring to determine how they affect the electronic structure and the crystal packing of Cu_2E clusters. The incorporation of DCzDBFDP (IV.III)^[6] and DtBCzDBFDP (IV.IV)^[6] into copper chalcogenide clusters was unsuccessful due to difficulties with synthesizing DCzDBF (IV.V) and DtBCzDBF (IV.VI) with high purity and yields. Therefore, a different literature procedure could be attempted to introduce these donating groups.^[7] Successful synthesis of DCzDBFDP (IV.III)^[6] and DtBCzDBFDP (IV.IV)^[6] would allow their incorporation in copper chalcogenide clusters.

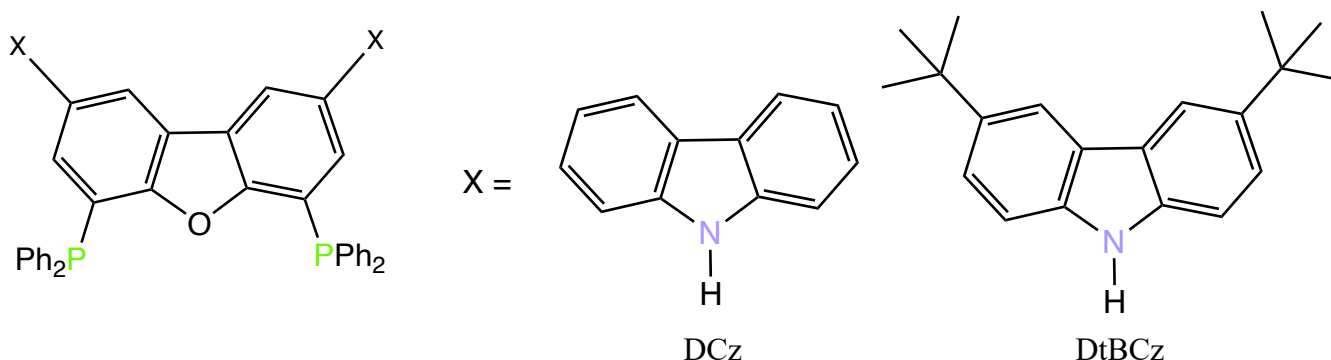


Figure 4.3: Substituted 4,6 - bis(diphenylphosphino)dibenzofuran.^[6]

It would be interesting to see how the electronic properties and the PLQYs of these complexes change when ranging from small donating groups such as $-\text{C}_2\text{H}_5$ to bigger donating groups such as carbazoles.

4.4 References

- [1] M. Nayyar, Chem 4491E Thesis: Luminescent Copper Chalcogenide Clusters, The University of Western Ontario **2020**.
- [2] K. Y. Li, Chem 4491E Thesis: Ligand Controlled Luminescence in Silver and Gold Chalcogenide Clusters, The University of Western Ontario **2021**.
- [3] K. Shimada, A. Kobayashi, Y. Ono, H. Ohara, T. Hasegawa, T. Taketsugu, E. Sakuda, S. Akagi, N. Kitamura, M. Kato, *J. Phys. Chem. C* **2016**, *120*, 16002–16011.
- [4] A. Eichhöfer, G. Buth, S. Lebedkin, M. Kühn, F. Weigend, *Inorg. Chem.* **2015**, *54*, 9413–9422.
- [5] B. Hu, C. Y. Su, D. Fenske, O. Fuhr, *Inorg. Chim. Acta* **2014**, *419*, 118–123.
- [6] M. Xie, C. Han, Q. Liang, J. Zhang, G. Xie, H. Xu, *Sci. Adv.* **2019**, *5*, 1–9.
- [7] D. Gudeika, D. Volyniuk, J. V. Grazulevicius, E. Skuodis, S. Y. Yu, W. T. Liou, L. Y. Chen, Y. J. Shiu, *Dye Pigment* **2016**, *130*, 298–305.

Appendices

Appendix 1.0 Permission to Reuse Copyright Material

Chapter 1, Figure 1.5 - John Wiley and Sons Reproduction Permission

5/24/22, 3:10 PM

RightsLink - Your Account

JOHN WILEY AND SONS LICENSE TERMS AND CONDITIONS

May 24, 2022

This Agreement between Ms. Mansha Nayyar ("You") and John Wiley and Sons ("John Wiley and Sons") consists of your license details and the terms and conditions provided by John Wiley and Sons and Copyright Clearance Center.

License Number	5313220556039
License date	May 20, 2022
Licensed Content Publisher	John Wiley and Sons
Licensed Content Publication	Chemistry - A European Journal
Licensed Content Title	Adamantyl- and Furanyl-Protected Nanoscale Silver Sulfide Clusters
Licensed Content Author	Sebastian Bestgen, Xiaoxun Yang, Ibrahim Issac, et al
Licensed Content Date	Jun 14, 2016
Licensed Content Volume	22
Licensed Content Issue	29
Licensed Content Pages	5
Type of Use	Dissertation/Thesis
Requestor type	University/Academic
Format	Print and electronic
Portion	Figure/table
Number of figures/tables	2
Will you be translating?	No
Title	Luminescent Group 11 Metal Chalcogen Clusters with Bidentate Phosphine Ligands
Institution name	Western University
Expected presentation date	Jun 2022
Portions	Figure 2 S-substructure of 1 consisting of a S13-core composed of S2- ions (orange) that is surrounded by 32 thiolates (yellow) in a distorted icosahedral fashion. Lines between S atoms are nonbinding and solely illustrate the geometric arrangement.
Requestor Location	Ms. Mansha Nayyar 1151 Richmond Street Chemistry Building, UWO London, ON N6A 3K7 Canada Attn: Ms. Mansha Nayyar
Publisher Tax ID	EU826007151
Total	0.00 CAD
Terms and Conditions	

Luminescence in Phosphine-Stabilized Copper Chalcogenide Cluster Molecules—A Comparative Study

Author: Andreas Eichhöfer, Gernot Buth, Sergei Lebedkin, et al

Publication: Inorganic Chemistry

Publisher: American Chemical Society

Date: Oct 1, 2015

Copyright © 2015, American Chemical Society



PERMISSION/LICENSE IS GRANTED FOR YOUR ORDER AT NO CHARGE

This type of permission/license, instead of the standard Terms and Conditions, is sent to you because no fee is being charged for your order. Please note the following:

- Permission is granted for your request in both print and electronic formats, and translations.
- If figures and/or tables were requested, they may be adapted or used in part.
- Please print this page for your records and send a copy of it to your publisher/graduate school.
- Appropriate credit for the requested material should be given as follows: "Reprinted (adapted) with permission from {COMPLETE REFERENCE CITATION}. Copyright {YEAR} American Chemical Society." Insert appropriate information in place of the capitalized words.
- One-time permission is granted only for the use specified in your RightsLink request. No additional uses are granted (such as derivative works or other editions). For any uses, please submit a new request.

If credit is given to another source for the material you requested from RightsLink, permission must be obtained from that source.

BACK

CLOSE WINDOW

Chapter 1, Figure 1.10 (b) - Elsevier Reproduction Permission

5/24/22, 3:10 PM

RightsLink - Your Account

ELSEVIER LICENSE TERMS AND CONDITIONS

May 24, 2022

This Agreement between Ms. Mansha Nayyar ("You") and Elsevier ("Elsevier") consists of your license details and the terms and conditions provided by Elsevier and Copyright Clearance Center.

License Number	5313210826140
License date	May 20, 2022
Licensed Content Publisher	Elsevier
Licensed Content Publication	Inorganica Chimica Acta
Licensed Content Title	Synthesis, characterization and optical properties of a series of binuclear copper chalcogenolato complexes
Licensed Content Author	Bing Hu, Cheng-Yong Su, Dieter Fenske, Olaf Fuhr
Licensed Content Date	Aug 1, 2014
Licensed Content Volume	419
Licensed Content Issue	n/a
Licensed Content Pages	6
Start Page	118
End Page	123
Type of Use	reuse in a thesis/dissertation
Portion	figures/tables/illustrations
Number of figures/tables/illustrations	5
Format	both print and electronic
Are you the author of this Elsevier article?	No
Will you be translating?	No
Title	Luminescent Group 11 Metal Chalcogen Clusters with Bidentate Phosphine Ligands
Institution name	Western University
Expected presentation date	Jun 2022
Portions	Fig. 5. Photographs of 1–5 and A under daylight (top) and UV light ($\lambda = 366$ nm; bottom).
Requestor Location	Ms. Mansha Nayyar 1151 Richmond Street Chemistry Building, UWO London, ON N6A 3K7 Canada Attn: Ms. Mansha Nayyar GB 494 6272 12
Publisher Tax ID	GB 494 6272 12
Total	0.00 CAD
Terms and Conditions	

Chapter 1, Figure 1.11 (b) and (c) - Royal Society of Chemistry Reproduction Permission

5/24/22, 3:09 PM

<https://marketplace.copyright.com/rs-ui-web/mp/license/60fa8eb2-9b9b-49d5-9fde-45db4ffcb8c9/052e8670-29f5-45e7-bc0e-09728cb5d6c9>



This is a License Agreement between Mansha Nayyar ("User") and Copyright Clearance Center, Inc. ("CCC") on behalf of the Rightsholder identified in the order details below. The license consists of the order details, the CCC Terms and Conditions below, and any Rightsholder Terms and Conditions which are included below. All payments must be made in full to CCC in accordance with the CCC Terms and Conditions below.

Order Date	20-May-2022	Type of Use	Republish in a thesis/dissertation
Order License ID	1223640-1	Publisher Portion	THE SOCIETY, Image/photo/illustration
ISSN	1359-7345		

LICENSED CONTENT

Publication Title	Chemical communications	Publication Type	Journal
Article Title	Crystal structure of a luminescent thiolated Ag nanocluster with an octahedral Ag ₆ (4+) core.	Start Page	300
		End Page	302
		Issue	3
Author/Editor	ROYAL SOCIETY OF CHEMISTRY (GREAT BRITAIN)	Volume	49
		URL	http://www.rsc.org/Publishing/journals/cc/Article.asp?Type=CurrentIssue
Date	01/01/1996		
Language	English		
Country	United Kingdom of Great Britain and Northern Ireland		
Rights holder	Royal Society of Chemistry		

REQUEST DETAILS

Portion Type	Image/photo/illustration	Distribution	Worldwide
Number of images / photos / illustrations	1	Translation	Original language of publication
Format (select all that apply)	Print, Electronic	Copies for the disabled?	No
Who will republish the content?	Academic institution	Minor editing privileges?	Yes
Duration of Use	Current edition and up to 5 years	Incidental promotional use?	No
Lifetime Unit Quantity	Up to 499	Currency	CAD
Rights Requested	Main product		

NEW WORK DETAILS

Title	Luminescent Group 11 Metal Chalcogen Clusters with Bidentate Phosphine Ligands	Institution name	Western University
		Expected presentation date	2022-06-22
Instructor name	Dr. J. F. Corrigan		

<https://marketplace.copyright.com/rs-ui-web/mp/license/60fa8eb2-9b9b-49d5-9fde-45db4ffcb8c9/052e8670-29f5-45e7-bc0e-09728cb5d6c9>

1/4

ADDITIONAL DETAILS

Order reference number	N/A	The requesting person / organization to appear on the license	Mansha Nayyar
-------------------------------	-----	--	---------------

REUSE CONTENT DETAILS

Title, description or numeric reference of the portion(s)	Fig 3	Title of the article/chapter the portion is from	Crystal structure of a luminescent thiolated Ag nanocluster with an octahedral Ag ₆ (4+) core.
Editor of portion(s)	Yang, Huayan; Lei, Jing; Wu, Binghui; Wang, Yu; Zhou, Meng; Xia, Andong; Zheng, Lansun; Zheng, Nanfeng	Author of portion(s)	Yang, Huayan; Lei, Jing; Wu, Binghui; Wang, Yu; Zhou, Meng; Xia, Andong; Zheng, Lansun; Zheng, Nanfeng
Volume of serial or monograph	49	Issue, if republishing an article from a serial	3
Page or page range of portion	300-302	Publication date of portion	2013-01-11

White Electroluminescent Phosphine-Chelated Copper Iodide Nanoclusters

Author: Mingchen Xie, Chunmiao Han, Jing Zhang, et al

Publication: Chemistry of Materials

Publisher: American Chemical Society

Date: Aug 1, 2017

Copyright © 2017, American Chemical Society



PERMISSION/LICENSE IS GRANTED FOR YOUR ORDER AT NO CHARGE

This type of permission/license, instead of the standard Terms and Conditions, is sent to you because no fee is being charged for your order. Please note the following:

- Permission is granted for your request in both print and electronic formats, and translations.
- If figures and/or tables were requested, they may be adapted or used in part.
- Please print this page for your records and send a copy of it to your publisher/graduate school.
- Appropriate credit for the requested material should be given as follows: "Reprinted (adapted) with permission from {COMPLETE REFERENCE CITATION}. Copyright {YEAR} American Chemical Society." Insert appropriate information in place of the capitalized words.
- One-time permission is granted only for the use specified in your RightsLink request. No additional uses are granted (such as derivative works or other editions). For any uses, please submit a new request.

If credit is given to another source for the material you requested from RightsLink, permission must be obtained from that source.

BACK

CLOSE WINDOW

White Electroluminescent Phosphine-Chelated Copper Iodide Nanoclusters



Author: Mingchen Xie, Chunmiao Han, Jing Zhang, et al

Publication: Chemistry of Materials

Publisher: American Chemical Society

Date: Aug 1, 2017

Copyright © 2017, American Chemical Society

PERMISSION/LICENSE IS GRANTED FOR YOUR ORDER AT NO CHARGE

This type of permission/license, instead of the standard Terms and Conditions, is sent to you because no fee is being charged for your order. Please note the following:

- Permission is granted for your request in both print and electronic formats, and translations.
- If figures and/or tables were requested, they may be adapted or used in part.
- Please print this page for your records and send a copy of it to your publisher/graduate school.
- Appropriate credit for the requested material should be given as follows: "Reprinted (adapted) with permission from {COMPLETE REFERENCE CITATION}. Copyright {YEAR} American Chemical Society." Insert appropriate information in place of the capitalized words.
- One-time permission is granted only for the use specified in your RightsLink request. No additional uses are granted (such as derivative works or other editions). For any uses, please submit a new request.

If credit is given to another source for the material you requested from RightsLink, permission must be obtained from that source.

BACK

CLOSE WINDOW

Appendix 2.0 Supporting Information for Chapter 2

Appendix 2.1: ^1H and $^{31}\text{P}\{^1\text{H}\}$ NMR data for compounds (2.3) - (2.7)

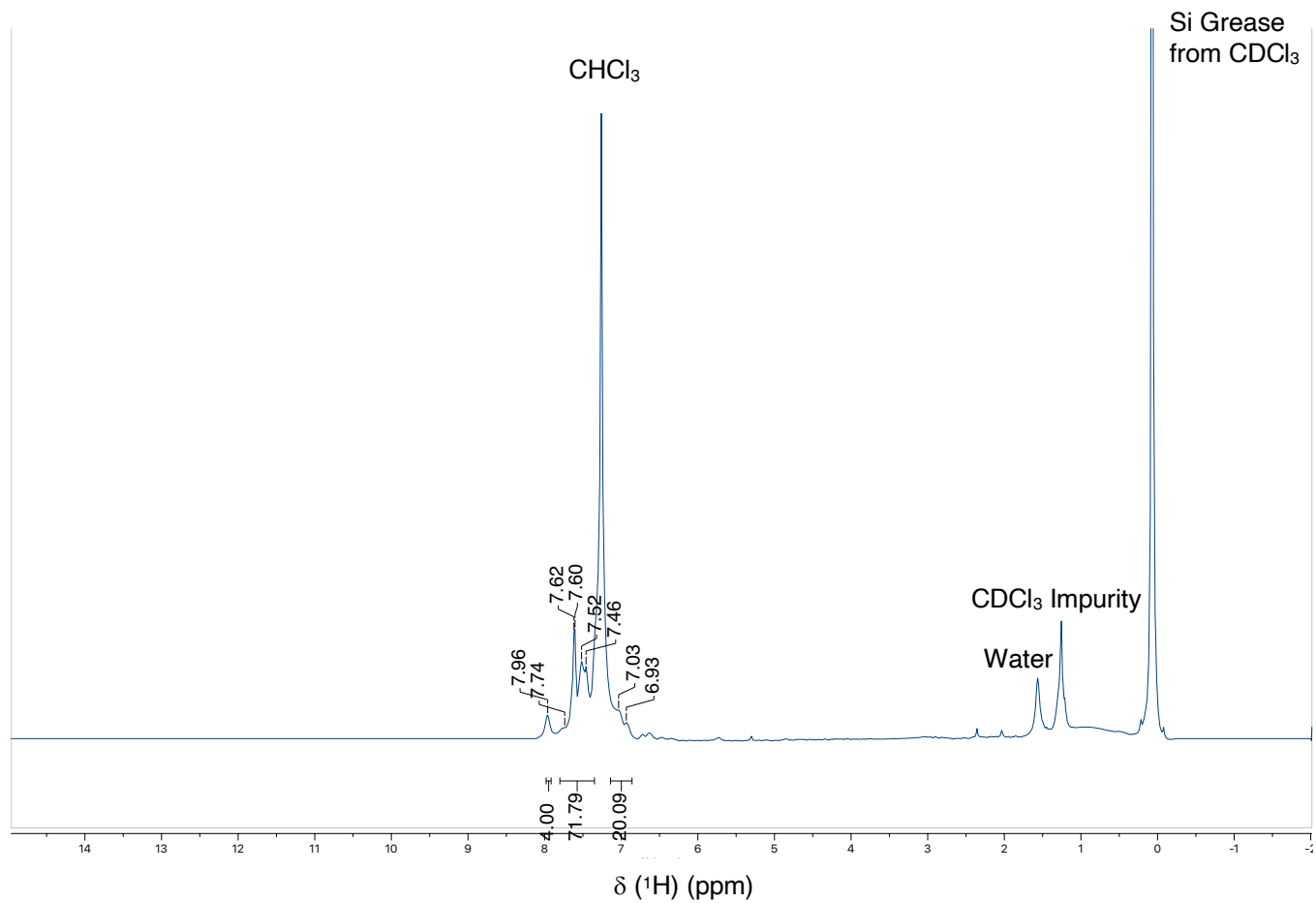


Figure S2.1: ^1H NMR spectrum in CDCl_3 (298 K) of $[\text{Cu}_4(\text{SePh})_4(\text{dbfdp})_2]$ (2.3)

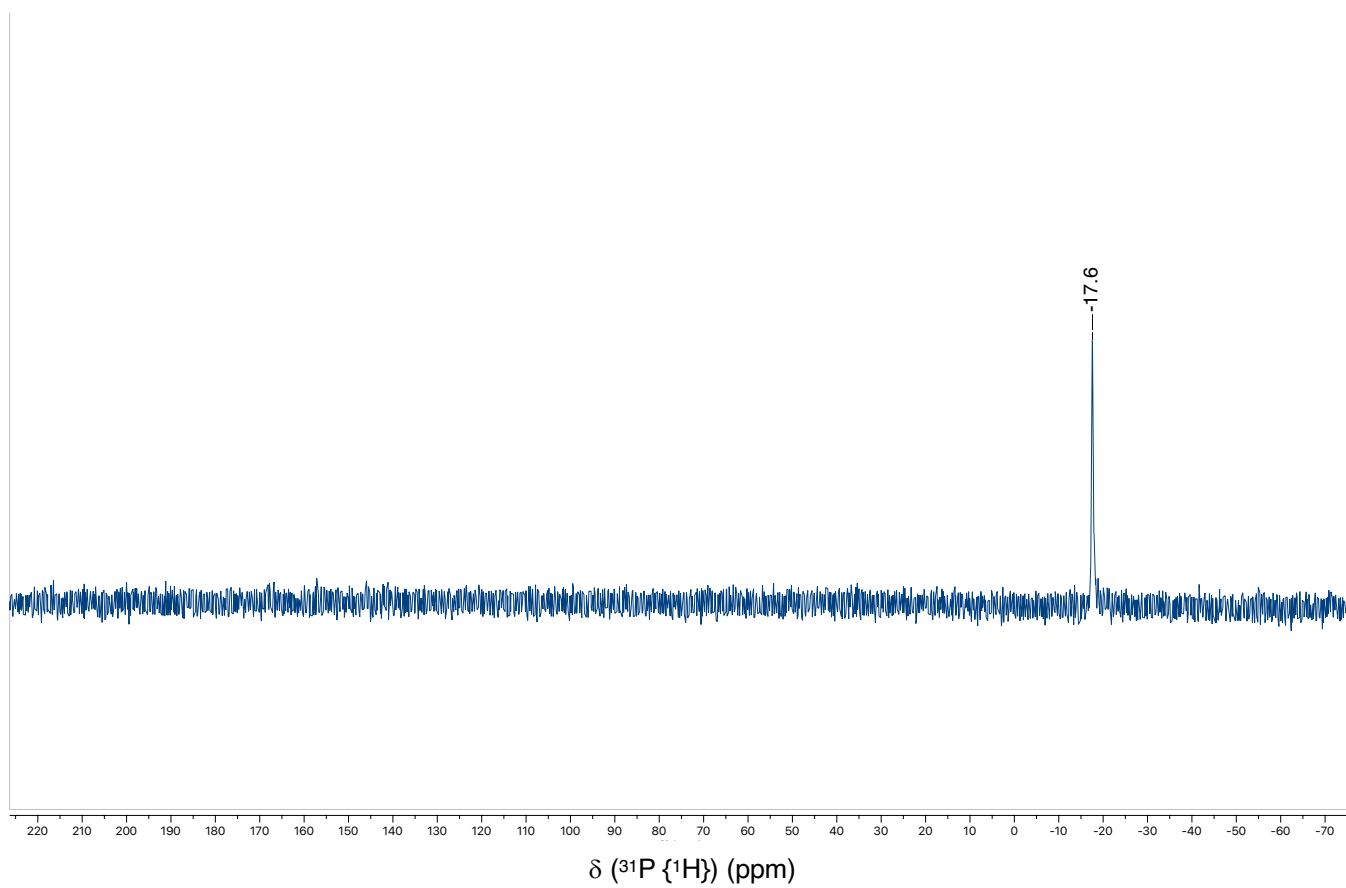


Figure S2.2: $^{31}\text{P}\{^1\text{H}\}$ NMR spectrum in CDCl_3 (298 K) of $[\text{Cu}_4(\text{SePh})_4(\text{dbfdp})_2]$ (**2.3**)

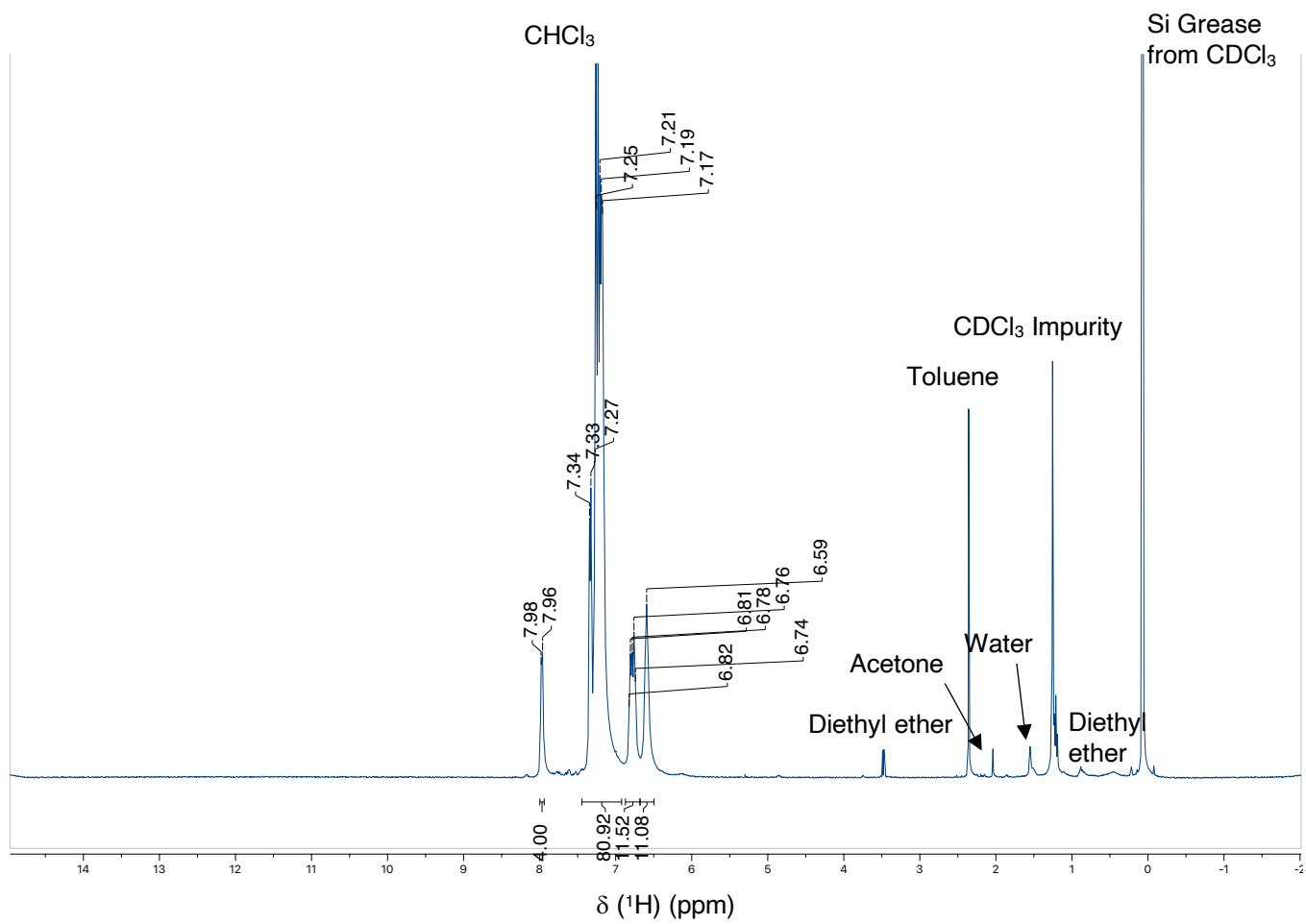


Figure S2.3: ^1H NMR spectrum in CDCl_3 (298 K) of $[\text{Ag}_6(\text{SePh})_6(\text{dbfdp})_2]$ (2.4)

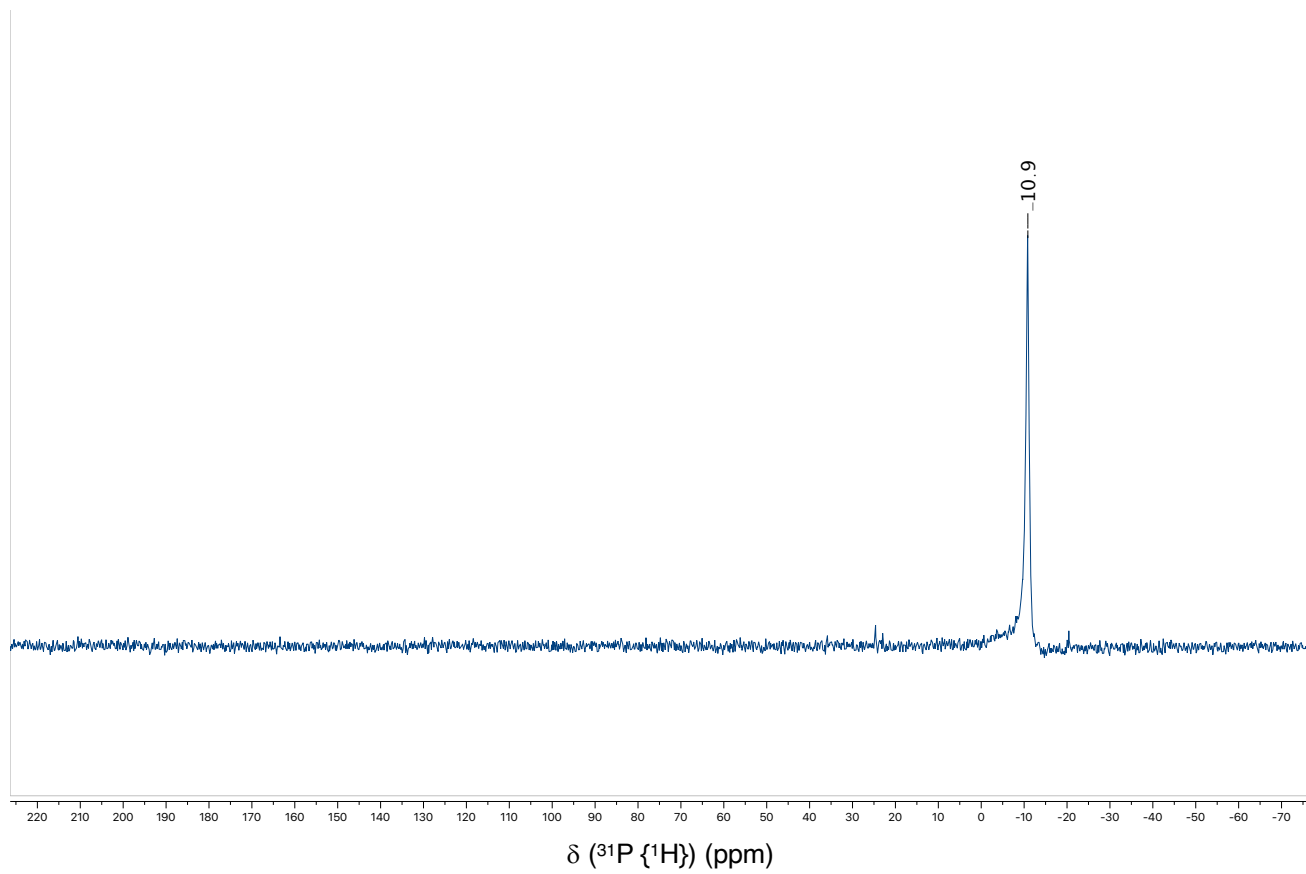


Figure S2.4: $^{31}\text{P}\{^1\text{H}\}$ NMR spectrum in CDCl_3 (298 K) of $[\text{Ag}_6(\text{SePh})_6(\text{dbfdp})_2]$ (**2.4**)

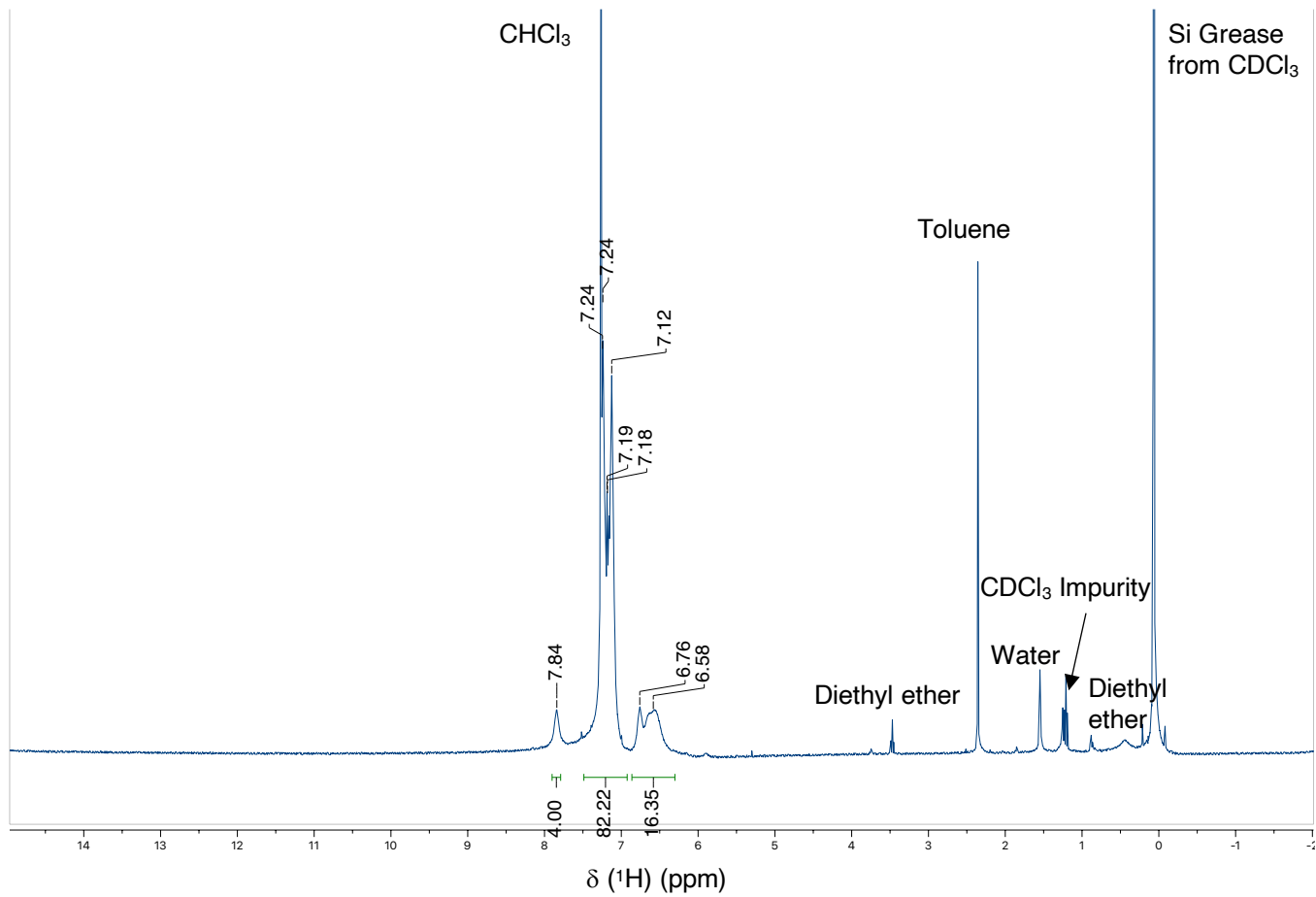


Figure S2.5: ^1H NMR spectrum in CDCl_3 (298 K) of $[\text{Cu}_5(\text{SPh})_5(\text{dbfdp})_2]$ (2.5)

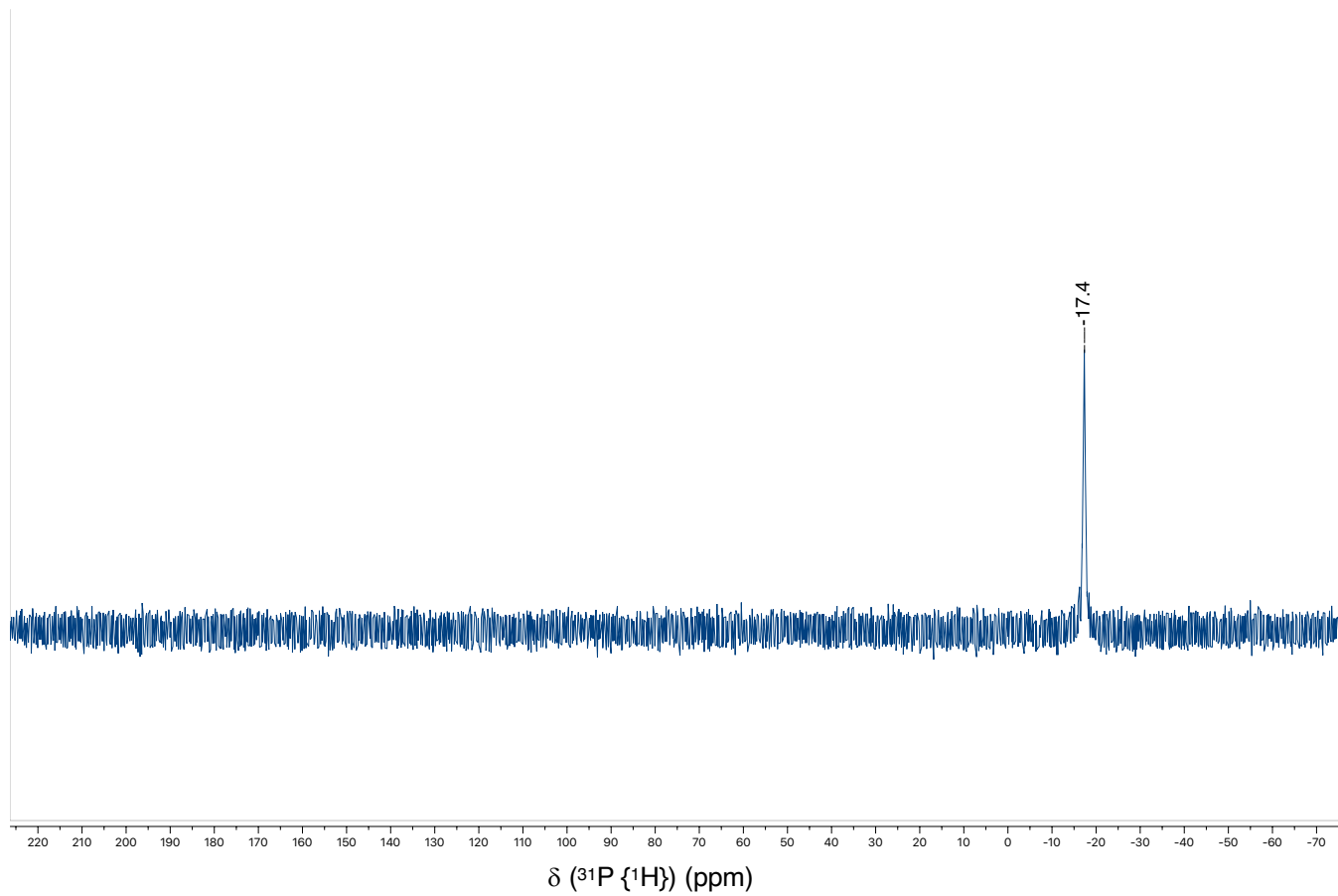


Figure S2.6: $^{31}\text{P}\{^1\text{H}\}$ NMR spectrum in CDCl_3 (298 K) of $[\text{Cu}_5(\text{SPh})_5(\text{dbfdp})_2]$ (**2.5**)

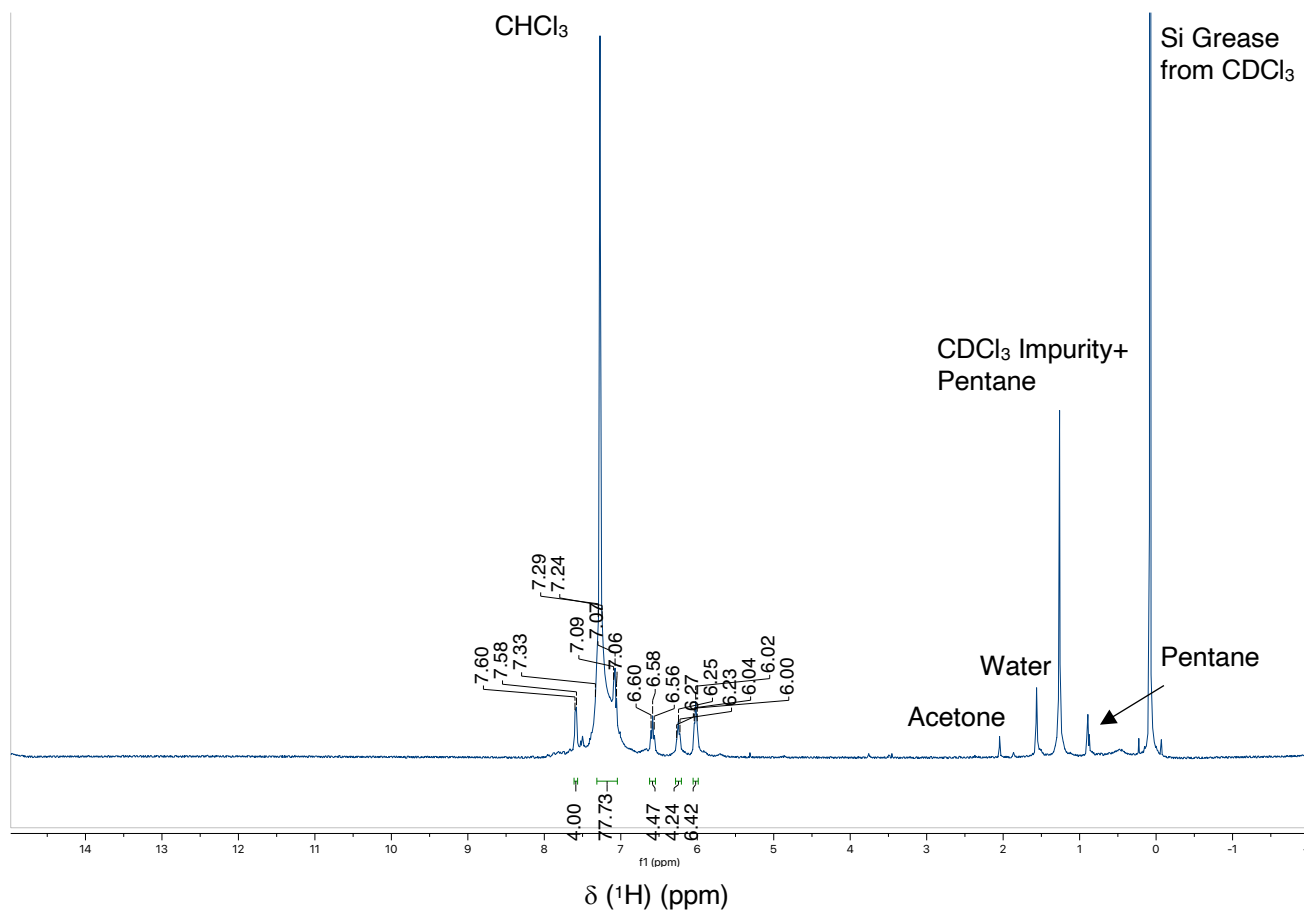


Figure S2.7: ¹H NMR spectrum in CDCl₃ (298 K) of [Cu₅(SPh)₄Cl(dbfdp)₂] (2.6)

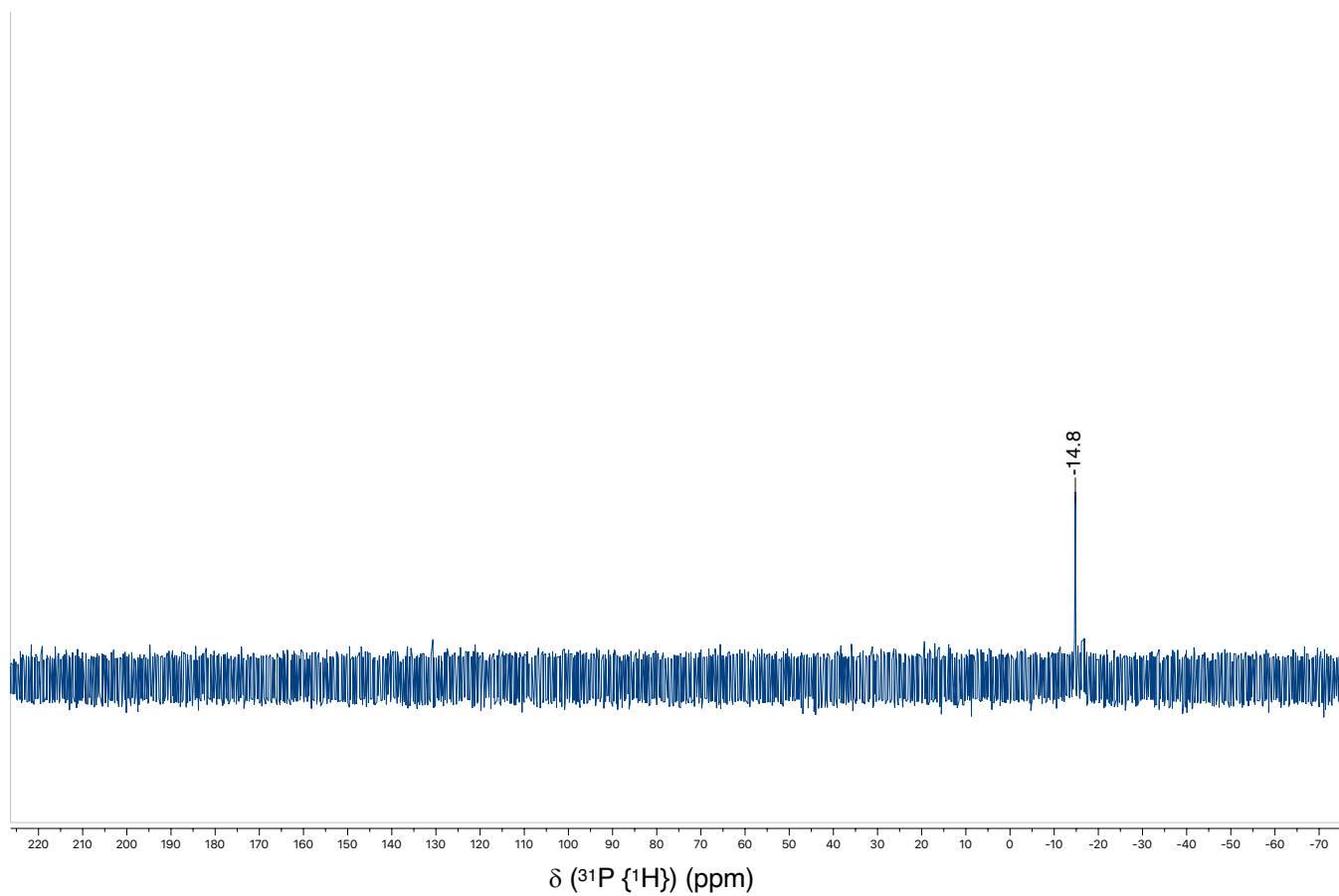


Figure S2.8: $^{31}\text{P}\{^1\text{H}\}$ NMR spectrum in CDCl_3 (298 K) of $[\text{Cu}_5(\text{SPh})_4\text{Cl}(\text{dbfdp})_2]$ (**2.6**)

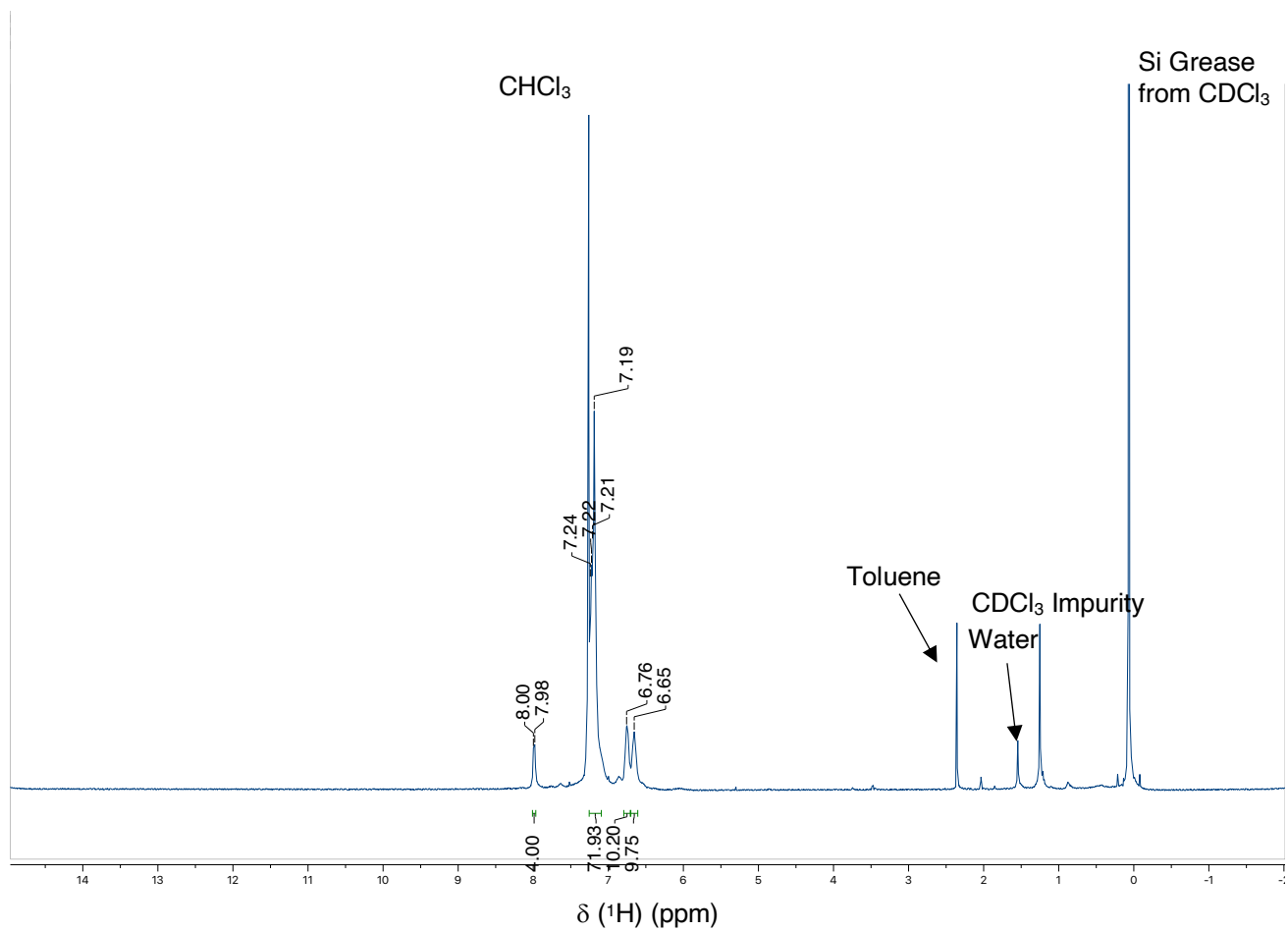


Figure S2.9: ^1H NMR spectrum in CDCl_3 (298 K) of $[\text{Ag}_4(\text{SPh})_4(\text{dbfdp})_2]$ (2.7)

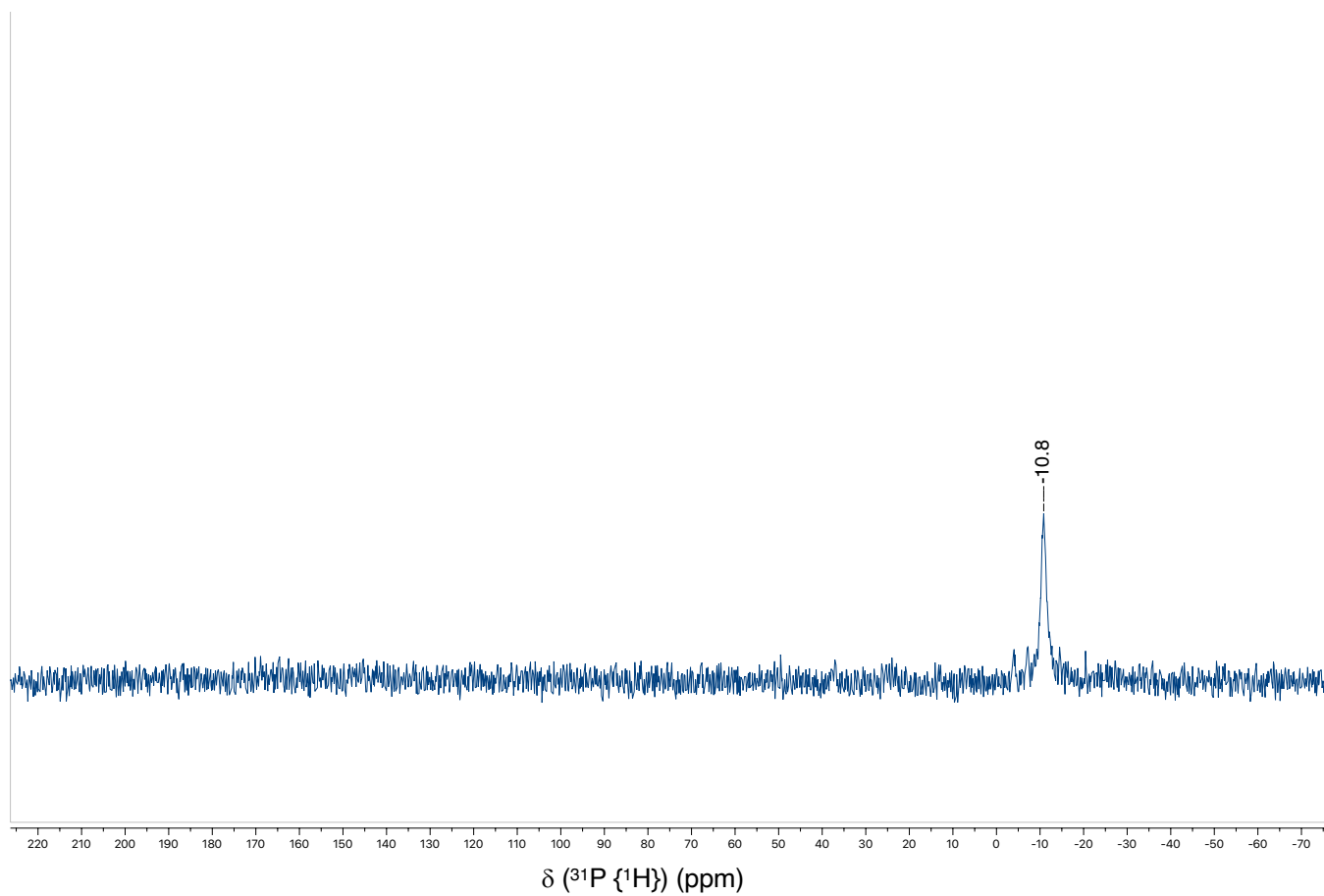


Figure S2.10: $^{31}\text{P}\{^1\text{H}\}$ NMR spectrum in CDCl_3 (298 K) of $[\text{Ag}_4(\text{SPh})_4(\text{dbfdp})_2]$ (2.7)

Appendix 2.2: X - ray structure analysis and data for compounds (2.3) - (2.7)

Table S2.1: Summary of Crystal Data of [Cu₄(SePh)₄(dbfdp)₂] (2.3)

Formula	C ₉₆ H ₇₂ Cu ₄ O ₂ P ₄ Se ₄
Formula Weight (g/mol)	1951.41
Crystal Dimensions (mm)	0.294 × 0.108 × 0.075
Crystal Color and Habit	yellow Needle
Crystal System	triclinic
Space Group	P -1
Temperature, K	110
a, Å	13.5232(8)
b, Å	13.8005(8)
c, Å	15.1254(9)
α, °	114.598(2)
β, °	97.365(2)
γ, °	98.677(2)
V, Å ³	2479.3(3)
Number of reflections to determine final unit cell	2665
Min and Max 2θ for cell determination, °	5.42, 60.94
Z	1
F(000)	976
ρ (g/cm ³)	1.307
λ, Å, (MoKα)	0.71073
μ, (cm ⁻¹)	2.421
Diffractometer Type	Bruker Kappa Axis Apex2
Scan Type(s)	phi and omega scans
Max 2θ for data collection, °	61.086
Measured fraction of data	0.998
Number of reflections measured	103703
Unique reflections measured	15156
R _{merge}	0.0434
Number of reflections included in refinement	15156
Cut off Threshold Expression	I > 2sigma(I)
Structure refined using	full matrix least-squares using F ²
Weighting Scheme	w=1/[sigma ² (Fo ²)+(0.0305P) ² +2.0109P] where P=(Fo ² +2Fc ²)/3
Number of parameters in least-squares	497
R ₁	0.0298
wR ₂	0.0681
R ₁ (all data)	0.0442
wR ₂ (all data)	0.0723
GOF	1.023
Maximum shift/error	0.002
Min & Max peak heights on final ΔF Map (e ⁻ /Å)	-0.507, 0.478

Where:

$$R_1 = \frac{\sum (|F_o| - |F_c|)}{\sum F_o}$$

$$wR_2 = [\sum(w(F_o^2 - F_c^2)^2) / \sum(w F_o^4)]^{1/2}$$

$$GOF = [\sum(w(F_o^2 - F_c^2)^2) / (No. of reflns. - No. of params.)]^{1/2}$$

Table S2.2: Selected bond lengths of $[Cu_4(SePh)_4(dbfdp)_2]$ (2.3)

Bond length	Å	Bond length	Å
Se1-Cu2	2.3651(3)	Cu1-Cu2	2.6246(4)
Se1-Cu1	2.4693(3)	Cu2-P2	2.2022(6)
Se2-Cu2	2.4009(3)	Se2-Cu1	2.5797(3)
Se2-Cu1'	2.4972(3)	Cu1-P1	2.2412(5)

Table S2.3: Selected bond angles of $[Cu_4(SePh)_4(dbfdp)_2]$ (2.3)

Bond angle	(°)	Bond angle	(°)
C37-Se1-Cu2	100.96(6)	P1-Cu1-Se2	119.691(17)
C37-Se1-Cu1	117.20(6)	Se1-Cu1-Se2	100.065(10)
Cu2-Se1-Cu1	65.723(10)	Se2'-Cu1-Se2	102.545(10)
C43-Se2-Cu2	109.76(6)	P1-Cu1-Cu2	115.214(17)
C43-Se2-Cu1'	116.94(6)	Se1-Cu1-Cu2	55.227(9)
Cu2-Se2-Cu1'	126.311(12)	Se2'-Cu1-Cu2	139.042(12)
C43-Se2-Cu1	108.48(6)	Se2-Cu1-Cu2	54.938(8)
Cu2-Se2-Cu1	63.482(9)	P2-Cu2-Se1	127.127(17)
Cu1'-Se2-Cu1	77.455(10)	P2-Cu2-Se2	124.217(17)
P1-Cu1-Se1	121.319(16)	Se1-Cu2-Se2	108.591(12)
P1-Cu1-Se2'	105.657(16)	P2-Cu2-Cu1	150.342(18)
Se1-Cu1-Se2'	105.411(11)	Se1-Cu2-Cu1	59.050(9)
		Se2-Cu2-Cu1	61.580(10)

Table S2.4: Summary of Crystal Data of $[Ag_6(SePh)_6(dbfdp)_2]$ (2.4)

Formula	$C_{108}H_{82}Ag_6O_2P_4Se_6$
Formula Weight (g/mol)	2656.59
Crystal Dimensions (mm)	$0.078 \times 0.054 \times 0.024$
Crystal Color and Habit	colourless Block
Crystal System	triclinic
Space Group	P -1
Temperature, K	110
a , Å	12.5939(14)
b , Å	14.4785(16)
c , Å	27.824(3)
α , °	96.174(2)
β , °	92.224(2)
γ , °	108.006(2)
V , Å ³	4783.1(9)
Number of reflections to determine final unit cell	9933
Min and Max 2θ for cell determination, °	4.84, 50.08
Z	2
F(000)	2584
ρ (g/cm ³)	1.845
λ , Å, (MoK α)	0.71073
μ , (cm ⁻¹)	3.605
Diffractometer Type	Bruker Kappa Axis Apex2
Scan Type(s)	phi and omega scans
Max 2θ for data collection, °	50.152
Measured fraction of data	0.998
Number of reflections measured	106451
Unique reflections measured	16922
R_{merge}	0.0815
Number of reflections included in refinement	16922
Cut off Threshold Expression	$I > 2\sigma(I)$
Structure refined using	full matrix least-squares using F^2
Weighting Scheme	$w = 1 / [\sigma^2(F_o^2) + (0.0721P)^2]$ where $P = (F_o^2 + 2F_c^2) / 3$
Number of parameters in least-squares	1135
R_1	0.0357
wR_2	0.0913
R_1 (all data)	0.0662
wR_2 (all data)	0.1313
GOF	1.112
Maximum shift/error	0.001
Min & Max peak heights on final ΔF Map (e/Å)	-1.795, 0.962

Where:

$$R_1 = \frac{\sum (|F_o| - |F_c|)}{\sum F_o}$$

$$wR_2 = \left[\frac{\sum (w(F_o^2 - F_c^2))^2}{\sum (w F_o^4)} \right]^{1/2}$$

$$GOF = \left[\frac{\sum (w(F_o^2 - F_c^2))^2}{(\text{No. of reflns.} - \text{No. of params.})} \right]^{1/2}$$

Table S2.5: Selected bond lengths of $[Ag_6(SePh)_6(dbfdp)_2]$ (2.4)

Bond length	Å	Bond length	Å
Ag1-P1	2.4644(19)	Ag4-Ag6	3.1174(8)
Ag1-Se1	2.6122(9)	Ag5-P4	2.4371(18)
Ag1-Se2	2.6634(9)	Ag5-Se4	2.5720(8)
Ag1-Ag3	2.9910(8)	Ag5-Se6	2.6572(9)
Ag1-Ag2	3.0147(8)	Ag5-Ag6	3.1320(8)
Ag2-P2	2.4395(19)	Ag6-Se6	2.5145(9)
Ag2-Se1	2.6105(9)	Ag6-Se5	2.5508(9)
Ag2-Se3	2.6243(9)	Ag6-Se3	2.8300(9)
Ag2-Ag3	3.0954(8)	Ag4-Se1	3.0222(9)
Ag3-Se2	2.5339(9)	Ag4-P3	2.4769(19)
Ag3-Se4	2.5978(9)	Ag4-Se5	2.6377(9)
Ag3-Se3	2.6668(10)	Ag4-Se4	2.6446(9)

Table S2.6: Selected bond angles of $[Ag_6(SePh)_6(dbfdp)_2]$ (2.4)

Bond angle	(°)	Bond angle	(°)
P1-Ag1-Se1	120.58(5)	Ag1-Ag3-Ag2	59.352(18)
P1-Ag1-Se2	112.04(5)	P3-Ag4-Se5	119.43(5)
Se1-Ag1-Se2	126.60(3)	P3-Ag4-Se4	116.34(5)
P1-Ag1-Ag3	163.40(5)	Se5-Ag4-Se4	119.52(3)
Se1-Ag1-Ag3	73.77(2)	P3-Ag4-Se1	120.19(5)
Se2-Ag1-Ag3	52.86(2)	Se5-Ag4-Se1	86.31(3)
P1-Ag1-Ag2	131.96(5)	Se4-Ag4-Se1	85.17(3)
Se1-Ag1-Ag2	54.72(2)	P3-Ag4-Ag6	131.19(5)
Se2-Ag1-Ag2	96.12(3)	Se5-Ag4-Ag6	51.80(2)
Ag3-Ag1-Ag2	62.048(19)	Se4-Ag4-Ag6	74.65(2)
P2-Ag2-Se1	126.39(5)	Se1-Ag4-Ag6	107.66(2)
P2-Ag2-Se3	125.44(5)	P4-Ag5-Se4	126.69(5)
Se1-Ag2-Se3	107.83(3)	P4-Ag5-Se6	111.39(5)
P2-Ag2-Ag1	103.49(5)	Se4-Ag5-Se6	119.00(3)
Se1-Ag2-Ag1	54.77(2)	P4-Ag5-Ag6	157.42(5)
Se3-Ag2-Ag1	113.04(3)	Se4-Ag5-Ag6	75.34(2)
P2-Ag2-Ag3	143.61(5)	Se6-Ag5-Ag6	50.68(2)
Se1-Ag2-Ag3	71.99(2)	Se6-Ag6-Se5	149.29(3)
Se3-Ag2-Ag3	54.84(2)	Se6-Ag6-Se3	126.07(3)
Ag1-Ag2-Ag3	58.600(17)	Se5-Ag6-Se3	84.25(3)
Se2-Ag3-Se4	136.33(3)	Se6-Ag6-Ag4	120.17(3)
Se2-Ag3-Se3	123.99(3)	Se5-Ag6-Ag4	54.36(2)
Se4-Ag3-Se3	99.41(3)	Se3-Ag6-Ag4	93.36(2)
Se2-Ag3-Ag1	56.92(2)	Se6-Ag6-Ag5	54.84(2)
Se4-Ag3-Ag1	113.79(3)	Se5-Ag6-Ag5	120.04(3)

Se3-Ag3-Ag1	112.52(3)	Se3-Ag6-Ag5	116.83(3)
Se2-Ag3-Ag2	96.93(3)	Ag4-Ag6-Ag5	68.176(19)
Se4-Ag3-Ag2	114.49(3)	Ag6-Se6-Ag5	74.49(3)
Se3-Ag3-Ag2	53.56(2)	Ag2-Se3-Ag6	115.92(3)
Ag2-Se1-Ag4	103.65(3)	Ag3-Se3-Ag6	98.42(3)
Ag1-Se1-Ag4	134.18(3)	Ag5-Se4-Ag3	133.73(3)
Ag3-Se2-Ag1	70.22(2)	Ag5-Se4-Ag4	84.34(3)
Ag2-Se3-Ag3	71.61(3)	Ag3-Se4-Ag4	101.96(3)
		Ag6-Se5-Ag4	73.84(3)

Table S2.7: Summary of Crystal Data of $[Cu_5(SPh)_5(dbfdp)_2]$ (2.5)

Formula	$C_{219}H_{180}Cu_{10}O_6P_8S_{10}$
Formula Weight (g/mol)	4111.38
Crystal Dimensions (mm)	$0.508 \times 0.202 \times 0.150$
Crystal Color and Habit	yellow block
Crystal System	monoclinic
Space Group	C 2/c
Temperature, K	110
a , Å	23.4828(9)
b , Å	17.2174(6)
c , Å	51.157(2)
α , °	90
β , °	92.064(2)
γ , °	90
V , Å ³	20669.9(13)
Number of reflections to determine final unit cell	9836
Min and Max 2θ for cell determination, °	4.8, 52.72
Z	4
F(000)	8448
ρ (g/cm)	1.321
λ , Å, (MoK α)	0.71073
μ , (cm ⁻¹)	1.224
Diffractometer Type	Bruker Kappa Axis Apex2
Scan Type(s)	phi and omega scans
Max 2θ for data collection, °	52.734
Measured fraction of data	0.999
Number of reflections measured	122609
Unique reflections measured	21109
R_{merge}	0.0558
Number of reflections included in refinement	21109
Cut off Threshold Expression	$I > 2\sigma(I)$
Structure refined using	full matrix least-squares using F^2
Weighting Scheme	$w=1/[\sigma^2(F_o^2)+(0.0701P)^2+68.0554P]$ where $P=(F_o^2+2F_c^2)/3$
Number of parameters in least-squares	1265
R_1	0.0462
wR_2	0.1317
R_1 (all data)	0.0641
wR_2 (all data)	0.1423
GOF	1.057
Maximum shift/error	0.003
Min & Max peak heights on final ΔF Map (e/Å)	-0.389, 1.244

Where:

$$R_1 = \frac{\sum ||F_o| - |F_c||}{\sum F_o}$$

$$wR_2 = \left[\frac{\sum (w(F_o^2 - F_c^2))^2}{\sum (w F_o^4)} \right]^{1/2}$$

$$GOF = \left[\frac{\sum (w(F_o^2 - F_c^2))^2}{(\text{No. of reflns.} - \text{No. of params.})} \right]^{1/2}$$

Table S2.8: Selected bond lengths of $[Cu_5(SPh)_5(dbfdp)_2]$ (2.5)

Bond length	Å	Bond length	Å
Cu1-P1	2.1876(10)	Cu3-S3	2.2674(9)
Cu1-S2	2.2279(10)	Cu3-S4	2.3280(10)
Cu1-S1	2.2991(10)	Cu3-Cu5	2.8223(6)
Cu1-Cu2	2.6942(6)	Cu4-P4	2.2168(12)
Cu2-P2	2.2266(10)	Cu4-S5	2.2429(11)
Cu2-S1	2.3874(10)	Cu4-S3	2.2766(10)
Cu2-S3	2.3945(9)	Cu5-S4	2.2111(10)
Cu2-S2	2.4494(10)	Cu5-S5	2.2426(11)
Cu3-P3	2.2617(10)	Cu5-S1	2.3073(10)

Table S2.9: Selected bond angles of $[Cu_5(SPh)_5(dbfdp)_2]$ (2.5)

Bond angle	(°)	Bond angle	(°)
P1-Cu1-S2	138.22(4)	Cu5-S1-Cu2	94.05(4)
P1-Cu1-S1	119.54(4)	Cu1-S2-Cu2	70.16(3)
S2-Cu1-S1	102.20(4)	Cu3-S3-Cu4	89.48(3)
P1-Cu1-Cu2	145.38(3)	Cu3-S3-Cu2	113.42(4)
S2-Cu1-Cu2	58.78(3)	Cu4-S3-Cu2	122.56(4)
S1-Cu1-Cu2	56.46(3)	Cu5-S4-Cu3	76.84(3)
P2-Cu2-S1	126.18(4)	Cu5-S5-Cu4	87.31(4)
P2-Cu2-S3	112.62(4)	S4-Cu3-Cu5	49.72(3)
S1-Cu2-S3	101.40(3)	P4-Cu4-S5	132.28(4)
P2-Cu2-S2	120.32(4)	P4-Cu4-S3	124.98(4)
S1-Cu2-S2	93.50(3)	S5-Cu4-S3	102.48(4)
S3-Cu2-S2	97.64(3)	S4-Cu5-S5	132.42(4)
P2-Cu2-Cu1	116.43(3)	S4-Cu5-S1	116.70(4)
S1-Cu2-Cu1	53.39(2)	S5-Cu5-S1	110.79(4)
S3-Cu2-Cu1	130.45(3)	S4-Cu5-Cu3	53.44(3)
S2-Cu2-Cu1	51.06(2)	S5-Cu5-Cu3	111.37(3)
P3-Cu3-S3	126.00(4)	S1-Cu5-Cu3	105.33(3)
P3-Cu3-S4	111.17(4)	Cu1-S1-Cu5	142.02(4)
S3-Cu3-S4	122.81(4)	Cu1-S1-Cu2	70.15(3)
P3-Cu3-Cu5	160.88(3)	S3-Cu3-Cu5	73.10(3)

Table S2.10: Summary of Crystal Data of $[Cu_5(SPh)_4Cl(dbfdp)_2]$ (2.6)

Formula	$C_{99}H_{78}Cl_7Cu_5O_2P_4S_4$
Formula Weight (g/mol)	2117.58
Crystal Dimensions (mm)	$0.656 \times 0.147 \times 0.034$
Crystal Color and Habit	colourless needle
Crystal System	monoclinic
Space Group	$P 2_1/m$
Temperature, K	110
a , Å	14.323(3)
b , Å	24.423(5)
c , Å	15.526(3)
α , °	90
β , °	101.145(3)
γ , °	90
V , Å ³	5328.9(18)
Number of reflections to determine final unit cell	9236
Min and Max 2θ for cell determination, °	4.42, 54.84
Z	2
F(000)	2152
ρ (g/cm ³)	1.320
λ , Å, (MoK α)	0.71073
μ , (cm ⁻¹)	1.339
Diffractometer Type	Bruker Kappa Axis Apex2
Scan Type(s)	phi and omega scans
Max 2θ for data collection, °	55.062
Measured fraction of data	0.999
Number of reflections measured	203032
Unique reflections measured	12542
R_{merge}	0.0666
Number of reflections included in refinement	12542
Cut off Threshold Expression	$I > 2\sigma(I)$
Structure refined using	full matrix least-squares using F^2
Weighting Scheme	$w=1/[\sigma^2(F_o^2)+(0.0523P)^2+17.3334P]$ where $P=(F_o^2+2F_c^2)/3$
Number of parameters in least-squares	574
R_1	0.0470
wR_2	0.1235
R_1 (all data)	0.0623
wR_2 (all data)	0.1324
GOF	1.050
Maximum shift/error	0.001
Min & Max peak heights on final ΔF Map (e/Å)	-1.691, 0.847

Where:

$$R_1 = \frac{\sum (|F_o| - |F_c|)}{\sum F_o}$$

$$wR_2 = \left[\frac{\sum (w(F_o^2 - F_c^2)^2)}{\sum (w F_o^4)} \right]^{1/2}$$

$$GOF = \left[\frac{\sum (w(F_o^2 - F_c^2)^2)}{(\text{No. of reflns.} - \text{No. of params.})} \right]^{1/2}$$

Table S2.11: Selected bond lengths of $[Cu_5(SPh)_4Cl(dbfdp)_2]$ (2.6)

Bond length	Å	Bond length	Å
Cu1-P1	2.2369(9)	Cu2-S1	2.2371(10)
Cu1-S1	2.2404(9)	Cu2-S3	2.2657(8)
Cu1-S2	2.3050(7)	Cu3-Cl1	2.2429(15)
Cu1-Cu2	2.9716(8)	Cu3-S2	2.2504(14)
Cu2-P2	2.2253(9)	Cu3-S3	2.2528(14)

Table S2.12: Selected bond angles of $[Cu_5(SPh)_4Cl(dbfdp)_2]$ (2.6)

Bond angle	(°)	Bond angle	(°)
P1-Cu1-S1	133.85(3)	P2-Cu2-Cu1	121.29(3)
P1-Cu1-S2	117.78(4)	S1-Cu2-Cu1	48.47(2)
S1-Cu1-S2	107.94(4)	S3-Cu2-Cu1	100.13(3)
P1-Cu1-Cu2	125.52(3)	S2-Cu3-S3	110.79(5)
S1-Cu1-Cu2	48.37(3)	Cu2-S1-Cu1	83.16(3)
S2-Cu1-Cu2	98.22(3)	Cu3-S3-Cu2	95.67(3)
P2-Cu2-S1	130.04(3)	Cu2 ¹ -S3-Cu2	127.13(6)
P2-Cu2-S3	116.54(4)	Cu1 ¹ -S2-Cu1	135.65(5)
S1-Cu2-S3	113.39(4)	C49-S3-Cu3	117.09(18)
Cu3-S2-Cu1'	93.64(3)	C49-S3-Cu2'	109.96(6)
C43-S2-Cu1	107.94(5)	Cu3-S3-Cu2'	95.67(3)
Cu3-S2-Cu1	93.64(3)	C49-S3-Cu2	109.96(6)

Table S2.13: Summary of Crystal Data of $[Ag_4(SPh)_4(dbfdp)_2]$ (2.7)

Formula	$C_{96}H_{72}Ag_4O_2P_4S_4$
Formula Weight (g/mol)	1941.13
Crystal Dimensions (mm)	$0.150 \times 0.026 \times 0.010$
Crystal Color and Habit	colourless Plate
Crystal System	triclinic
Space Group	P -1
Temperature, K	110
a , Å	12.4171(11)
b , Å	13.0644(11)
c , Å	15.1584(13)
α , °	94.234(3)
β , °	98.414(3)
γ , °	117.988(3)
V , Å ³	2119.3(3)
Number of reflections to determine final unit cell	3352
Min and Max 2θ for cell determination, °	6.02, 34.66
Z	1
F(000)	976
ρ (g/cm ³)	1.521
λ , Å, (MoK α)	0.71073
μ , (cm ⁻¹)	1.133
Diffractometer Type	Bruker Kappa Axis Apex2
Scan Type(s)	phi and omega scans
Max 2θ for data collection, °	41.652
Measured fraction of data	0.993
Number of reflections measured	17109
Unique reflections measured	4394
R_{merge}	0.0947
Number of reflections included in refinement	4394
Cut off Threshold Expression	$I > 2\sigma(I)$
Structure refined using	full matrix least-squares using F ²
Weighting Scheme	$w=1/[\sigma^2(F_o^2)+(0.0483P)^2+8.1486P]$ where $P=(F_o^2+2F_c^2)/3$
Number of parameters in least-squares	800
R_1	0.0482
wR_2	0.0989
R_1 (all data)	0.1116
wR_2 (all data)	0.1295
GOF	1.016
Maximum shift/error	0.000
Min & Max peak heights on final ΔF Map (e/Å)	-0.426, 0.576

Where:

$$R_1 = \frac{\sum (|F_o| - |F_c|)}{\sum F_o}$$

$$wR_2 = \left[\frac{\sum (w(F_o^2 - F_c^2)^2)}{\sum (w F_o^4)} \right]^{1/2}$$

$$GOF = \left[\frac{\sum (w(F_o^2 - F_c^2)^2)}{(\text{No. of reflns.} - \text{No. of params.})} \right]^{1/2}$$

Table S2.14: Selected bond lengths of $[Ag_4(SPh)_4(dbfdp)_2]$ (2.7) (Molecule shows disorder, $_1$ – fraction 1, $_2$ – fraction 2)

Bond length	Å	Bond length	Å
Ag1_1-P2_1	2.416(8)	Ag1_2-S2_2	2.302(18)
Ag1_1-S1_1	2.442(8)	Ag1_2-P2_2	2.422(9)
Ag1_1-S2_1	2.897(16)	Ag1_2-S1_2	2.464(9)
Ag2_1-P1_1	2.414(8)	Ag2_2-P1_2	2.413(9)
Ag2_1-S2_1	2.507(9)	Ag2_2-S2_2	2.503(9)
Ag2_1-S1_1	2.584(8)	Ag2_2-S1_2	2.582(10)

Table S2.15: Selected bond angles of $[Ag_4(SPh)_4(dbfdp)_2]$ (2.7) (Molecule shows disorder, $_1$ – fraction 1, $_2$ – fraction 2)

Bond angle	(°)	Bond angle	(°)
P2_1-Ag1_1-S1_1	136.2(4)	S2_2-Ag1_2-P2_2	126.2(4)
P2_1-Ag1_1-S2_1	109.4(3)	S2_2-Ag1_2-S1_2	94.3(5)
S1_1-Ag1_1-S2_1	114.2(4)	P2_2-Ag1_2-S1_2	133.4(4)
P1_1-Ag2_1-S2_1	142.6(4)	P1_2-Ag2_2-S2_2	140.4(5)
P1_1-Ag2_1-S1_1	123.8(4)	P1_2-Ag2_2-S1_2	124.7(4)
S2_1-Ag2_1-S1_1	92.5(4)	S2_2-Ag2_2-S1_2	92.5(4)
Ag1_1-S1_1-Ag2_1	103.8(3)	Ag1_2-S1_2-Ag2_2	101.5(4)
Ag2_1-S2_1-Ag1_1	80.7(4)	Ag1_2-S2_2-Ag2_2	101.6(6)

Appendix 3.0 Supporting Information for Chapter 3

Appendix 3.1: ^1H , $^{13}\text{C}\{^1\text{H}\}$ and $^{31}\text{P}\{^1\text{H}\}$ NMR data for compounds (3.1) and (3.2)

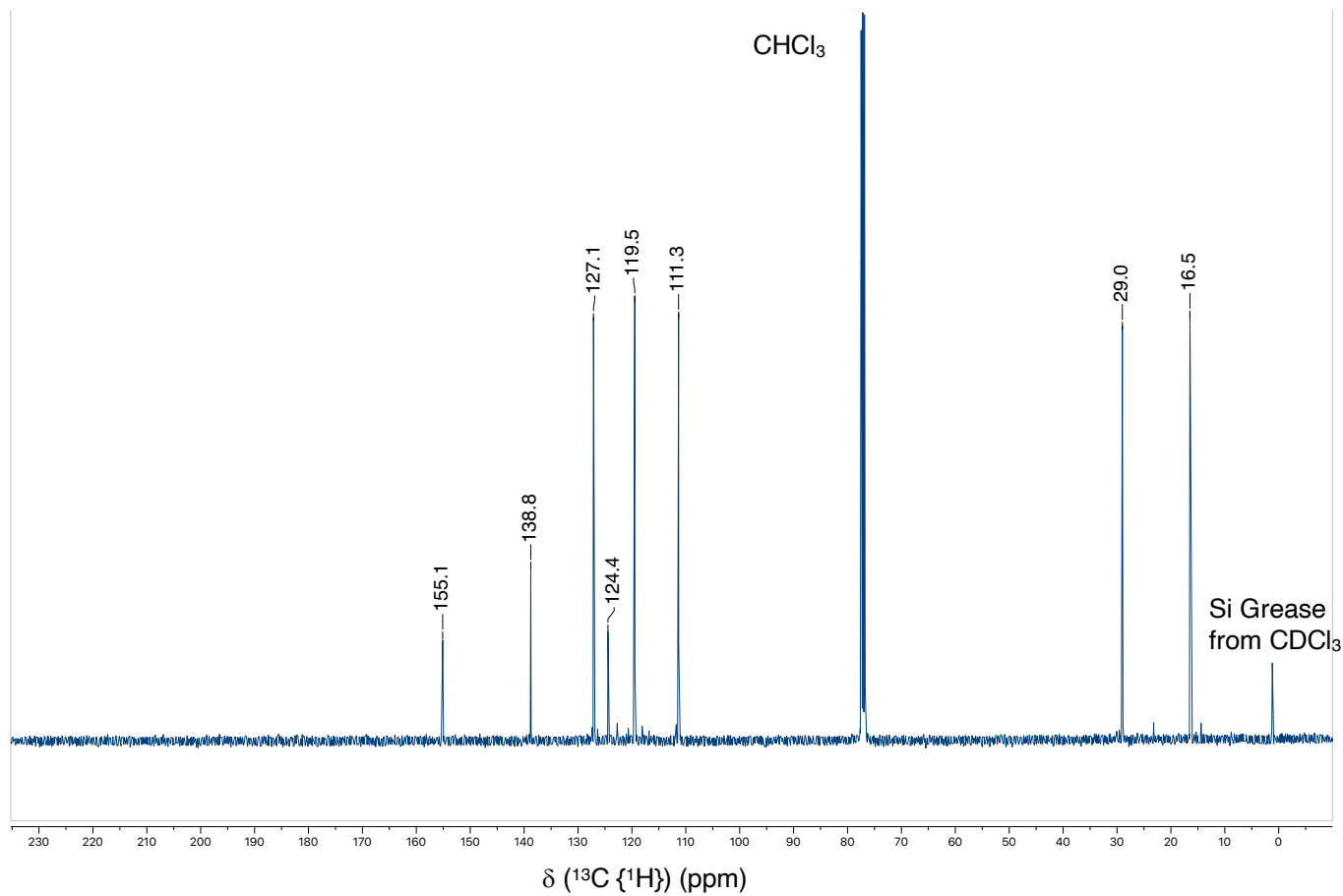


Figure S3.1: $^{13}\text{C}\{^1\text{H}\}$ NMR spectrum in CDCl_3 (298 K) of (EtDBF) (3.1)

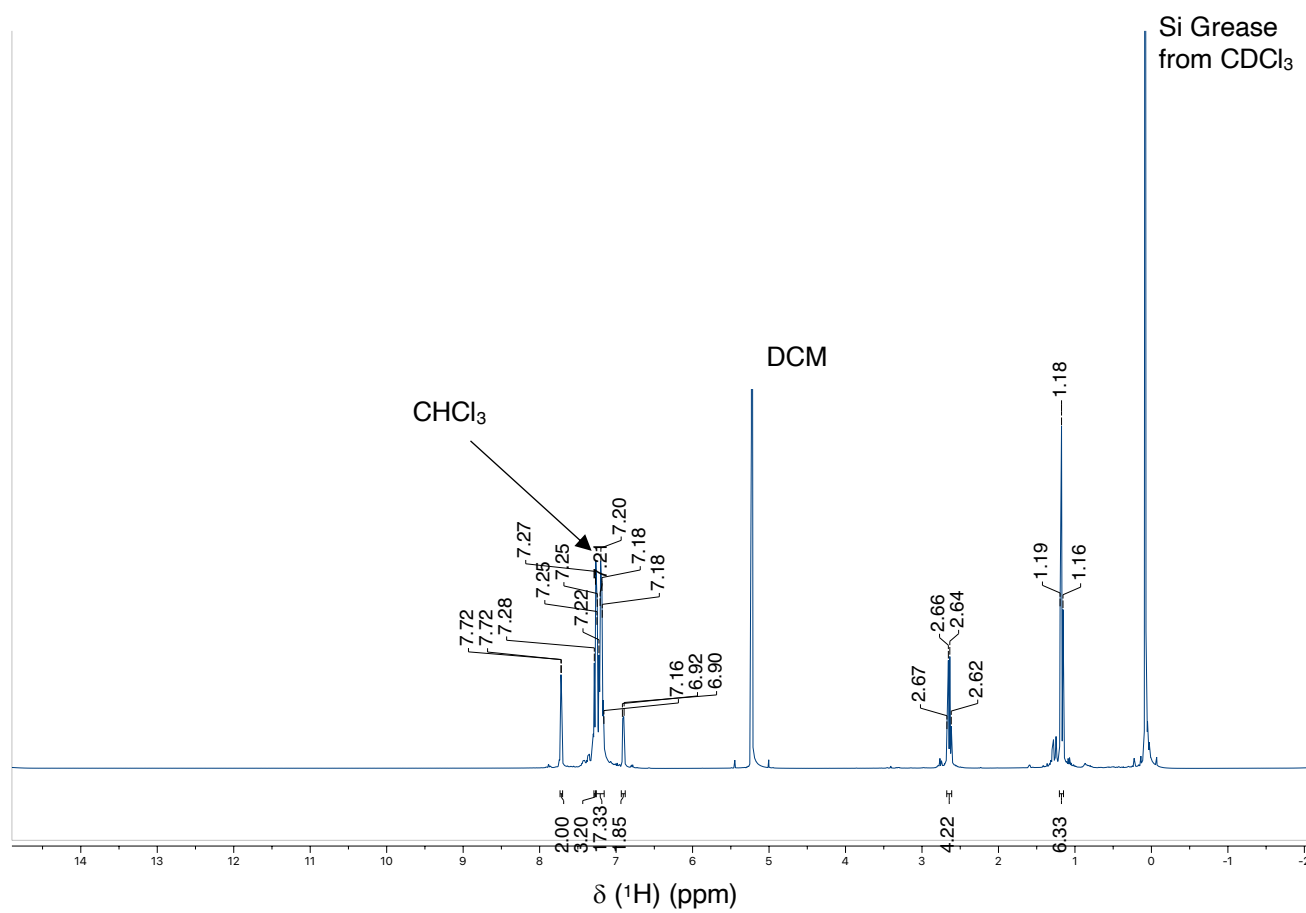


Figure S3.2: ^1H NMR spectrum in CDCl_3 (298 K) of (EtDBFDP) (3.2)

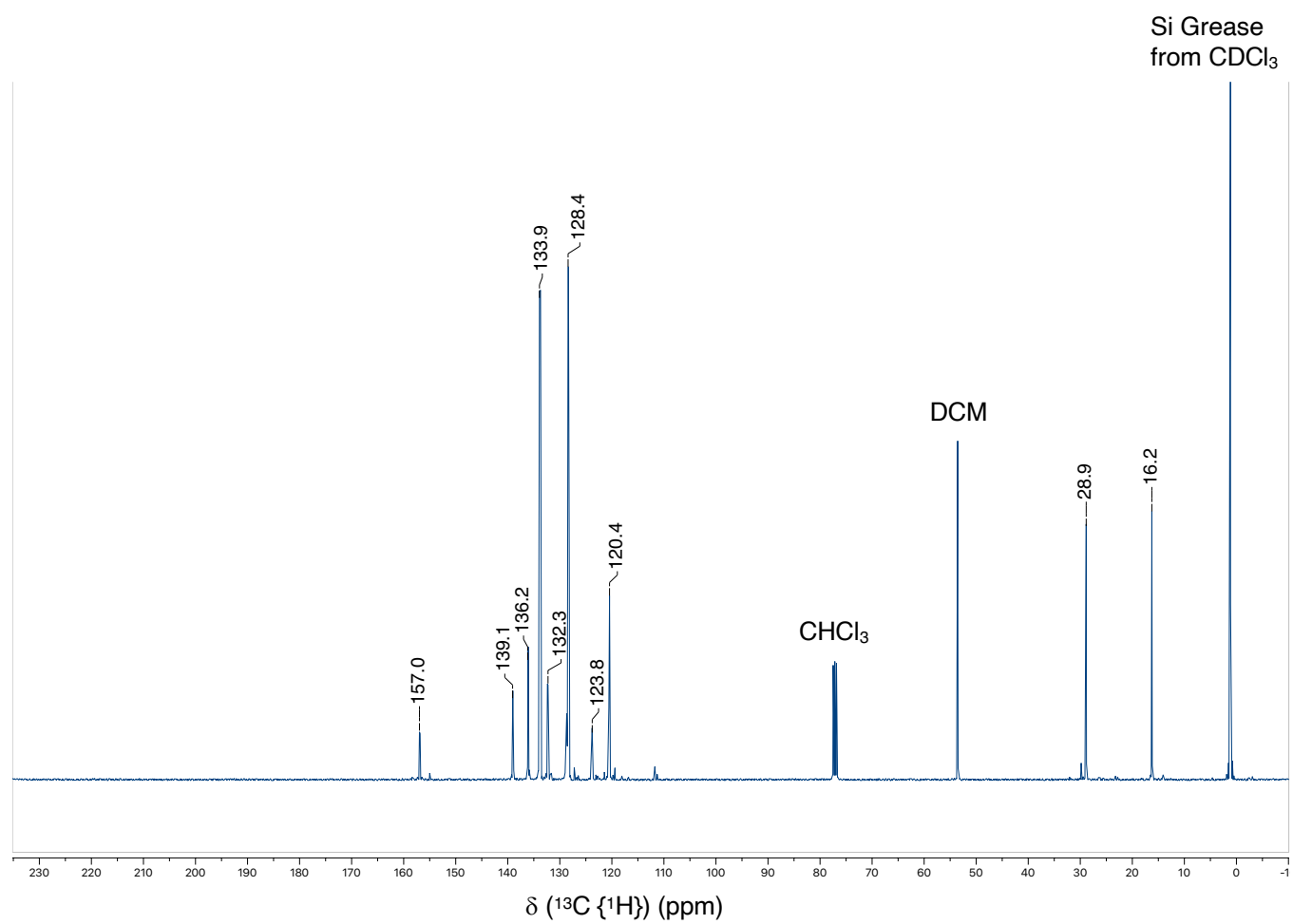


Figure S3.3: $^{13}\text{C}\{^1\text{H}\}$ NMR spectrum in CDCl_3 (298 K) of (EtDBFDP) (3.2)

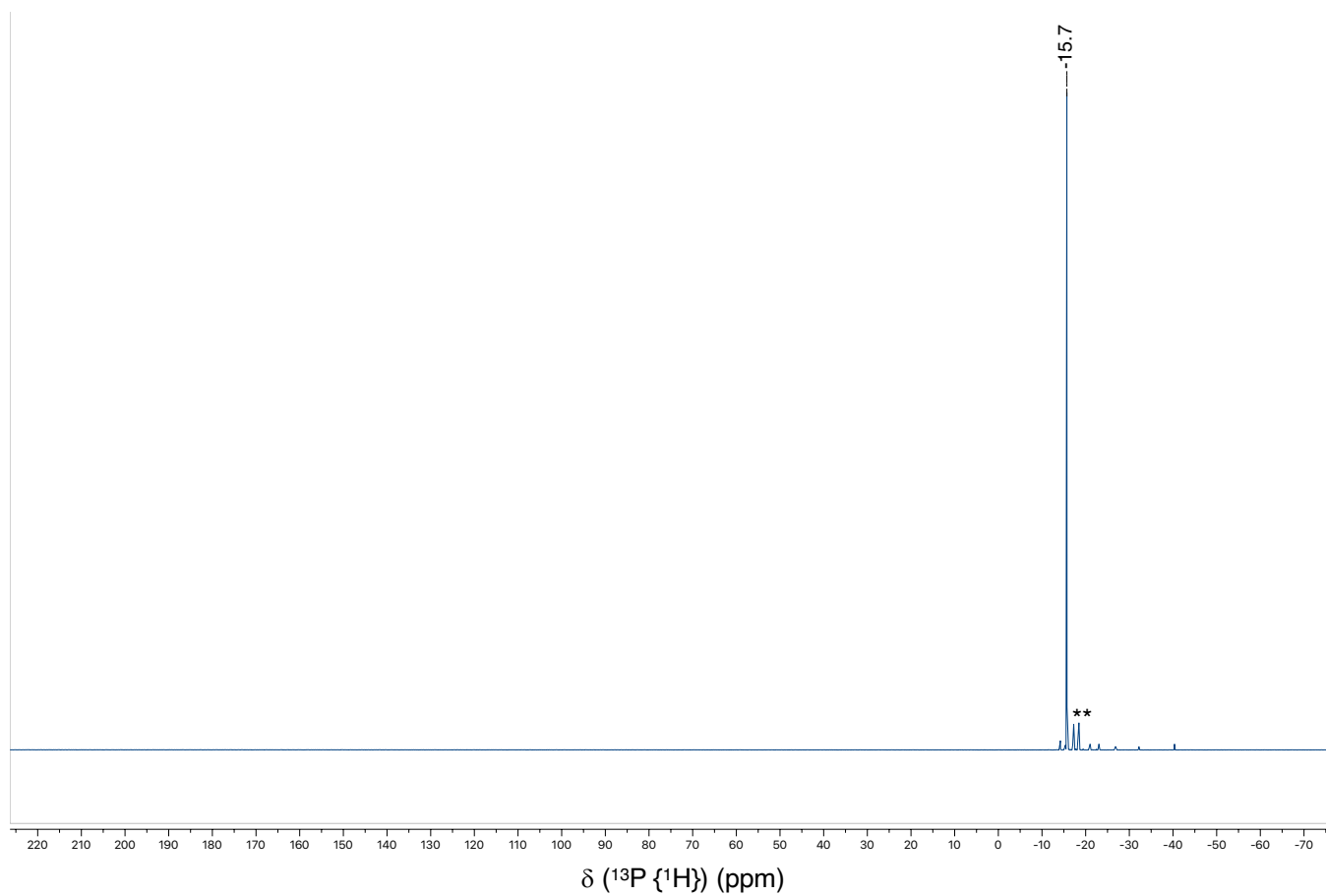


Figure S3.4: $^{31}\text{P}\{^1\text{H}\}$ NMR spectrum in CDCl_3 (298 K) of (EtDBFDP) (3.2) (* unknown impurities)

Appendix 3.2: X - ray structure analysis and data for (3.3)

Table S3.1: Summary of Crystal Data of $[Cu_{12}Se_6(etdbfdp)_2]$ (3.3)

Formula	$C_{168}H_{152}Cu_{12}O_6P_8Se_6$
Formula Weight (g/mol)	3750.89
Crystal Dimensions (mm)	$0.284 \times 0.114 \times 0.026$
Crystal Color and Habit	orange plate
Crystal System	monoclinic
Space Group	$P 2_1/c$
Temperature, K	110
a , Å	17.3502(18)
b , Å	24.097(3)
c , Å	18.749(2)
α , °	90
β , °	108.8800(10)
γ , °	90
V , Å ³	7416.7(14)
Number of reflections to determine final unit cell	4333
Min and Max 2θ for cell determination, °	5.56, 45.78
Z	2
F(000)	3760
ρ (g/cm)	1.680
λ , Å, (MoK α)	0.71073
μ , (cm ⁻¹)	3.299
Diffractometer Type	Bruker Kappa Axis Apex2
Scan Type(s)	phi and omega scans
Max 2θ for data collection, °	45.52
Measured fraction of data	0.998
Number of reflections measured	82278
Unique reflections measured	10000
R_{merge}	0.1249
Number of reflections included in refinement	10000
Cut off Threshold Expression	$I > 2\sigma(I)$
Structure refined using	full matrix least-squares using F^2
Weighting Scheme	$w=1/[\sigma^2(F_o^2)+(0.0697P)^2+7.2989P]$ where $P=(F_o^2+2F_c^2)/3$
Number of parameters in least-squares	935
R_1	0.0548
wR_2	0.1223
R_1 (all data)	0.1255
wR_2 (all data)	0.1532
GOF	1.027
Maximum shift/error	0.001
Min & Max peak heights on final ΔF Map (e ⁻ /Å)	-0.553, 0.714

Where:

$$R_1 = \sum | |F_o| - |F_c| | / \sum F_o$$

$$wR_2 = [\sum (w(F_o^2 - F_c^2)^2) / \sum (w F_o^4)]^{1/2}$$

$$GOF = [\sum (w(F_o^2 - F_c^2)^2) / (\text{No. of reflns.} - \text{No. of params.})]^{1/2}$$

Table S3.2: Selected bond lengths of $[Cu_{12}Se_6(etdbfdp)_2]$ (3.3)

Bond length	Å	Bond length	Å
Se1-Cu2	2.3606(14)	Cu1-Cu2	2.9563(17)
Se1-Cu1	2.3632(15)	Cu1-Cu3	2.9868(15)
Se1-Cu4	2.3820(15)	Cu2-P2	2.318(3)
Se1-Cu3	2.3835(15)	Cu2-Cu5	2.6200(16)
Se2-Cu6	2.2718(16)	Cu2-Cu6	2.7848(17)
Se2-Cu5'	2.3060(14)	Cu2-Cu4	2.8484(15)
Se2-Cu3'	2.4588(16)	Cu3-P3	2.298(3)
Se2-Cu2	2.4624(15)	Cu3-Cu5	2.6189(16)
Se3-Cu5	2.2705(14)	Cu3-Cu6	2.6907(17)
Se3-Cu6	2.3186(16)	Cu3-Cu4	2.8771(17)
Se3-Cu1	2.4626(15)	Cu4-P4	2.305(3)
Se3-Cu4'	2.4632(16)	Cu4-Cu6	2.6339(17)
Cu1-P1	2.300(3)	Cu4-Cu5	2.7112(16)
Cu1-Cu6	2.5966(16)	Cu5-Cu6	2.8344(16)
Cu1-Cu5	2.7122(16)	Cu5'-Cu6	2.8477(16)

Table S3.3: Selected bond angles of $[Cu_{12}Se_6(etdbfdp)_2]$ (3.3)

Bond angle	(°)	Bond angle	(°)
Cu2-Se1-Cu1	77.49(5)	Se1-Cu4-Cu6	103.00(6)
Cu2-Se1-Cu4	73.82(5)	Se3-Cu4-Cu6	53.99(4)
Cu1-Se1-Cu4	120.60(6)	P4-Cu4-Cu5'	144.64(9)
Cu2-Se1-Cu3	120.92(6)	Se1-Cu4-Cu5'	99.86(5)
Cu1-Se1-Cu3	77.99(5)	Se3-Cu4-Cu5'	51.78(4)
Cu4-Se1-Cu3	74.27(5)	Cu6-Cu4-Cu5'	64.03(4)
Cu6-Se2-Cu5	76.93(5)	P4-Cu4-Cu2	129.29(9)
Cu6-Se2-Cu3	69.20(5)	Se1-Cu4-Cu2	52.74(4)
Cu5-Se2-Cu3	66.60(5)	Se3-Cu4-Cu2	106.75(5)
Cu6-Se2-Cu2	71.93(5)	Cu6-Cu4-Cu2	104.16(5)
Cu5-Se2-Cu2	66.56(5)	Cu5-Cu4-Cu2	56.17(4)
Cu3-Se2-Cu2	124.04(5)	P4-Cu4-Cu3	112.38(9)
Cu5-Se3-Cu6'	76.28(5)	Se1-Cu4-Cu3	52.89(4)
Cu5-Se3-Cu1	69.79(5)	Se3-Cu4-Cu3	112.12(5)
Cu6'-Se3-Cu1	65.71(5)	Cu6-Cu4-Cu3	58.25(4)
Cu5-Se3-Cu4	69.75(5)	Cu5'-Cu4-Cu3	101.47(5)
Cu6'-Se3-Cu4	66.77(5)	Cu2-Cu4-Cu3	92.26(4)

Cu1-Se3-Cu4	122.86(5)	Se3-Cu5-Se2	164.66(7)
P1-Cu1-Se1	112.23(9)	Se3-Cu5-Cu3	125.38(6)
P1-Cu1-Se3	100.17(8)	Se2-Cu5-Cu3	59.50(4)
Se1-Cu1-Se3	147.32(6)	Se3-Cu5-Cu2	121.44(6)
P1-Cu1-Cu6'	119.11(9)	Se2-Cu5-Cu2	59.58(4)
Se1-Cu1-Cu6'	103.31(5)	Cu3-Cu5-Cu2	112.11(5)
Se3-Cu1-Cu6'	54.48(4)	Se3-Cu5-Cu4	58.47(4)
P1-Cu1-Cu5	145.58(9)	Se2-Cu5-Cu4	124.03(6)
Se1-Cu1-Cu5	98.76(5)	Cu3-Cu5-Cu4	156.55(6)
Se3-Cu1-Cu5	51.78(4)	Cu2-Cu5-Cu4	64.56(4)
Cu6'-Cu1-Cu5	64.50(4)	Se3-Cu5-Cu1	58.44(4)
P1-Cu1-Cu2	109.85(9)	Se2-Cu5-Cu1	127.39(6)
Se1-Cu1-Cu2	51.22(4)	Cu3-Cu5-Cu1	68.12(4)
Se3-Cu1-Cu2	114.24(5)	Cu2-Cu5-Cu1	157.72(6)
Cu6'-Cu1-Cu2	59.78(4)	Cu4-Cu5-Cu1	105.81(5)
Cu5-Cu1-Cu2	100.99(5)	Se3-Cu5-Cu6'	52.62(4)
P1-Cu1-Cu3	139.14(9)	Se2-Cu5-Cu6'	142.61(6)
Se1-Cu1-Cu3	51.31(4)	Cu3-Cu5-Cu6'	105.30(5)
Se3-Cu1-Cu3	105.43(5)	Cu2-Cu5-Cu6'	104.92(5)
Cu6'-Cu1-Cu3	101.70(5)	Cu4-Cu5-Cu6'	56.66(4)
Cu5-Cu1-Cu3	54.46(4)	Cu1-Cu5-Cu6'	55.78(4)
Cu2-Cu1-Cu3	87.97(4)	Se3-Cu5-Cu6	144.24(6)
P2-Cu2-Se1	117.28(9)	Se2-Cu5-Cu6	50.99(4)
P2-Cu2-Se2	96.78(8)	Cu3-Cu5-Cu6	58.79(4)
Se1-Cu2-Se2	145.81(6)	Cu2-Cu5-Cu6	61.07(4)
P2-Cu2-Cu5'	125.94(9)	Cu4-Cu5-Cu6	103.75(5)
Se1-Cu2-Cu5'	103.08(5)	Cu1-Cu5-Cu6	105.12(5)
Se2-Cu2-Cu5'	53.86(4)	Cu6'-Cu5-Cu6	91.63(5)
P2-Cu2-Cu6'	135.84(8)	Se2-Cu6-Se3	168.47(6)
Se1-Cu2-Cu6'	97.98(5)	Se2-Cu6-Cu1	122.62(6)
Se2-Cu2-Cu6'	50.86(4)	Se3-Cu6-Cu1	59.81(5)
Cu5'-Cu2-Cu6'	63.51(4)	Se2-Cu6-Cu4	123.47(6)
P2-Cu2-Cu4	120.02(8)	Se3-Cu6-Cu4	59.24(4)
Se1-Cu2-Cu4	53.43(4)	Cu1-Cu6-Cu4	111.59(6)
Se2-Cu2-Cu4	113.04(5)	Se2-Cu6-Cu3	58.68(5)
Cu5'-Cu2-Cu4	59.27(4)	Se3-Cu6-Cu3	124.49(6)
Cu6'-Cu2-Cu4	101.87(5)	Cu1-Cu6-Cu3	156.15(6)
P2-Cu2-Cu1	132.44(8)	Cu4-Cu6-Cu3	65.40(5)
Se1-Cu2-Cu1	51.29(4)	Se2-Cu6-Cu2	57.21(4)
Se2-Cu2-Cu1	103.75(5)	Se3-Cu6-Cu2	126.34(6)
Cu5'-Cu2-Cu1	100.48(5)	Cu1-Cu6-Cu2	66.54(4)
Cu6'-Cu2-Cu1	53.68(4)	Cu4-Cu6-Cu2	153.58(5)
Cu4-Cu2-Cu1	90.47(4)	Cu3-Cu6-Cu2	105.05(5)
P3-Cu3-Se1	111.62(9)	Se2-Cu6-Cu5'	140.43(6)
P3-Cu3-Se2	100.53(9)	Se3-Cu6-Cu5'	51.09(4)
Se1-Cu3-Se2	147.69(6)	Cu1-Cu6-Cu5'	59.73(4)
P3-Cu3-Cu5	128.11(10)	Cu4-Cu6-Cu5'	59.31(4)

Se1-Cu3-Cu5	100.86(5)	Cu3-Cu6-Cu5 ⁷	103.10(5)
Se2-Cu3-Cu5	53.91(4)	Cu2-Cu6-Cu5 ⁷	102.31(5)
P3-Cu3-Cu6	138.94(9)	Se2-Cu6-Cu5	52.07(4)
Se1-Cu3-Cu6	101.30(5)	Se3-Cu6-Cu5	139.45(6)
Se2-Cu3-Cu6	52.12(4)	Cu1-Cu6-Cu5	103.97(5)
Cu5-Cu3-Cu6	64.85(4)	Cu4-Cu6-Cu5	102.36(5)
P3-Cu3-Cu4	129.86(9)	Cu3-Cu6-Cu5	56.36(4)
Se1-Cu3-Cu4	52.84(4)	Cu2-Cu6-Cu5	55.43(4)
Se2-Cu3-Cu4	108.02(5)	Cu5 ⁷ -Cu6-Cu5	88.37(5)
Cu5-Cu3-Cu4	101.96(5)	Cu5-Cu3-Cu1	57.42(4)
Cu6-Cu3-Cu4	56.35(4)	Cu6-Cu3-Cu1	101.97(5)
P3-Cu3-Cu1	117.64(9)	Cu4-Cu3-Cu1	89.30(4)
Se1-Cu3-Cu1	50.70(4)	P4-Cu4-Se1	108.40(9)
Se2-Cu3-Cu1	111.17(5)	P4-Cu4-Se3	103.70(9)
P4-Cu4-Cu6	126.55(8)	Se1-Cu4-Se3	147.83(6)

Curriculum Vitae

Mansha Nayyar

Education

- M.Sc. The University of Western Ontario (September 2020 - June 2022), “Luminescent Group 11 Metal Chalcogen Clusters with Bidentate Phosphine Ligands”, supervised by Dr. John F. Corrigan
 - Courses taken:
 - CHEM 9507Q (Advanced Chem Communications)
 - CHEM 9754R (Powder Diffraction)
 - CHEM 9513S (Intro. Physical Organic Chem)
 - CHEM 9555T (Organic Photochemistry)
- Honours B.Sc. The University of Western Ontario (September 2016 - April 2020), Honours Specialization in Chemistry

Publications and Presentations

- Publications
 - “Luminescent Group 11 Metal Chalcogenolate Clusters with Conjugated Diphosphine Ligands” (In preparation to be submitted June 2022)
- Presentations
 - 105th Canadian Chemistry Conference and Exhibition (CCCE 2022) (In person, June 2022): “Luminescent Group 11 Metal Chalcogenolate Clusters with Conjugated Diphosphine Ligands” (presentation)
 - 24th Chemistry and Biochemistry Graduate Research Conference (CBGRC) (Virtual, November 19, 2021), “Luminescent Group 11 Metal Chalcogenolate Clusters” (presentation)
 - 51st IUPAC General Assembly, 48th World Chemistry Congress, 104th Canadian Chemistry Conference and Exhibition (CCCE 2021) (Virtual, July 2021): “Luminescent Group 11 Metal Chalcogenolate Clusters” (poster)
 - 48th Southern Ontario Undergraduate Student Chemistry Conference (Virtual, June 2020): “Luminescent Copper Chalcogenide Clusters” (presentation)

Scholarships and Awards

- Scholarships
 - Queen Elizabeth II Graduate Scholarships in Science and Technology (QEII - GSST), 2022 - 2023 (Valued: \$15,000) - declined
 - Queen Elizabeth II Graduate Scholarships in Science and Technology (QEII - GSST), fall 2021 - summer 2022 (Valued: \$15,000)
- Awards
 - CSC Travel Award, June 2022 (Award based on research excellence to travel to Canadian Chemistry Conference and Exhibition (CCCE 2022), valued: \$1000)
 - 24th Chemistry and Biochemistry Graduate Research Conference (CBGRC), November 19, 2021 (Best presentation, valued: \$75)
 - 48th Southern Ontario Undergraduate Student Chemistry Conference, June 2020 (Best presentation, valued: \$200)

Outreach

- Inspiring Diversity in Science, Technology, Engineering & Math (IDSTEM) Conference, March 12 - 13, 2022, Western University (Virtual - poster judge)

Certifications

- Supporting Disclosures of GBSV at Western, April 2022
- WHMIS, The University of Western Ontario, January 2021
- Laboratory Safety and Hazardous Waste Management, The University of Western Ontario, September 2019
- Worker Health and Safety Awareness, The University of Western Ontario, September 2019

Teaching experience

- Teaching Mentor: Supervised and taught laboratory techniques to two 4491E students (fall 2021 - winter 2022) and (fall 2020 - winter 2021), and summer student (summer 2021)
- Teaching Assistant: Instructed and supervised third year chemistry student laboratories (fall 2021 and fall 2020) and first year integrated science laboratories (winter 2021)

Laboratory Skills

- Organic and inorganic synthetic skills: Schlenk techniques, glove box, titration, TLC, flash column chromatography, distillation under inert conditions and crystallization
- Analysis and characterization skills: NMR Spectroscopy, ATR - IR Spectroscopy, UV - Vis Spectroscopy (also solid-state UV - Vis) and Mass Spectrometry
- Proficient in Chem Draw and Mestre Nova